

# On the *ab initio* determination of higher-order force constants at nonstationary reference geometries

Wesley D. Allen and Attila G. Császár  
*Department of Chemistry, Stanford University, Stanford, California 94305*

(Received 17 August 1992; accepted 26 October 1992)

Several complementary analyses have been performed in an investigation of the use of reference geometric structures which are not stationary at a given level of theory in the prediction of improved equilibrium anharmonic molecular force fields. Diatomic paradigms for the procedure were established by constructing empirical potential energy functions for the nitrogen and fluorine molecules which not only reproduce the available Rydberg–Klein–Rees data but also provide reliable derivatives through fourth order for ranges of 0.4 Å or greater around the equilibrium bond distance. For comparison, analogous curves were determined at the double- $\zeta$  plus polarization (DZP) restricted Hartree–Fock (RHF) level of theory, and the quartic force fields for N<sub>2</sub> and F<sub>2</sub> were also obtained at the experimental  $r_e$  structures using a (8s5p3d2f1g) basis set and the coupled-cluster singles and doubles method augmented by a perturbative contribution from connected triple excitations [CCSD(T)]. The results substantiate the ability of RHF theory to predict correlation-quality, higher-order force constants if an accurate reference geometry from experiment or a higher level of theory is employed. The theoretical foundations of this technique as applied to polyatomic molecular systems have been systematically explored. Mechanisms were analyzed which address the nonzero force dilemma by using various choices of internal coordinates to shift the equilibrium point of theoretical potential energy surfaces. Examples are presented in which the variations in predicted spectroscopic constants arising from different shift coordinate sets are non-negligible. A Cartesian projection scheme for higher-order force fields was developed and implemented to avert internal-coordinate dependences; formulas for higher-order projection matrices and higher-order derivatives of the external variables of a molecular system were concurrently derived. A formalism for the transformation of force fields between internal and Cartesian representations was also constructed which is applicable to arbitrary order. In addition to N<sub>2</sub> and F<sub>2</sub>, case studies were performed on the F<sub>2</sub>O and N<sub>2</sub>O molecules, for which electron correlation effects are of unusual importance. Quartic force fields are reported for F<sub>2</sub>O and N<sub>2</sub>O at the DZP and TZ(2d1f) CCSD(T) levels of theory, respectively, which provide the best data sets currently available and facilitate the assessment of experimental force constants. The CCSD(T) results are reproduced remarkably well by RHF predictions at the experimental equilibrium structures of these molecules but not at the corresponding RHF optimum geometries. Finally, practical recommendations are made for predictions of higher-order force constants at nonstationary points.

## I. DIATOMIC PARADIGMS

The theoretical determination of harmonic and anharmonic molecular force fields by *ab initio* methods has become one of the most common and successful applications of computational quantum chemistry.<sup>1–17</sup> There are several factors which influence the quality of these theoretical predictions,<sup>1,2,9–12</sup> the choice of the reference geometry being one of the most vexing but poorly appreciated considerations. Since the inception of computational quantum chemistry, a controversy has persisted as to whether force constants should be evaluated at optimized theoretical geometries or at experimental equilibrium structures. In fact, in the opinion of Pulay *et al.*,<sup>10</sup> “the choice of reference geometry is the most difficult problem confronting the systematic *ab initio* calculation of force constants.” Ostensibly the evaluation of force constants in a theoretical vibrational analysis at a point other than the optimized theoretical structure is unphysical in that nonzero forces are gen-

erally present on all the atoms and the system is not at equilibrium. Nevertheless, as discussed below, the selection of nonstationary reference geometries has considerable merit provided that appropriate procedures are implemented to circumvent the nonzero force dilemma. In this preview (Sec. I) a novel analysis of this topic is presented for the diatomic molecules N<sub>2</sub> and F<sub>2</sub> in order to highlight pertinent issues and to establish paradigms for the investigation of polyatomic systems.

In 1966 Schwendeman<sup>18</sup> was one of the first to observe that *ab initio* force constants for diatomic molecules tend to lie significantly closer to their experimental counterparts if they are evaluated at experimental equilibrium bond distances. Consequently, it was argued that theoretical predictions of force constants should be carried out whenever feasible at experimental  $r_e$  structures, which are generally known for the low-lying electronic states of common diatomic molecules. It is possible to elaborate on this argument extensively using the voluminous theoretical and ex-

perimental data now available for the  $N_2$  and  $F_2$  molecules. The strategy employed here for this purpose is to find an analytic representation of experimental, Rydberg–Klein–Rees<sup>19</sup> (RKR) and theoretical [double- $\zeta$  plus polarization (DZP) restricted Hartree–Fock (RHF)]<sup>20</sup> potential curves via a fit to a number of energy points, and subsequently to determine force constants analytically through fourth order as a function of bond distance. Thus, at any particular bond length within a given range, DZP RHF predictions for the potential energy derivatives of various orders can be compared to “exact” experimental values. The  $N_2$  and  $F_2$  examples are chosen not only because precise empirical data are available but also because they exhibit very different levels of agreement between theoretical and experimental equilibrium structures. Specifically, for the nitrogen molecule the DZP RHF equilibrium distance is 0.015 Å too short, which is an acceptable disparity, whereas for  $F_2$  this difference is 0.077 Å, which is anomalously large for this standard level of theory.

In the empirical RKR potentials of the ground electronic states of the nitrogen<sup>21</sup> and fluorine<sup>22</sup> molecules, the classical turning points for each quantized vibrational level are given up to  $v=22$  and  $v=23$  for  $N_2$  and  $F_2$ , respectively. These data points span the ranges  $r(N_2) \in (0.887, 1.559)$  Å and  $r(F_2) \in (1.165, 2.786)$  Å, the most notable separations therein appearing as 0.091 and 0.125 Å gaps about the respective  $r_e$  values of 1.0977 and 1.4119 Å.<sup>23</sup> The task of constructing potential functions not only to fit the RKR data points but also to provide reliable derivatives through fourth order is replete with pitfalls. Spline function techniques are clearly incapable of generating curves with smooth higher derivatives. Alternatively, numerous analytic forms for diatomic potentials have been developed for global fits to experimental data, and enlightening comparative studies exist for several of them.<sup>24,25</sup> However, extensive preliminary testing here of Morse and Varshni functions and modifications thereof revealed that commonly used reference potentials containing three to five parameters are not sufficiently flexible to yield higher-order derivatives whose accuracy is maintained over extended bond-length intervals. Attempts were made to ameliorate this problem by augmenting these reference potentials with unconstrained polynomial expansions in the variable  $\xi = \exp(\rho) - 1$ , where  $\rho$  is the Simons–Parr–Finlan coordinate  $(r - r_e)/r$ .<sup>26</sup> Such polynomial fitting procedures only gave rise to erratic higher-order force constants as a consequence of the uncertainty in the RKR points.

The optimal procedure which was formulated for extracting potential energy derivatives from the RKR data involved the transformation relation (in atomic units):

$$V(r) = E_e(r) + \frac{\xi^2}{r} = A + B \tan^{-1}[Z(r)] + \frac{\xi^2}{r}, \quad (1)$$

where  $E_e(r)$  denotes the molecular electronic energy,  $\zeta$  is the atomic number of the nuclear centers, and  $Z(r)$  is a dimensionless, monotonic function satisfying the boundary conditions  $\lim_{r \rightarrow \infty} Z(r) = +\infty$  and  $\lim_{r \rightarrow 0} Z(r) = -\infty$ . For both  $N_2$  and  $F_2$  the constants  $A$  and  $B$  in Eq. (1) were

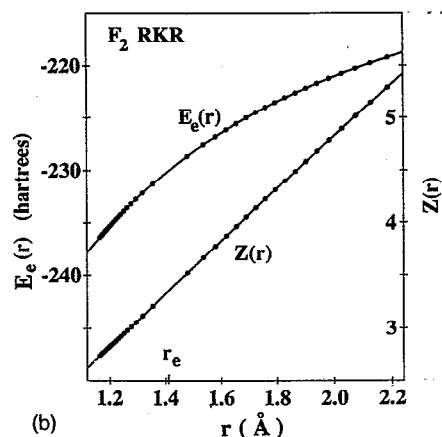
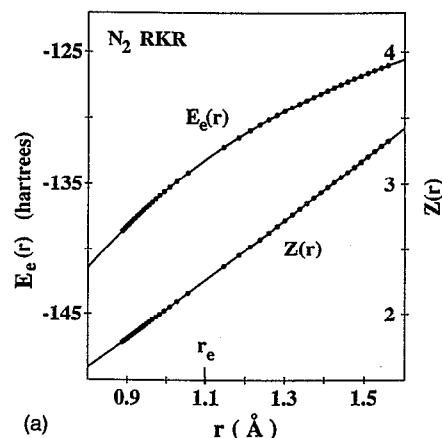


FIG. 1. Plots of the  $E_e(r)$  and  $Z(r)$  representations of the experimental RKR data for (a)  $N_2$  and (b)  $F_2$ .

selected to give the exact separated-atom energy<sup>27</sup> at infinite distance and the correlated, relativistic united-atom electronic energy<sup>28</sup> at  $r=0$ . The transformation of the RKR data for  $V(r)$  yields the  $E_e(r)$  and  $Z(r)$  points plotted in Figs. 1(a) and 1(b) for  $N_2$  and  $F_2$ , respectively. The linearity of the RKR data sets in the  $Z(r)$  representation is striking, indicating that the expansion of  $Z(r)$  about  $r_e$  converges rapidly. For the range of intermediate bond distances of concern here,  $Z(r)$  can thus be written as

$$Z(r) = z_0 + z_1(r - r_e) + \sum_{n=2}^K z_n(r - r_e)^n, \quad (2)$$

in which the  $z_0$  and  $z_1$  coefficients are found to be at least an order of magnitude greater than their higher-order analogs if  $r$  is expressed in Å (see Table I below). Nevertheless, to satisfactorily fit the RKR data out to  $r(N_2) = 1.6$  Å and  $r(F_2) = 2.4$  Å, the upper limit  $K$  in Eq. (2) must be extended to 7 and 11 for  $N_2$  and  $F_2$ , respectively.

Extensive spectroscopic studies have firmly established the dissociation energies, equilibrium bond lengths, and quadratic force constants of  $N_2$  and  $F_2$ ,<sup>21–23</sup> thus providing values for  $E_e(r_e)$ ,  $E'_e(r_e)$ , and  $E''_e(r_e)$  and allowing  $z_0$ ,  $z_1$ , and  $z_2$  to be ascertained unequivocally. In addition, the observed  $\alpha_e$  and  $\omega_e x_e$  constants<sup>23</sup> for  $N_2$  yield  $V'''(r_e) = -169.6$  aJ Å<sup>-3</sup> and  $V''''(r_e) = 997.6$  aJ Å<sup>-4</sup>, values

TABLE I.  $V(r)$  parameters for  $N_2$  and  $F_2$ .<sup>a</sup>

	$N_2$		$F_2$	
	DZP RHF	RKR	DZP RHF	RKR
$A$	-199.295 94 <sup>b</sup>	-199.565 8 <sup>c</sup>	-365.323 62 <sup>b</sup>	-364.503 9 <sup>c</sup>
$B$	180.748 4( $\pi^{-1}$ ) <sup>b</sup>	180.748 4( $\pi^{-1}$ ) <sup>c</sup>	329.790 6( $\pi^{-1}$ ) <sup>b</sup>	329.790 6( $\pi^{-1}$ ) <sup>c</sup>
$r_e$	1.082 707 <sup>d</sup>	1.097 685 <sup>e</sup>	1.334 980 <sup>d</sup>	1.411 930 <sup>e</sup>
$z_0$	2.258 028 37	2.258 029 34 <sup>f</sup>	3.353 860 00	3.353 861 20 <sup>f</sup>
$z_1$	2.344 700 20	2.281 151 14	2.806 251 88	2.508 708 05
$z_2$	0.237 794	0.127 367	0.172 260	0.009 460
$z_3$	-0.046 999	-0.099 744	-0.013 602	-0.039 633
$z_4$	-0.031 175	-0.026 538	0.008 768	0.017 855 [8]
$z_5$	0.034 471	0.047 202 [3]	-0.020 785	0.027 784 [8]
$z_6$	-0.023 815 [1]	0.012 127 [4]	0.048 361 [5]	-0.010 575 [9]
$z_7$	0.049 402 [1]	0.020 027 [4]	-0.034 520 [5]	-0.078 191 [9]
$z_8$	0.030 502 [2]	...	-0.006 187 [6]	-0.094 601 [10]
$z_9$	-0.081 551 [2]	...	0.010 441 [6]	0.215 908 [10]
$z_{10}$	...	...	-0.000 380 [7]	0.116 726 [11]
$z_{11}$	...	...	0.000 808 [7]	-0.181 962 [11]

Intervals of fit, $r$ (Å):			
[1] (0.85, 1.45)	[2] (0.85,1.56)	[3] (0.88,1.38)	[4] (0.88, 1.56)
[5] (1.09, 1.83)	[6] (1.09,2.06)	[7] (1.09,2.26)	[8] (1.25, 1.73)
[9] (1.25, 1.91)	[10] (1.25,2.08)	[11] (1.25,2.33)	

<sup>a</sup>The functional form of the  $V(r)$  potentials is given in Eqs. (1) and (2). Units:  $A$  and  $B$  in hartree,  $r_e$  in Å, and  $z_n$  parameters in Å<sup>-n</sup>. The unconstrained  $z_n$  quantities were determined from least-squares fits to RKR and DZP RHF energy points as described in the text using the intervals enumerated in brackets adjacent to each entry. The  $z_n$  constants listed without brackets were evaluated from energy and derivative data for each potential curve at the corresponding equilibrium distance, these data being determined directly in the DZP RHF case and by means of the  $\alpha_e$  and  $\omega_e x_e$  spectroscopic constants of Refs. 21, 22, and 23 in the RKR case.

<sup>b</sup>The  $B$  parameters for the DZP RHF potentials were set to the corresponding RKR values, and the  $A$  constants in these potentials were subsequently selected as eight-digit values which reproduce the analogous RKR  $z_0$  parameters within roundoff error.

<sup>c</sup>The  $A$  and  $B$  parameters for the RKR curves were chosen to reproduce the correlated, relativistic electronic energies for the separated-atom (Ref. 27) and united-atom (Ref. 28) limits.

<sup>d</sup>Precisely determined  $r_e$  values obtained from RHF analytic gradients.

<sup>e</sup>Spectroscopic values from Ref. 23.

<sup>f</sup>The  $z_0$  values in the RKR curves were ascertained from the empirically derived (Refs. 21–23) dissociation energies (in hartree)  $D_e(N_2)=0.3640$  and  $D_e(F_2)=0.060\ 945$ .

which are in excellent agreement with theoretical predictions of  $-170.5$  aJ Å<sup>-3</sup> and  $1005.0$  aJ Å<sup>-4</sup>, respectively, obtained here<sup>29</sup> with a large basis set denoted as PZ(3d2f1g) used in conjunction with the coupled-cluster singles and doubles method augmented by a perturbative contribution from connected triple excitations [CCSD(T)].<sup>20</sup> By constraining the third and fourth derivatives of the RKR potential curve for  $N_2$  to the empirical values arising from  $\alpha_e$  and  $\omega_e x_e$ , the corresponding  $z_3$  and  $z_4$  coefficients in Eq. (2) were determined. In the case of  $F_2$ ,  $V'''(r_e) = -36.39$  aJ Å<sup>-3</sup> and  $V''''(r_e) = 231.0$  aJ Å<sup>-4</sup> are given by the experimental  $\alpha_e$  and  $\omega_e x_e$  constants.<sup>22</sup> The former value was confirmed by subsequent PZ(3d2f1g) CCSD(T) predictions, but the latter value was brought into question.<sup>30</sup> Accordingly,  $z_3$  for  $F_2$  was evaluated from the empirically deduced  $V'''(r_e)$  value while  $z_4$  was left as an adjustable parameter.

The unconstrained  $z_n$  parameters in Eq. (2) were found via least-squares fits to the residuals remaining after deflation of the dominant, fixed lower-order terms in  $Z(r)$ . To ascertain derivatives of the RKR potential curves accurately, the fits must be performed sequentially rather than simultaneously to ensure that the  $z_n \cdot n!$  values are

approximations to the  $r$  derivatives of  $Z$  and not merely phenomenological constants. By analysis of model Varshni potential functions for  $N_2$  and  $F_2$ , a cutoff interval for each order was estimated about  $r_e$  within which the associated  $z_n$  term contributes less than  $20$  cm<sup>-1</sup> to  $V(r)$ . These cutoff intervals were utilized in a fitting procedure involving successively larger ranges of  $r$ , in which the various  $z_n$  constants were found either individually or in pairs by fixing all previously determined, lower-order constants in Eq. (2) and then fitting the selected terms to the RKR points lying inside the ensuing cutoff interval for the next higher-order contribution. The RKR points for small internuclear distances in both molecules are somewhat uncertain, and in the case of  $F_2$  it was necessary to exclude the points for  $r(F_2) < 1.25$  Å because the scatter contained therein<sup>31</sup> deteriorated the fits of the higher-order  $z_n$  coefficients.

All parameters involved in the RKR potential functions for  $N_2$  and  $F_2$  are listed in Table I along with the intervals employed in the fitting procedure. For comparison with the RKR curves, DZP RHF potential energy functions were constructed analogously by computing and then fitting energy points around the theoretical equilibrium geometry using the same intervals as in the RKR

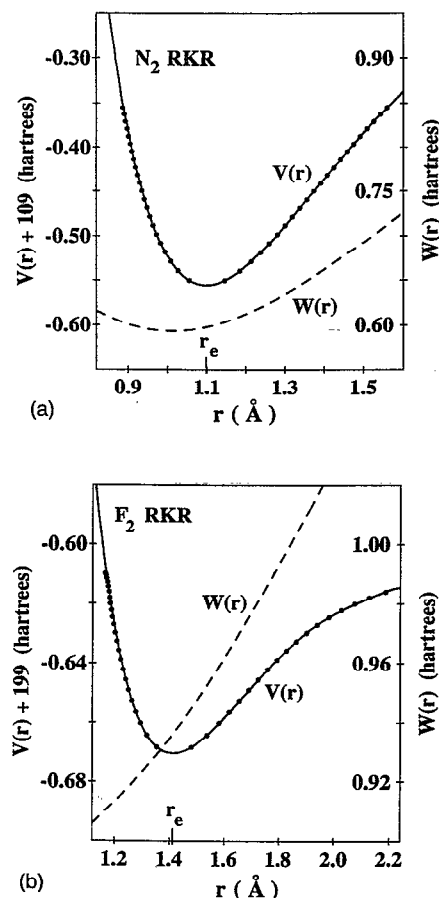


FIG. 2. Plots of the fitted RKR potential curves and the difference function  $W(r) \equiv V_{\text{RHF}}(r) - V_{\text{RKR}}(r)$  for (a)  $\text{N}_2$  and (b)  $\text{F}_2$ .

analyses. The final DZP RHF parameters for  $\text{N}_2$  and  $\text{F}_2$  are also given in Table I along with their RKR counterparts. Prior to the fit, the values of the  $A$ ,  $B$ ,  $r_0$ ,  $z_0$ , and  $z_1$  constants listed in Table I were selected to amend the  $V(r)$  functional form to describe the RHF potential curves. Analytic third-derivative techniques<sup>32–35</sup> were then used to precisely determine the DZP RHF quintic force fields of  $\text{N}_2$  and  $\text{F}_2$  at the theoretical  $r_e$  distances via numerical differentiation, and these force constants were used to constrain the values of  $z_2$ – $z_5$ .<sup>36</sup> The validity of the  $V(r)$  representations was confirmed by tests of DZP RHF higher-order derivative predictions at representative points. For example, for  $\text{N}_2$  at  $r=0.92$  Å,  $V'''$ ,  $V''''$ , and  $V'''''$  are predicted by Eqs. (1) and (2) to be  $-511.9$  aJ Å<sup>-3</sup>,  $3048$  aJ Å<sup>-4</sup>, and  $-1.95 \times 10^4$  aJ Å<sup>-5</sup>, in order, as compared to  $-511.5$ ,  $3035$ , and  $-1.91 \times 10^4$  from direct evaluation by RHF analytic derivative methods. In addition, for  $\text{F}_2$  at  $r=1.55$  Å,  $V''' = -17.11$  aJ Å<sup>-3</sup>,  $V'''' = 95.10$  aJ Å<sup>-4</sup>, and  $V''''' = -474$  aJ Å<sup>-5</sup> are given by Eqs. (1) and (2) vs  $-17.10$ ,  $94.82$ , and  $-479$  by direct evaluation. This high level of agreement bolsters confidence in the analogous RKR derivative predictions, even though the accuracy of the RKR results is surely somewhat diminished by the uncertainty of the input data and the smaller number of reliable constraints.

Plots of the RKR potential curves as well as those of  $W(r)$ , defined as  $V_{\text{RHF}}(r) - V_{\text{RKR}}(r)$ , appear in Figs. 2(a) and 2(b) for  $\text{N}_2$  and  $\text{F}_2$ , respectively. In Figs. 3(a)–3(d) the first through fourth derivatives of the RKR functions for  $E_e(r)$  and  $V(r)$  are plotted, and in Figs. 4(a) and 4(b) the percent errors in the DZP RHF electronic energy derivatives for  $\text{N}_2$  and  $\text{F}_2$  are shown as functions of the internuclear distance. Finally, numerical comparisons of RKR and DZP RHF derivatives of  $E_e(r)$  and  $V(r)$  are presented at both the theoretical and experimental  $r_e$  bond distances in Tables II and III, wherein the aforementioned  $PZ(3d2f1g)$  CCSD(T) predictions are also given for reference.

There are several salient points which are elucidated by the analysis of the  $\text{N}_2$  and  $\text{F}_2$  potential energy curves:

(1) Because the total energy is a sum of two parts, viz., the electronic energy and the nuclear–nuclear repulsion energy ( $V_N$ ), all derivatives of  $V(r)$  are comprised of two sizeable terms, which happen to be opposite in sign. The data in Tables II and III clearly exemplify this generalization. The theoretical prediction of force constants is thus seen to be a rather unbalanced procedure vis-à-vis cancellation of errors, because the  $V_N$  contribution and its derivatives are obtained exactly while the  $E_e$  term and its derivatives are determined only approximately. A delicate balance of the two terms of opposite sign may thus arise, in which case the associated force constant predictions depend strongly on the level of theory.

(2) The  $E_e$  and  $V_N$  contributions to the quadratic force constants nearly cancel each other, but for the higher-order force constants the contributions of the derivatives of  $V_N$  become increasingly dominant. Note from the data in Tables II and III that for  $\text{N}_2$  at the experimental geometry,  $E_e'/V_N' = -1.00$ ,  $E_e''/V_N'' = -0.87$ ,  $E_e'''/V_N''' = -0.63$ , and  $E_e''''/V_N'''' = -0.38$ , whereas in the  $\text{F}_2$  case these ratios are  $-1.00$ ,  $-0.96$ ,  $-0.87$ , and  $-0.74$ , respectively. Inspection of the plots in Figs. 3(a)–3(d) reveals that this behavior is not restricted to the experimental bond distance alone. In particular, the  $V(r)$  derivative curves shift away from the  $r$  axis as the order of the derivative is increased, indicating a relative aggrandizement of the  $V_N$  contributions. It can thus be inferred that higher-order bond stretching derivatives depend strongly on core–core nuclear repulsions and that the cancellation of the  $E_e$  and  $V_N$  derivative terms decreases substantially in higher order. This conclusion is in accord with the original data reported by Schwendeman,<sup>18(a)</sup> who listed the ratios of electronic to nuclear-repulsion contributions to quadratic, cubic, and quartic force constants of 13 diatomic molecules. In related work, Schwendeman<sup>18(b)</sup> also argued that the cancellation of  $E_e''$  and  $V_N''$  terms can be interpreted as causing the error in RHF theoretical bond lengths to be pseudo-first-order rather than second order, as would have been expected otherwise.

(3) By all accounts the accuracy of the DZP RHF predictions for the electronic energy derivatives of both  $\text{N}_2$  and  $\text{F}_2$  is remarkable on a percentage basis; however, the theoretical

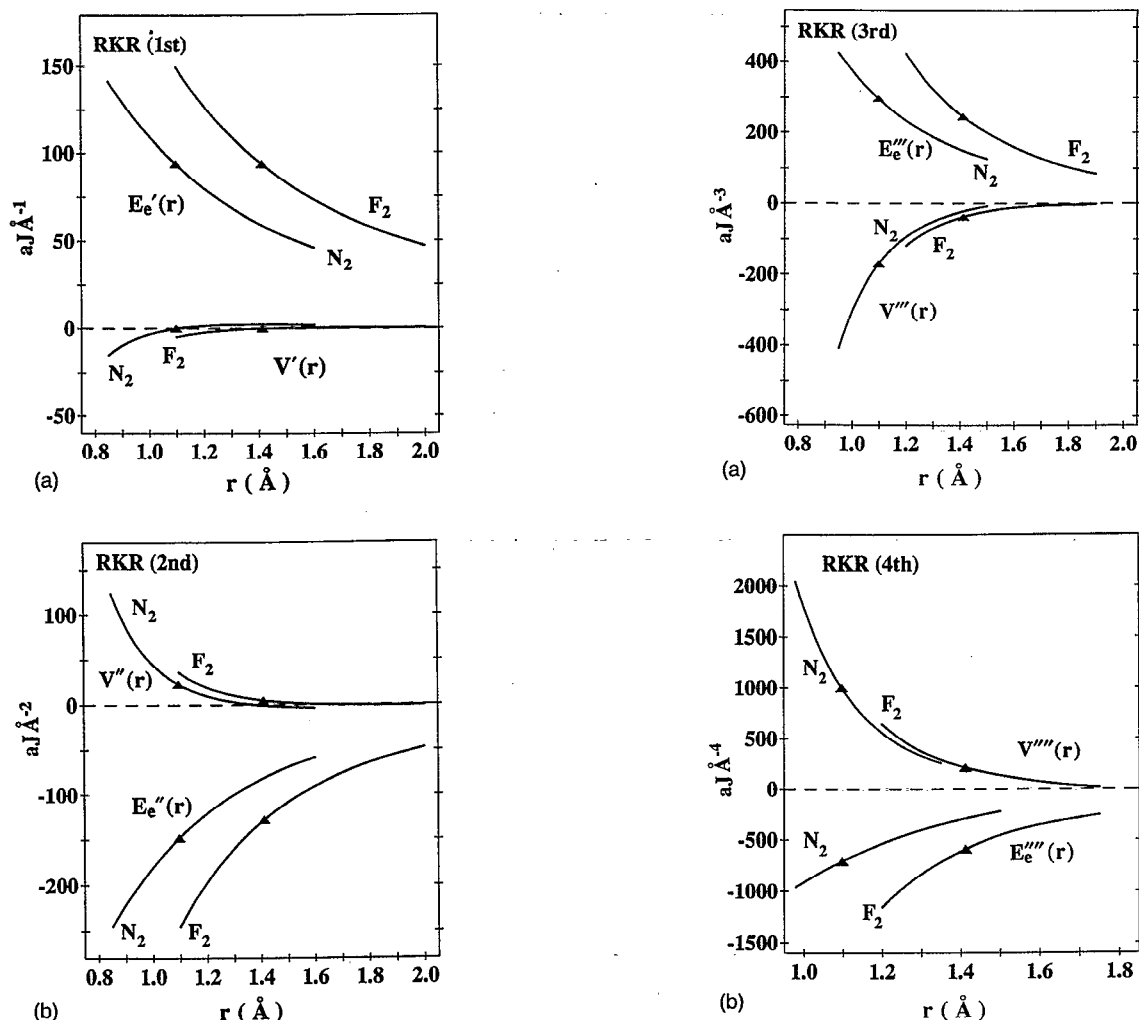


FIG. 3. RKR derivative functions for N<sub>2</sub> and F<sub>2</sub>: (a) first, (b) second, (c) third, and (d) fourth.

predictions for the second derivatives of  $V(r)$  are much less accurate than those of  $E_e(r)$ , a disparity which becomes smaller for higher-order derivatives. As shown in Figs. 4(a) and 4(b), the errors in the DZP RHF derivatives of  $E_e(r)$  through fourth order are well under 10% for both N<sub>2</sub> and F<sub>2</sub> over bond-length intervals of 0.5 Å or greater encompassing  $r_e$ . Because the errors in  $E_e''$ ,  $E_e'''$ , and  $E_e''''$  are comparable, the fact that the  $V'''$  predictions are much poorer than the  $V''''$  and  $V''''''$  results is a direct consequence of the aforementioned cancellation of nuclear repulsion and electronic energy terms. Note as a specific example that the theoretical  $E_e''$  value for N<sub>2</sub> is in error by only 3.0% at the experimental  $r_e$  distance, but the corresponding discrepancy for  $V'''$  is 19.4% (see Table II); in contrast,  $E_e''''$  and  $V''''''$  for N<sub>2</sub> are predicted to comparable accuracies of 5.6 and 3.9%, respectively. These observations are consistent with those of Pulay, Meyer, and Boggs,<sup>37</sup> who have reported correlation contributions of less than 1% to the cubic and quartic constants of several diatomic hydrides. It seems clear that the  $E_e(r)$  function and its derivatives and not the corresponding  $V(r)$  curves should be considered the best measure of theoretical performance.

(4) While correlation effects are most prominent in deter-

mining the first derivatives of  $V(r)$  and consequently optimum bond lengths, it should not be construed from this fact that the correlation contribution to  $E_e'$  is in a relative sense greater than the analogous contributions to the higher derivatives. Because RHF potential curves typically dissociate to products which are erroneously high in energy, the correlation energy usually becomes much larger as bond distances are elongated. Moreover, uncorrelated optimum bond lengths are usually too short (at least for molecules involving first-row atoms) and correlation contributions to higher-order derivatives are generally small on a percentage basis. As a result, the conventional view<sup>1,38</sup> on this issue has been that the correlation energy can be well approximated as a linear function of  $r$  with positive slope for intermediate bond distances near  $r_e$ . Exceptions do exist, however; Michalska *et al.*<sup>38</sup> showed that for LiH and Li<sub>2</sub> the optimum bond lengths predicted at the 6-311G\*\* RHF level of theory are longer than the experimental values and the correlation energy is actually a decreasing function of  $r$  near the equilibrium distance. In the particular cases of N<sub>2</sub> and F<sub>2</sub>, the first derivative of the correlation energy,  $W'(r)$ ,<sup>39</sup> is clearly positive near  $r_e$ , as seen in Figs. 2(a) and 2(b), and the curvature of  $W(r)$  is much smaller than that of  $V(r)$ . The linear approximation is

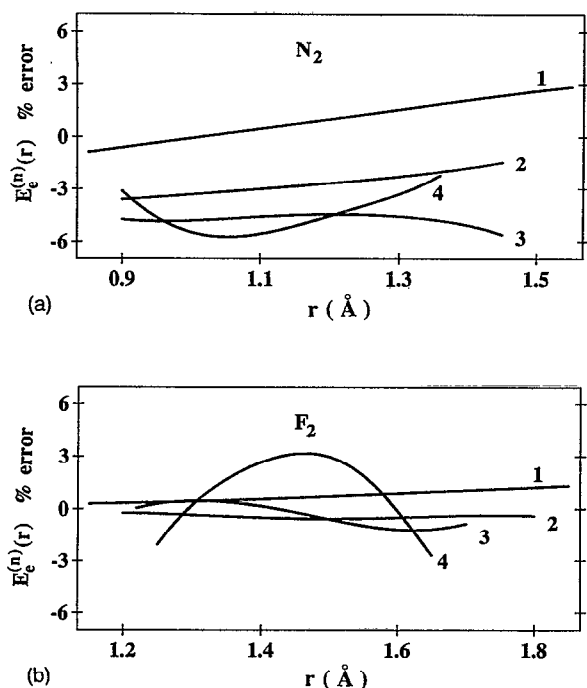


FIG. 4. Percent error curves for the DZP RHF electronic energy derivatives of (a)  $N_2$  and (b)  $F_2$  as referenced to the analogous RKR functions. The experimental data do not determine the RKR third and fourth derivatives to better than 1%; hence, some of the structure in the percent error curves at third and fourth order may be artifactual.

particularly good for bond distances greater than 1.2 Å in these molecules, even though for smaller distances  $W'''(r)$  cannot be neglected, as highlighted by the fact that  $W(r)$  for  $N_2$  actually goes through a minimum near  $r=1.0$  Å. This conclusion notwithstanding, the plots in Fig. 4 reveal that in the case of  $F_2$  the percentage errors in the DZP RHF values for  $E'_e$  are comparable to those for  $E''_e$ ,  $E'''_e$ , and  $E''''_e$  over a wide range of bond distances and in the  $N_2$  example are actually much smaller. Thus, at the RHF level

the  $E'_e$  predictions are *not* inherently less accurate on a percentage basis than their higher-order analogs, but rather the cancellation of the  $V_N$  and  $E_e$  derivative terms causes the absolute error in  $E'_e$  to be of greater significance in the determination of the total energy derivative than in higher-order cases.

(5) If theoretical derivatives of the total energy are compared to experimental values at the same geometry, despite cancellation problems in the  $V_N$  and  $E_e$  terms, RHF theory is quite successful in predicting force constants. Note in Table III that for  $F_2$  the "pure" theoretical quadratic force constant of  $8.82 \text{ aJ } \text{Å}^{-2}$  is 87% larger than the empirical value of  $4.70 \text{ aJ } \text{Å}^{-2}$ , but the error comes almost exclusively from the drastically different reference geometries on which the force constants are based. A direct comparison at the experimental  $r_e$  structure reveals a much smaller error of 14.1%, and at the theoretical  $r_e$  distance the disparity is only 7.3%. The agreement for  $V''''$  and  $V'''''$  is even better, provided once again that a direct comparison of quantities at the same geometry is made. For example, at the experimental  $r_e$  structure, the DZP RHF cubic force constant for  $F_2$  ( $-36.18 \text{ aJ } \text{Å}^{-3}$ ) differs from the experimental value ( $-36.39 \text{ aJ } \text{Å}^{-3}$ ) by only 0.6%. Because  $F_2$  is recognized as a pathological case for computational quantum chemistry,<sup>40</sup> it is remarkable that the errors in the second, third, and fourth derivatives of  $E_e(r)$  are considerably smaller for  $F_2$  than for  $N_2$  [cf. Figs. 4(a) and 4(b)]! This comparison serves to emphasize that the choice of reference geometry is critical in the *ab initio* prediction of high-order force constants.

From the analysis of the RKR and DZP RHF potential energy curves of  $N_2$  and  $F_2$ , it is clear that there are merits to the selection of nonstationary reference geometries in force field predictions. However, this approach in-

TABLE II. A comparison of DZP RHF theoretical and RKR experimental data for the electronic ( $E_e$ ) and total ( $V$ ) energies of  $N_2$  and their geometric derivatives through fourth order.<sup>a</sup>

	At $r_e(\text{DZP RHF})=1.082\ 707\ \text{Å}$			At $r_e(\text{expt})^b=1.097\ 685\ \text{Å}$			PZ(3d2f1g) CCSD(T) <sup>c</sup>
	DZP RHF	RKR	% error	DZP RHF	RKR	% error	
$E_e(N_2)$	-132.907 896	-133.503 919	-0.45	-132.580 357	-133.177 747	-0.45	-133.029 426
$E'_e$	96.437	96.074	0.38	94.255	93.823	0.46	93.766
$E''_e$	-147.88	-152.54	-3.1	-143.55	-148.01	-3.0	-147.63
$E'''_e$	294.1	308.4	-4.6	283.9	297.6	-4.6	296.7
$E''''_e$	-692.1	-733.8	-5.7	-665.5	-704.9	-5.6	-697.5
$V(N_2)$	-108.958 964	-109.554 988	-0.54	-108.958 210	-109.555 600	-0.55	-109.407 271
$V'$	0.00	-0.3632	...	0.4315	0.00	...	-0.0556
$V''$	30.26	25.60	18.2	27.40	22.94	19.4	23.31
$V'''$	-199.5	-185.2	7.7	-183.3	-169.6	8.1	-170.5
$V''''$	1131.4	1089.8	3.8	1037.0	997.6	3.9	1005.0

<sup>a</sup>The DZP RHF and RKR results were extracted from the potential-energy functions detailed in Table I. All energies are given in hartree, whereas all derivatives correspond to energies measured in aJ and distances in Å. The percent errors are given as  $100(\text{RHF}/\text{RKR}-1)$ .

<sup>b</sup>Reference 23.

<sup>c</sup>Highly correlated theoretical predictions. See Sec. IV for details.

TABLE III. A comparison of DZP RHF theoretical and RKR experimental data for the electronic ( $E_e$ ) and total ( $V$ ) energies of  $F_2$  and their geometric derivatives through fourth order.<sup>a</sup>

	At $r_e(\text{DZP RHF})=1.334\,980\text{ \AA}$			At $r_e(\text{expt})=1.411\,930\text{ \AA}$			PZ(3d2,1g) CCSD(T)
	DZP RHF	RKR	% error	DZP RHF	RKR	% error	
$E_e(F_2)$	-230.847 255	-231.773 494	-0.40	-229.092 257	-230.027 524	-0.41	-229.724 951
$E_e'$	104.859	104.371	0.47	94.277	93.741	0.57	93.735
$E_e''$	-148.28	-148.98	-0.5	-127.42	-128.08	-0.5	-128.00
$E_e'''$	298.1	296.8	0.4	245.9	245.7	0.08	247.1
$E_e''''$	-755.4	-745.8	1.3	-604.6	-588.0	2.8	-622.5
$V(F_2)$	-198.739 402	-199.665 641	-0.46	-198.734 278	-199.669 545	-0.47	-199.366 961
$V'$	0.00	-0.4873	...	0.5365	0.00	...	-0.0044
$V''$	8.818	8.217	7.3	5.365	4.703	14.1	4.778
$V'''$	-54.95	-56.24	-2.3	-36.18	-36.39	-0.6	-34.99
$V''''$	302.3	311.9	-3.1	194.7	211.3	-7.9	176.8

<sup>a</sup>See footnotes a-c of Table II.

roduces new problems in *ab initio* determinations of force constants, which is the subject of the remainder of this article.

## II. REVIEW: SELECTION OF REFERENCE GEOMETRY

In theoretical predictions of molecular force fields appearing in the literature, various choices have been implemented for the reference geometric structure: (a) the optimum geometry at the level of theory used in the force constant evaluation, (b) an experimental  $r_e$ ,  $r_0$ ,  $r_s$ ,  $r_z$ ,  $r_\omega$ ,  $r_g$ ,  $r_m$ , or  $r_\alpha$  structure,<sup>41</sup> (c) an optimum geometry from a higher level of theory, or (d) an empirically corrected theoretical geometry. Additional possibilities are prescribed, standard geometries<sup>42</sup> or empirically corrected experimental geometries, e.g., an experimental  $r_s$  structure to which corrections have been added to better approximate  $r_e$  parameters.<sup>43</sup> While option (a) is preferred conceptually and is the most common choice by far, there are several bond types known for which moderate levels of theory, even ones including extensive treatments of electron correlation, yield optimum geometric parameters containing substantial errors. In these cases the corresponding force constant predictions are deteriorated merely as a consequence of deficient reference geometries, as exemplified by the case of  $F_2$  above. Such considerations led to the recommendation of choice (b) in the early work of Schwendeman,<sup>18</sup> but for many polyatomic molecules of interest, precise experimental geometries are simply not available. An additional complication apparent from the analysis in Sec. I is that sizeable variations in predicted bond stretching force constants can arise even from the small differences between empirical  $r_e$  parameters and various vibrationally averaged analogs, thus hindering systematic comparisons of force fields based on phenomenologically different reference structures.

The selection of the reference geometry according to option (c) or (d) generally improves the accuracy of the theoretical force field without establishing a dependence on experimental structure determinations for the particular compound under investigation. A notable example of the efficacy of option (c) is contained in the analysis of vibra-

tional anharmonicity in the HOF and  $F_2O$  molecules by Thiel *et al.*,<sup>13</sup> in which RHF cubic force constants determined at CCSD optimum geometries were found to be in remarkable agreement with their CCSD counterparts. The viability of option (d) was established in the 1970s by Blom and Altona<sup>8</sup> and Pulay and co-workers.<sup>9,10,44</sup> In this approach, which is predicated on the occurrence of systematic errors in theoretical structural predictions, empirical offset values for specific bond types are appended to optimized internal coordinates obtained at a standard level of theory in order to approximate true  $r_e$  structures. Standard offset values at both self-consistent-field (SCF) and correlated levels of theory have been proposed on the basis of several quantum chemical investigations,<sup>9,45-52</sup> the most extensive list being constructed for SCF studies with the 4-21G basis set.<sup>9,10,45-47</sup> In more recent applications, Pulay and co-workers<sup>53</sup> have modified the original procedure by employing standard offset forces for specific bond types rather than shifts in the structural parameters themselves. Naturally, the use of option (d) may be ill-advised for unusually bonded chemical systems.

In effect, shifting the reference geometry from a local minimum to a nonstationary point is equivalent<sup>2,13</sup> to modifying the original theoretical surface  $V(\mathbf{s})$  to

$$V^{\text{shift}}(\mathbf{s}, \mathcal{R}) = V(\mathbf{s}) - \mathbf{g}^{\text{shift}} \cdot (\mathcal{R} - \mathcal{R}^{\text{shift}}), \quad (3)$$

where  $\mathcal{R}$  denotes a complete set of internal coordinates perhaps distinct from  $\mathbf{s}$ ,  $\mathcal{R}^{\text{shift}}$  is comprised of the values of these coordinates at the shifted reference geometry, and  $\mathbf{g}^{\text{shift}}$  is the corresponding gradient vector at  $\mathcal{R}^{\text{shift}}$  given by the particular level of theory. Since this procedure can be accomplished with any complete and nonredundant set of internal coordinates, the shifted surface is not uniquely defined, and for this reason an implicit dependence of  $V^{\text{shift}}$  on  $\mathcal{R}$  is indicated in Eq. (3). This dependence is elucidated when the various choices of the shift term are expanded in Cartesian coordinates, leading to identical first-order terms in the Cartesian space but different higher-order terms. For example, in the  $N_2$  and  $F_2$  cases discussed above, each DZP RHF potential curve could be modified to have a minimum

at the experimental  $r_e$  distance by adding a shift term which is linear in any one of the geometrical coordinates mentioned in Sec. I, namely  $r$ ,  $\rho=(r-r_e)/r$ , or  $\xi=\exp(\rho)-1$ . Each choice would give rise to different quadratic, cubic, and quartic force constants with respect to  $r$  because  $\rho$  and  $\xi$  are nonlinear functions of the bond distance. Although this problem is not widely appreciated, it has been recognized previously by Pulay<sup>1,2</sup> as it pertains to quadratic force constants; however, no attempt has been made to study it systematically, to show the analogous effect on higher-order force constants, or to ascertain quantitatively the magnitude of the problem. Thus, the purpose of the present paper is to provide a thorough analysis of the selection of nonstationary reference geometries in theoretical determinations of higher-order force constants by investigating both the analytical foundations of the procedure and numerical results for representative molecules.

### III. THEORETICAL FOUNDATIONS

#### A. Geometric derivative relations

The basis for analytical considerations of the shifted molecular potential energy surface in Eq. (3) is the dependence of the associated internal coordinate sets on the Cartesian coordinates of the nuclear centers. Let  $\{\zeta_\alpha; \alpha=1,2,\dots,3N\}$  represent a complete and nonredundant set of curvilinear displacement variables defined with respect to an arbitrary reference configuration of an  $N$ -atom molecule,<sup>54-57</sup> including both the set of internal displacement coordinates  $\{s_p; p=1,2,\dots,M\}$  and the external displacement variables  $\{\tau_\eta; \eta=1,2,\dots,L\}$ . For nonlinear and linear molecules,  $(L,M)=(6,3N-6)$  and  $(5,3N-5)$ , respectively. The space of generalized external variables is generated by the mapping  $\tau_\eta(\mathbf{x})=\tau_\eta^\circ(\mathbf{q})$ , where  $\tau_\eta^\circ(\mathbf{x})$  represents a canonical set of translational and rotational coordinates which are orthogonal to the internal variables at the reference configuration, and  $\mathbf{q}=\mathbf{u}\mathbf{x}$  denotes a set of rectilinear coordinates resulting from an arbitrary linear transformation ( $\mathbf{u}$ ) of rank  $3N$  of the Cartesian variables  $\mathbf{x}$ . To maintain consistency in the following analysis, the indices utilized to enumerate the various types of coordinates are  $\{p,q\}$ , internal;  $\{\eta,\omega\}$ , external;  $\{i,j,\sigma\}$ , Cartesian; and  $\{\alpha,\beta,\gamma,\delta,\epsilon\}$ , general.

The displacement coordinates  $\zeta_\alpha$  can be represented by an expansion in the set of rectilinear Cartesian displacement variables  $\{x_i\}$  according to

$$\zeta_\alpha = \sum_{i_1}^{3N} B_{i_1}^\alpha x_{i_1} + \frac{1}{2} \sum_{i_1 i_2}^{3N} B_{i_1 i_2}^\alpha x_{i_1} x_{i_2} + \frac{1}{6} \sum_{i_1 i_2 i_3}^{3N} B_{i_1 i_2 i_3}^\alpha x_{i_1} x_{i_2} x_{i_3} + \frac{1}{24} \sum_{i_1 i_2 i_3 i_4}^{3N} B_{i_1 i_2 i_3 i_4}^\alpha x_{i_1} x_{i_2} x_{i_3} x_{i_4} + \dots \quad (4)$$

where the various  $B_{i_1 i_2 \dots i_n}^\alpha$  coefficients for the internal and external spaces are defined by

$$B_{i_1 i_2 \dots i_n}^\alpha \equiv \left( \frac{\partial^n s_p}{\partial x_{i_1} \partial x_{i_2} \dots \partial x_{i_n}} \right) \quad (5)$$

and

$$B_{i_1 i_2 \dots i_n}^\eta \equiv \left( \frac{\partial^n \tau_\eta}{\partial x_{i_1} \partial x_{i_2} \dots \partial x_{i_n}} \right), \quad (6)$$

both sets of geometric derivatives being evaluated at the reference configuration. A complementary expansion can be developed for  $x_i$  in terms of the set  $\{\zeta_\alpha\}$ :

$$x_i = \sum_{\alpha}^{3N} A_{\alpha}^i \zeta_{\alpha} + \frac{1}{2} \sum_{\alpha\beta}^{3N} A_{\alpha\beta}^i \zeta_{\alpha} \zeta_{\beta} + \frac{1}{6} \sum_{\alpha\beta\gamma}^{3N} A_{\alpha\beta\gamma}^i \zeta_{\alpha} \zeta_{\beta} \zeta_{\gamma} + \frac{1}{24} \sum_{\alpha\beta\gamma\delta}^{3N} A_{\alpha\beta\gamma\delta}^i \zeta_{\alpha} \zeta_{\beta} \zeta_{\gamma} \zeta_{\delta} + \dots \quad (7)$$

Substitution of Eq. (7) into Eq. (4) yields the first-order condition

$$\sum_i^{3N} B_i^\alpha A_{\beta}^i = \delta_{\alpha\beta}, \quad (8)$$

in which  $B_i^\alpha$  can be partitioned by defining  $(\mathbf{B}_1)_{pi} = B_i^p$  and  $(\mathbf{B}_2)_{\eta i} = B_i^\eta$  for the internal and external spaces, respectively. The quantities  $(\mathbf{B}_1)_{pi}$  are elements of the familiar  $\mathbf{B}$  matrix of Eliashevich and Wilson,<sup>54,55</sup> for which simple formulas are known for all commonly used sets of internal coordinates. The matrix formulation of Eq. (8) is

$$\begin{bmatrix} \mathbf{B}_1 \\ \mathbf{B}_2 \end{bmatrix} \begin{bmatrix} \mathbf{A}_1 & \mathbf{A}_2 \end{bmatrix} = \begin{bmatrix} \mathbf{B}_1 \mathbf{A}_1 & \mathbf{B}_1 \mathbf{A}_2 \\ \mathbf{B}_2 \mathbf{A}_1 & \mathbf{B}_2 \mathbf{A}_2 \end{bmatrix} = \begin{bmatrix} \mathbf{I}_M & \mathbf{0} \\ \mathbf{0} & \mathbf{I}_L \end{bmatrix}, \quad (9)$$

where  $(\mathbf{A}_1)_{ip} \equiv A_p^i$  and  $(\mathbf{A}_2)_{i\eta} \equiv A_\eta^i$  refer to internal and external partitions of the inverse  $\mathbf{B}$  matrix, and  $\mathbf{I}_M$  and  $\mathbf{I}_L$  are  $M$ - and  $L$ -dimensional identity matrices, respectively. For canonical sets of external variables  $\tau_\eta^\circ(\mathbf{x})$ , the elements of  $\mathbf{B}_2^\circ \mathbf{B}_1^T$  are identically equal to zero, i.e., the first-order orthogonality relation

$$\sum_{i_1}^{3N} B_{i_1}^{\circ,\eta} B_{i_1}^p = 0 \quad (10)$$

holds at the reference configuration (see Appendix A). For the space of generalized external variables  $\tau_\eta(\mathbf{x})$ ,  $\mathbf{B}_2 = \mathbf{B}_2^\circ \mathbf{u}^{-1}$ , and hence the associated orthogonality condition is

$$(\mathbf{B}_2 \mathbf{u} \mathbf{B}_1^T) = \mathbf{0}. \quad (11)$$

As a consequence of Eq. (11), the composite  $\mathbf{A}$  matrix in Eq. (9) can be constructed from the expressions

$$\mathbf{A}_1 = \mathbf{u} \mathbf{B}_1^T (\mathbf{B}_1 \mathbf{u} \mathbf{B}_1^T)^{-1} \quad (12)$$

and

$$\mathbf{A}_2 = \mathbf{u}^T \mathbf{B}_2^T (\mathbf{B}_2 \mathbf{u}^T \mathbf{B}_2^T)^{-1}. \quad (13)$$

These partitions also yield the left inverse of  $\mathbf{B}$ . Specifically, after defining

$$\mathbf{Y} \equiv \mathbf{A} \mathbf{B} = \begin{bmatrix} \mathbf{A}_1 & \mathbf{A}_2 \end{bmatrix} \begin{bmatrix} \mathbf{B}_1 \\ \mathbf{B}_2 \end{bmatrix} = \mathbf{A}_1 \mathbf{B}_1 + \mathbf{A}_2 \mathbf{B}_2, \quad (14)$$

the following system of equations arises after successive projections on  $\mathbf{Y}$  with  $\mathbf{B}_1$  and  $\mathbf{B}_2$ :

$$\begin{bmatrix} \mathbf{B}_1 \\ \mathbf{B}_2 \end{bmatrix} \mathbf{Y} = \begin{bmatrix} \mathbf{B}_1 \\ \mathbf{B}_2 \end{bmatrix}. \quad (15)$$

If the set of internal and external variables is complete and nonredundant, then the partitioned **B** matrix in Eq. (15) has a unique inverse, and **Y** is thus equivalent to the  $3N \times 3N$  identity matrix  $I_{3N}$ .

The standard body-fixed axis system employed in the separation of molecular vibration and rotation is determined by the Sayvetz conditions,<sup>56,58,59</sup> which can be invoked by using external variables for which **u** is a diagonal matrix containing triads of the reciprocal atomic masses.<sup>1,9,60</sup> This choice is necessitated in applications involving the transformation of tensor quantities from Cartesian to internal coordinate representations, as in transformations of dipole-moment or polarizability derivatives. However, in analogous transformations of scalar molecular properties, such as potential energy derivatives, the choice of the body-fixed system is not restricted. In these cases it is desirable to select a canonical set of external variables such that **u** in Eqs. (12) and (13) is the identity matrix in order to simplify the mathematical transformations of concern.

The analogs of Eq. (8) through fourth order arising from the reciprocity of Eqs. (4) and (7) are

$$\sum_{i_1}^{3N} B_{i_1}^\alpha A_{\beta\gamma}^{i_1} + \sum_{i_1 i_2}^{3N} B_{i_1 i_2}^\alpha A_{\beta\gamma}^{i_1 i_2} = 0, \tag{16}$$

$$\begin{aligned} \sum_{i_1}^{3N} B_{i_1}^\alpha A_{\beta\gamma\delta}^{i_1} + \sum_{i_1 i_2}^{3N} B_{i_1 i_2}^\alpha A^{i_1 i_2} \{\beta\gamma, \delta\} \\ + \sum_{i_1 i_2 i_3}^{3N} B_{i_1 i_2 i_3}^\alpha A_{\beta\gamma}^{i_1 i_2} A_{\delta}^{i_3} = 0, \end{aligned} \tag{17}$$

and

$$\begin{aligned} \sum_{i_1}^{3N} B_{i_1}^\alpha A_{\beta\gamma\delta\epsilon}^{i_1} + \sum_{i_1 i_2}^{3N} B_{i_1 i_2}^\alpha A^{i_1 i_2} \{\beta\gamma\delta, \epsilon\} + \sum_{i_1 i_2}^{3N} B_{i_1 i_2}^\alpha A^{i_1 i_2} \{\beta\gamma, \delta\epsilon\} \\ + \sum_{i_1 i_2 i_3}^{3N} B_{i_1 i_2 i_3}^\alpha A^{i_1 i_2 i_3} \{\beta\gamma, \delta, \epsilon\} \\ + \sum_{i_1 i_2 i_3 i_4}^{3N} B_{i_1 i_2 i_3 i_4}^\alpha A_{\beta\gamma}^{i_1 i_2} A_{\delta}^{i_3} A_{\epsilon}^{i_4} = 0, \end{aligned} \tag{18}$$

which are applicable regardless of whether the indices  $\alpha, \beta, \gamma, \delta,$  and  $\epsilon$  represent internal or external variables. In Eqs. (17) and (18), the following general notation has been introduced:

$$\begin{aligned} X^{\alpha_1 \alpha_2 \dots \alpha_n} \{\beta_1 \gamma_1 \dots, \beta_2 \gamma_2 \dots, \dots, \beta_n \gamma_n \dots\} \\ \equiv \sum_{\mathcal{J}'} X^{\alpha_1 \alpha_2 \dots \alpha_n} [\mathcal{C}_{\mathcal{J}'}(\beta_1 \gamma_1 \dots, \beta_2 \gamma_2 \dots, \dots, \beta_n \gamma_n \dots)], \end{aligned} \tag{19}$$

where  $X$  is an arbitrary quantity,  $\mathcal{J}'$  enumerates all unique combinations  $\mathcal{C}_{\mathcal{J}'}$  of a given composite list of indices, and

$$\begin{aligned} X^{\alpha_1 \alpha_2 \dots \alpha_n} \{\beta_1 \gamma_1 \dots, \beta_2 \gamma_2 \dots, \dots, \beta_n \gamma_n \dots\} \\ \equiv X_{\beta_1 \gamma_1 \dots}^{\alpha_1} X_{\beta_2 \gamma_2 \dots}^{\alpha_2} \dots X_{\beta_n \gamma_n \dots}^{\alpha_n}. \end{aligned} \tag{20}$$

For example, in Eq. (17)

TABLE IV. Number of terms represented by the brace notation<sup>a</sup> for the quantities  $A^{i_1 i_2 \dots i_n}, B^{p_1 p_2 \dots p_n}, C^{q_1 q_2 \dots q_n},$  and  $W^{q_1 q_2 \dots q_n}.$

$A^{i_1 i_2 \dots i_n}, B^{p_1 p_2 \dots p_n},$ and $C^{q_1 q_2 \dots q_n}$	
$\{\beta_1, \beta_2\}$	1
$\{\beta_1 \beta_2 \beta_3\}$	1
$\{\beta_1 \beta_2, \beta_3\}$	3
$\{\beta_1, \beta_2, \beta_3\}$	1
$\{\beta_1 \beta_2 \beta_3 \beta_4\}$	1
$\{\beta_1 \beta_2 \beta_3, \beta_4\}$	4
$\{\beta_1 \beta_2, \beta_3 \beta_4\}$	3
$\{\beta_1 \beta_2, \beta_3, \beta_4\}$	6
$\{\beta_1, \beta_2, \beta_3, \beta_4\}$	1
$\{\beta_1 \beta_2 \beta_3 \beta_4 \beta_5\}$	1
$\{\beta_1 \beta_2 \beta_3 \beta_4, \beta_5\}$	5
$\{\beta_1 \beta_2 \beta_3, \beta_4 \beta_5\}$	10
$\{\beta_1 \beta_2 \beta_3, \beta_4, \beta_5\}$	10
$\{\beta_1 \beta_2, \beta_3 \beta_4, \beta_5\}$	15
$\{\beta_1 \beta_2, \beta_3, \beta_4, \beta_5\}$	10
$\{\beta_1, \beta_2, \beta_3, \beta_4, \beta_5\}$	1
$\{\beta_1 \beta_2 \beta_3 \beta_4 \beta_5 \beta_6\}$	1
$\{\beta_1 \beta_2 \beta_3 \beta_4 \beta_5, \beta_6\}$	6
$\{\beta_1 \beta_2 \beta_3 \beta_4, \beta_5 \beta_6\}$	15
$\{\beta_1 \beta_2 \beta_3, \beta_4 \beta_5 \beta_6\}$	20
$\{\beta_1 \beta_2 \beta_3 \beta_4, \beta_5, \beta_6\}$	15
$\{\beta_1 \beta_2 \beta_3, \beta_4 \beta_5, \beta_6\}$	60
$\{\beta_1 \beta_2 \beta_3, \beta_4, \beta_5, \beta_6\}$	20
$\{\beta_1 \beta_2, \beta_3 \beta_4, \beta_5, \beta_6\}$	90
$\{\beta_1 \beta_2, \beta_3, \beta_4, \beta_5, \beta_6\}$	15
$\{\beta_1, \beta_2, \beta_3, \beta_4, \beta_5, \beta_6\}$	1
$W^{q_1}$	
$\{p_1, p_2 p_3\}$	3
$\{p_1, p_2 p_3 p_4\}$	4
$\{p_1 p_2, p_3 p_4\}$	6
$\{p_1, p_2 p_3 p_4 p_5\}$	5
$\{p_1 p_2, p_3 p_4 p_5\}$	10
$\{p_1 p_2 p_3, p_4 p_5\}$	10
$\{p_1, p_2 p_3 p_4 p_5 p_6\}$	6
$\{p_1 p_2, p_3 p_4 p_5 p_6\}$	15
$\{p_1 p_2 p_3, p_4 p_5 p_6\}$	20
$\{p_1 p_2 p_3 p_4, p_5 p_6\}$	15
$W^{q_1 q_2}$	
$\{p_1, p_2 p_3, p_4 p_5\}$	15
$\{p_1, p_2 p_3 p_4, p_5 p_6\}$	60
$\{p_1 p_2, p_3 p_4, p_5 p_6\}$	45

<sup>a</sup>The number of unique combinations of indices arising in the notation of Eq. (19) is given. The index  $\beta_n$  represents either a Cartesian-coordinate index  $i_n$  or an internal-coordinate index  $p_n$ . Because the superscripts in Eq. (19) can be interchanged in the equations of the text, permutations of the indices in the table are not unique. Moreover, reordering of the index partitions does not give distinct contributions in the  $A^{i_1 i_2 \dots i_n}, B^{p_1 p_2 \dots p_n},$  and  $C^{q_1 q_2 \dots q_n}$  cases but does so for the  $W^{q_1 q_2 \dots q_n}$  terms. Thus, the number of terms for  $W^{q_1} \{p_1 p_2, p_3 p_4\}$  is twice that for  $A^{i_1 i_2} \{p_1 p_2, p_3 p_4\},$  for example.

$$\begin{aligned} A^{i_1 i_2} \{\beta\gamma, \delta\} &\equiv A^{i_1 i_2} [\beta\gamma, \delta] + A^{i_1 i_2} [\beta\delta, \gamma] + A^{i_1 i_2} [\gamma\delta, \beta] \\ &\equiv A_{\beta\gamma}^{i_1} A_{\delta}^{i_2} + A_{\beta\delta}^{i_1} A_{\gamma}^{i_2} + A_{\gamma\delta}^{i_1} A_{\beta}^{i_2}. \end{aligned} \tag{21}$$

The notation summarized in Eqs. (19) and (20) is also used in numerous expressions involving  $B_{i_1 i_2 \dots i_n}^\alpha$  derivatives given below; in each case the number of terms represented by the braces in Eq. (19) is listed in Table IV.

Expressions for the higher-order internal-coordinate derivatives  $B_{i_1 i_2}^p$ ,  $B_{i_1 i_2 i_3}^p$ , and  $B_{i_1 i_2 i_3 i_4}^p$  can be derived via direct, albeit tedious, differentiation of the basic functional forms for the various types of internal coordinates in common usage, specifically, bond distances, Simons–Parr–Finlan variables, valence bond angles, linear-bending coordinates, out-of-plane bending angles, and dihedral torsional angles.<sup>61–64</sup> All of the corresponding equations have been derived independently in this study and coded in the program INTDER,<sup>65</sup> many of these expressions have been tabulated elsewhere.<sup>56,62,63,66–69</sup>

The  $A_{\alpha\beta}^i$ ,  $A_{\alpha\beta\gamma}^i$  and  $A_{\alpha\beta\gamma\delta}^i$  quantities in Eq. (7) are generally not amenable to direct evaluation, but these higher-order expansion coefficients may be determined indirectly from the complementary  $B_{i_1 i_2 \dots i_n}^p$  derivatives using Eqs. (16)–(18). In manipulations involving these equations, it is useful to define the following notation:

$$C_{\beta_1 \beta_2 \dots \beta_n}^\alpha \equiv \sum_{i_1 i_2 \dots i_n}^{3N} B_{i_1 i_2 \dots i_n}^\alpha A_{\beta_1}^{i_1} A_{\beta_2}^{i_2} \dots A_{\beta_n}^{i_n}. \quad (22)$$

Subsequently, Eq. (16) can be written in matrix form as

$$\begin{bmatrix} \mathbf{B}_1 \\ \mathbf{B}_2 \end{bmatrix} \mathbf{A}_{\beta\gamma} = - \begin{bmatrix} \mathbf{c}_1^{\beta\gamma} \\ \mathbf{c}_2^{\beta\gamma} \end{bmatrix}, \quad (23)$$

where the vector components  $(\mathbf{A}_{\beta\gamma})_\sigma$ ,  $(\mathbf{c}_1^{\beta\gamma})_p$  and  $(\mathbf{c}_2^{\beta\gamma})_\eta$  are equated with the elements  $A_{\beta\gamma}^\sigma$ ,  $C_{\beta\gamma}^p$  and  $C_{\beta\gamma}^\eta$  respectively. By inverting Eq. (23) using Eqs. (12) and (13), it is found that

$$\mathbf{A}_{\beta\gamma} = -\mathbf{A}_1 \mathbf{c}_1^{\beta\gamma} - \mathbf{A}_2 \mathbf{c}_2^{\beta\gamma}, \quad (24)$$

or in expanded, component form

$$A_{\beta\gamma}^\sigma = - \sum_{i_1 i_2}^{3N} A_{\beta}^{i_1} A_{\gamma}^{i_2} (F_{\sigma i_1 i_2} + G_{\sigma i_1 i_2}), \quad (25)$$

where

$$F_{\sigma i_1 i_2 \dots i_n} \equiv \sum_p^M A_p^\sigma B_{i_1 i_2 \dots i_n}^p \quad (26)$$

and

$$G_{\sigma i_1 i_2 \dots i_n} \equiv \sum_\eta^L A_\eta^\sigma B_{i_1 i_2 \dots i_n}^\eta. \quad (27)$$

In an analogous fashion, Eq. (17) can be inverted to yield

$$A_{\beta\gamma\delta}^\sigma = - \sum_p^M A_p^\sigma \left( C_{\beta\gamma\delta}^p + \sum_{i_1 i_2}^{3N} B_{i_1 i_2}^p A^{i_1 i_2} \{\beta\gamma, \delta\} \right) - \sum_\eta^L A_\eta^\sigma \left( C_{\beta\gamma\delta}^\eta + \sum_{i_1 i_2}^{3N} B_{i_1 i_2}^\eta A^{i_1 i_2} \{\beta\gamma, \delta\} \right), \quad (28)$$

which upon rearrangement gives

$$A_{\beta\gamma\delta}^\sigma = - \sum_{i_1 i_2}^{3N} (A_{\beta}^{i_1} A_{\gamma}^{i_2} + A_{\gamma}^{i_1} A_{\beta}^{i_2} + A_{\delta}^{i_1} A_{\beta\gamma}^{i_2}) (F_{\sigma i_1 i_2} + G_{\sigma i_1 i_2}) - \sum_{i_1 i_2 i_3}^{3N} A_{\beta}^{i_1} A_{\gamma}^{i_2} A_{\delta}^{i_3} (F_{\sigma i_1 i_2 i_3} + G_{\sigma i_1 i_2 i_3}) \quad (29)$$

if the explicit form of  $A^{i_1 i_2} \{\beta\gamma, \delta\}$  is employed. In brief, after determination of the elements  $A_{\beta\gamma}^\sigma$  via Eq. (25), the higher-order coefficients  $A_{\beta\gamma\delta}^\sigma$  can be evaluated from Eq. (29) by explicitly inverting only the first-order  $\mathbf{B}$  matrix. This approach illustrates the general, sequential procedure by which  $A_{\beta_1 \beta_2 \dots \beta_n}^\sigma$  coefficients can be efficaciously determined from lower-order counterparts and  $B_{i_1 i_2 \dots i_n}^\alpha$  derivatives.

## B. Force constant transformations between internal and Cartesian spaces

The marked curvilinearity of the internal coordinates of a molecular system causes the general transformation of potential energy derivatives between internal and Cartesian spaces to be decidedly nonlinear, a consequence which is paramount to the analysis of Eq. (3). To facilitate the specification of the resulting transformation equations, superscripts and subscripts are used to denote internal- and Cartesian-coordinate derivatives, respectively. For example,  $V_i$  refers to the  $i$ th component of the Cartesian gradient, and  $V^{p_1 p_2 p_3}$  corresponds to the cubic force constant involving internal coordinates  $p_1$ ,  $p_2$ , and  $p_3$ . Because the molecular potential energy surface does not depend on the external variables of the system, the components of the Cartesian gradient can be determined via a linear transformation of the internal forces alone:

$$V_i = \sum_p^M V^p \left( \frac{\partial S_p}{\partial x_i} \right) = \sum_p^M V^p (\mathbf{B}_1)_{pi}. \quad (30)$$

The inversion of this first-order expression using Eq. (8) yields

$$V^p = \sum_i^{3N} V_i (\mathbf{A}_1)_{ip}, \quad (31)$$

in which  $V^p$  is invariant to the choice of  $\mathbf{u}$  in Eq. (12).<sup>70</sup> By direct differentiation of Eq. (30), the following expression is found for the quadratic force constant matrix in Cartesian coordinates:

$$V_{i_1 i_2} = \sum_{p_1}^M V^{p_1} \left( \frac{\partial^2 S_{p_1}}{\partial x_{i_1} \partial x_{i_2}} \right) + \sum_{p_1 p_2}^M V^{p_1 p_2} B_{i_1}^{p_1} B_{i_2}^{p_2} = \sum_{p_1}^M V^{p_1} B_{i_1 i_2}^{p_1} + \sum_{p_1 p_2}^M V^{p_1 p_2} B_{i_1}^{p_1} B_{i_2}^{p_2}. \quad (32)$$

Upon multiplication of Eq. (32) by the product  $A_{q_1}^{i_1} A_{q_2}^{i_2}$  and summation over  $i_1$  and  $i_2$ , the constant  $V^{q_1 q_2}$  is isolated on the right-hand side, and after rearrangement and reindexing an expression for the quadratic force constant matrix in internal coordinates is obtained, viz.,

$$V^{p_1 p_2} = \sum_{i_1 i_2}^{3N} V_{i_1 i_2} A_{p_1}^{i_1} A_{p_2}^{i_2} - \sum_q^M V^q C_{p_1 p_2}^q. \quad (33)$$

The primary significance of Eqs. (32) and (33) is that the Cartesian and internal quadratic force constant matrices cannot be interconverted by a linear transformation alone because  $B_{i_1 i_2}^{p_1}$  and hence  $C_{p_1 p_2}^q$  are generally nonzero for

curvilinear internal coordinates. However, if the forces at the reference geometry are zero, as in case (a) of Sec. II, the transformation in fact becomes linear, as pointed out by Pulay.<sup>2</sup>

An expression for the cubic force constant matrix in Cartesian coordinates arises by direct differentiation of Eq. (32). Specifically,

$$V_{i_1 i_2 i_3} = \sum_{p_1}^M V^{p_1} B^{p_1} \{i_1 i_2 i_3\} + \sum_{p_1 p_2}^M V^{p_1 p_2} B^{p_1 p_2} \{i_1 i_2, i_3\} + \sum_{p_1 p_2 p_3}^M V^{p_1 p_2 p_3} B^{p_1 p_2 p_3} \{i_1, i_2, i_3\}, \quad (34)$$

where the brace notation of Eq. (19) has been invoked (see Table IV). Manipulations analogous to those leading to Eq. (33) provide an equation for the internal-coordinate third derivatives:

$$V^{p_1 p_2 p_3} = \sum_{i_1 i_2 i_3}^{3N} V_{i_1 i_2 i_3} A^{i_1 i_2 i_3} \{p_1, p_2, p_3\} - \sum_q^M W^q \{p_1, p_2, p_3\} - \sum_q^M V^q C_{p_1 p_2 p_3}^q, \quad (35)$$

in which the brace notation in the second term refers to the quantity

$$W^{\alpha_1 \alpha_2 \dots \alpha_n} [\beta_0 \gamma_0 \dots, \beta_1 \gamma_1 \dots, \beta_2 \gamma_2 \dots, \dots, \beta_n \gamma_n \dots] \equiv V^{\alpha_1 \alpha_2 \dots \alpha_n} \beta_0 \gamma_0 \dots C_{\beta_1 \gamma_1 \dots}^{\alpha_1} C_{\beta_2 \gamma_2 \dots}^{\alpha_2} \dots C_{\beta_n \gamma_n \dots}^{\alpha_n}. \quad (36)$$

As shown by Eqs. (34) and (35), a direct linear transformation between the Cartesian and internal cubic force constant matrices is never valid, even if the *ab initio* force field is determined at a stationary point and all the  $V^q$  derivatives are zero.

The analogous fourth-order transformation equations are

$$V_{i_1 i_2 i_3 i_4} = \sum_{p_1}^M V^{p_1} B^{p_1} \{i_1 i_2 i_3 i_4\} + \sum_{p_1 p_2}^M V^{p_1 p_2} [B^{p_1 p_2} \{i_1 i_2 i_3, i_4\} + B^{p_1 p_2} \{i_1 i_2, i_3 i_4\}]$$

$$V_{i_1 i_2 \dots i_n} = \sum_{K=1}^n \left[ \sum_{p_1 p_2 \dots p_K}^M V^{p_1 p_2 \dots p_K} \sum_{\mathcal{V}=1}^{\mathcal{L}_a(K,n)} B^{p_1 p_2 \dots p_K} \{ \mathcal{P}_{a, \mathcal{V}}^{(K,n)}(i_1 i_2 \dots i_n) \} \right] \quad (39)$$

and

$$V^{p_1 p_2 \dots p_n} = \sum_{i_1 i_2 \dots i_n}^{3N} V_{i_1 i_2 \dots i_n} A^{i_1 i_2 \dots i_n} \{p_1, p_2, \dots, p_n\} - \sum_{q_1}^M V^{q_1} C_{p_1 p_2 \dots p_n}^{q_1} - \sum_{K=2}^{n-1} \left[ \sum_{q_1 q_2 \dots q_K}^M \sum_{\mathcal{V}=1}^{\mathcal{L}_b(K,n)} V^{q_1 q_2 \dots q_K} C_{\mathcal{V}}^{(K,n)} \{ \mathcal{P}_{b, \mathcal{V}}^{(K,n)}(p_1 p_2 \dots p_n) \} \right] + \sum_{q_1 q_2 \dots q_{K-1}}^M \sum_{\mathcal{V}=1}^{\mathcal{L}_c(K,n)} W^{q_1 q_2 \dots q_{K-1}} \{ \mathcal{P}_{c, \mathcal{V}}^{(K,n)}(p_1 p_2 \dots p_n) \}. \quad (40)$$

$$+ \sum_{p_1 p_2 p_3}^M V^{p_1 p_2 p_3} B^{p_1 p_2 p_3} \{i_1 i_2, i_3, i_4\} + \sum_{p_1 p_2 p_3 p_4}^M V^{p_1 p_2 p_3 p_4} B^{p_1 p_2 p_3 p_4} \{i_1, i_2, i_3, i_4\} \quad (37)$$

and

$$V^{p_1 p_2 p_3 p_4} = \sum_{i_1 i_2 i_3 i_4}^{3N} V_{i_1 i_2 i_3 i_4} A^{i_1 i_2 i_3 i_4} \{p_1, p_2, p_3, p_4\} - \sum_{q_1}^M [W^{q_1} \{p_1, p_2, p_3, p_4\} + W^{q_1} \{p_1 p_2, p_3 p_4\}] - \sum_{q_1 q_2}^M V^{q_1 q_2} C^{q_1 q_2} \{p_1 p_2, p_3 p_4\} - \sum_{q_1}^M V^{q_1} C_{p_1 p_2 p_3 p_4}^{q_1}. \quad (38)$$

Thus, to determine Cartesian derivatives through fourth order from internal-coordinate force constants, Eqs. (30), (32), (34), and (37) are utilized directly. In contrast, to determine quartic force fields in internal coordinates from Cartesian derivatives, Eqs. (31), (33), (35), and (38) are applied in succession, at each step using the lower-order results given by the previous transformation. Note that by sequential forward and backward transformations through intermediate Cartesian representations, Eqs. (30)–(38) facilitate general nonlinear transformations of molecular force fields between different internal coordinate sets.

As illustrated above, the general procedure for generating the set of  $n$ th-order transformation equations begins with the direct differentiation of the  $(n-1)$ th-order Cartesian derivative expression, thus allowing  $V_{i_1 i_2 \dots i_n}$  to be evaluated from the internal-coordinate derivatives  $\{V^{p_1 p_2 \dots p_K}; K = 1, 2, \dots, n\}$ . By multiplying the result by  $A_{q_1}^{i_1} A_{q_2}^{i_2} \dots A_{q_n}^{i_n}$  and summing over  $i_1, i_2, \dots, i_n$ , a relationship between particular  $V^{q_1 q_2 \dots q_n}$  constants and the set  $\{V_{i_1 i_2 \dots i_n}\}$  is found which involves the lower-order derivatives  $\{V^{p_1 p_2 \dots p_K}; K = 1, 2, \dots, n-1\}$ . Rearrangement and reindexing yields the final form for the internal derivatives  $V^{p_1 p_2 \dots p_n}$ . With the aid of several new definitions, the general transformation equations can be written in the following abstract form:

TABLE V. Number of partitions [ $\mathcal{L}_a(K,n)$ ,  $\mathcal{L}_b(K,n)$ ,  $\mathcal{L}_c(K,n)$ ] in the sums of Eqs. (39) and (40) for quintic through octic transformations.

$n \setminus K$	2	3	4	5	6	7
5	(2,1,3)	(2,0,1)	(1,0,0)	...	...	...
6	(3,2,4)	(3,1,2)	(2,0,0)	(1,0,0)	...	...
7	(3,2,5)	(4,1,4)	(3,0,1)	(2,0,0)	(1,0,0)	...
8	(4,3,6)	(4,1,6)	(5,1,2)	(3,0,0)	(2,0,0)	(1,0,0)

The related operators  $\mathcal{P}_{\gamma}^{(K,n)}$  for  $\gamma = a, b$ , and  $c$  partition lists of  $n$  elements into  $K$  segments under the restriction that the initial lexical ordering is maintained. In symbolic form

$$\mathcal{P}_{\gamma}^{(K,n)}(\alpha_1 \alpha_2 \dots \alpha_n) = (\alpha_1 \alpha_2 \dots \alpha_{j_1} \alpha_{j_1+1} \alpha_{j_1+2} \dots \alpha_{j_2} \dots \alpha_{j_{K-2}+1} \alpha_{j_{K-2}+2} \dots \alpha_{j_{K-1}} \alpha_{j_{K-1}+1} \dots \alpha_{j_K}), \tag{41}$$

where the upper segment boundaries are indexed as  $(j_1, j_2, j_3, \dots, j_{K-1}, j_K)$ , the corresponding segment lengths are  $(l_1, l_2 = j_2 - j_1, l_3 = j_3 - j_2, \dots, l_n = j_K - j_{K-1})$ , and  $j_K = n$ . The particular partitions included in each summation over  $\mathcal{N}$  are governed by sets of rules which apply for the different cases  $\gamma = a, b$ , and  $c$ . If  $\gamma = a$ , then  $\mathcal{N}$  enumerates all partition operators for which the segment lengths sequentially decrease, i.e.,  $l_1 \geq l_2 \geq \dots \geq l_n$ . The operators included for  $\gamma = b$  are the same as those for  $\gamma = a$  except that all instances in which a segment length of 1 appears are excluded. For  $\gamma = c$ , the segment-length rules are  $l_2 \geq l_3 \geq \dots \geq l_n$  and  $l_i \neq 1$  for  $i \geq 2$ ;  $l_1$  is unrestricted. In Table V the number of partitions in each sum,  $\mathcal{L}_\gamma(K,n)$ , is given for  $n = 5, 6, 7, 8$  and  $K = 2, 3, \dots, n - 1$ .

Because the *ab initio* determination of complete sextic force fields is becoming increasingly realistic,<sup>71</sup> it is worthwhile to report the explicit forms of the sextic transformation equations as illustrative applications of Eqs. (39) and (40). Specifically,

$$\begin{aligned} V_{i_1 i_2 i_3 i_4 i_5 i_6} = & \sum_{P_1}^M V^{P_1} B^{P_1} \{i_1 i_2 i_3 i_4 i_5 i_6\} + \sum_{P_1 P_2}^M V^{P_1 P_2} [B^{P_1 P_2} \{i_1 i_2 i_3 i_4 i_5 i_6\} + B^{P_1 P_2} \{i_1 i_2 i_3 i_4 i_5 i_6\} + B^{P_1 P_2} \{i_1 i_2 i_3 i_4 i_5 i_6\}] \\ & + \sum_{P_1 P_2 P_3}^M V^{P_1 P_2 P_3} [B^{P_1 P_2 P_3} \{i_1 i_2 i_3 i_4 i_5 i_6\} + B^{P_1 P_2 P_3} \{i_1 i_2 i_3 i_4 i_5 i_6\} + B^{P_1 P_2 P_3} \{i_1 i_2 i_3 i_4 i_5 i_6\}] \\ & + \sum_{P_1 P_2 P_3 P_4}^M V^{P_1 P_2 P_3 P_4} [B^{P_1 P_2 P_3 P_4} \{i_1 i_2 i_3 i_4 i_5 i_6\} + B^{P_1 P_2 P_3 P_4} \{i_1 i_2 i_3 i_4 i_5 i_6\}] \\ & + \sum_{P_1 P_2 P_3 P_4 P_5}^M V^{P_1 P_2 P_3 P_4 P_5} B^{P_1 P_2 P_3 P_4 P_5} \{i_1 i_2 i_3 i_4 i_5 i_6\} + \sum_{P_1 P_2 P_3 P_4 P_5 P_6}^M V^{P_1 P_2 P_3 P_4 P_5 P_6} B^{P_1 P_2 P_3 P_4 P_5 P_6} \{i_1 i_2 i_3 i_4 i_5 i_6\} \end{aligned} \tag{42}$$

and

$$\begin{aligned} V^{P_1 P_2 P_3 P_4 P_5 P_6} = & \sum_{i_1 i_2 i_3 i_4 i_5 i_6}^{3N} V_{i_1 i_2 i_3 i_4 i_5 i_6} A^{i_1 i_2 i_3 i_4 i_5 i_6} \{p_1, p_2, p_3, p_4, p_5, p_6\} - \sum_{q_1}^M V^{q_1} C^{q_1}_{P_1 P_2 P_3 P_4 P_5 P_6} - \sum_{q_1 q_2}^M V^{q_1 q_2} [C^{q_1 q_2} \{p_1 p_2 p_3 p_4 p_5 p_6\} \\ & + C^{q_1 q_2} \{p_1 p_2 p_3 p_4 p_5 p_6\}] - \sum_{q_1 q_2 q_3}^M V^{q_1 q_2 q_3} C^{q_1 q_2 q_3} \{p_1 p_2 p_3 p_4 p_5 p_6\} - \sum_{q_1}^M [W^{q_1} \{p_1, p_2, p_3, p_4, p_5, p_6\} \\ & + W^{q_1} \{p_1 p_2 p_3 p_4 p_5 p_6\} + W^{q_1} \{p_1 p_2 p_3 p_4 p_5 p_6\} + W^{q_1} \{p_1 p_2 p_3 p_4 p_5 p_6\}] \\ & - \sum_{q_1 q_2}^M [W^{q_1 q_2} \{p_1, p_2, p_3, p_4, p_5, p_6\} + W^{q_1 q_2} \{p_1 p_2 p_3 p_4 p_5 p_6\}], \end{aligned} \tag{43}$$

in which the nonvanishing terms arising as the index  $K$  in Eqs. (39) and (40) increases are listed in order. The clearly discernible structure of Eqs. (42) and (43) belies the complexity therein; for example, the  $W^{q_1 q_2} \{p_1, p_2, p_3, p_4, p_5, p_6\}$  contribution alone involves a total of 60 distinct terms. Indeed, the plethora of individual terms in the sextic transformation equations is a hindrance to their practical implementation.

### C. Selection of shift coordinates

The key principle embodied in the nonlinear transformation equations of the preceding section is that the nonvanishing internal gradients which arise when an *ab initio* force field is computed at a nonstationary reference geometry in fact contribute to all higher-order derivatives in alternate Cartesian- and internal-coordinate representa-

tions. Consequently, an improper choice of shift coordinates in Eq. (3) can engender anomalous higher-order force constants in a given representation, thus warranting considerations of the analytical underpinnings of the selection of the shift coordinates.

The choice of Cartesian coordinates for the shift term in Eq. (3) leads to spurious characteristics of the shifted surface. Consider the expansion

$$\begin{aligned} V(\mathbf{x}) = & V_0 + \sum_{i_1}^{3N} V_{i_1} x_{i_1} + \frac{1}{2} \sum_{i_1 i_2}^{3N} V_{i_1 i_2} x_{i_1} x_{i_2} \\ & + \frac{1}{6} \sum_{i_1 i_2 i_3}^{3N} V_{i_1 i_2 i_3} x_{i_1} x_{i_2} x_{i_3} \\ & + \frac{1}{24} \sum_{i_1 i_2 i_3 i_4}^{3N} V_{i_1 i_2 i_3 i_4} x_{i_1} x_{i_2} x_{i_3} x_{i_4} + \dots \end{aligned} \quad (44)$$

While  $V(\mathbf{x})$  must remain unchanged upon an arbitrary rotation of the entire molecular system, the individual terms in Eq. (44) are *not* rotationally invariant on an order by order basis. Therefore, the application of the shift term using Cartesian coordinates, i.e., mere neglect of the linear term in Eq. (44), must be considered invalid because this shift term contains rotational dependence and thus the resulting shifted surface does also. One manifestation of this rotational dependence arises whenever the harmonic approximation is used to determine the vibrational normal modes of a molecule via diagonalization of the mass-weighted Cartesian Hessian at a nonstationary point. The eigenvalues for the rectilinear translational modes are rigorously zero, regardless of the choice of reference geometry.<sup>55,56</sup> However, the eigenvalues corresponding to curvilinear rotational motions are equal to zero only if the quadratic force field is computed at a stationary point, because the presence of any rotational variable which has the same symmetry as a vibrational coordinate will effect coupling of rotations to internal modes if nonzero forces exist. The resulting rotational "frequencies" may be as much as a few hundred  $\text{cm}^{-1}$  in magnitude, and if low-frequency vibrations are present in the molecule, the vibration-rotation mixing may be considerable. In the present context the existence of spurious rotational frequencies is attributed to the rotational dependence of the underlying shifted potential energy surface on which the vibrational analysis is formally based.

The most obvious procedure for circumventing the coupling of vibrations to rotations at a nonstationary point involves the transformation of the Cartesian derivatives to some set of internal coordinates according to Eqs. (31) and (33) followed by the utilization of the FG matrix method<sup>55</sup> to determine the vibrational frequencies and normal modes of the molecule in the internal space. In essence, this approach amounts to the application of the shift term in Eq. (3) using the working set of internal coordinates because the internal forces in this representation are completely neglected in solving the vibrational secular problem. Therefore, the final vibrational frequencies are not unique, as discussed in the Sec. II above. For example,

at the DZP RHF level of theory,<sup>20</sup> the predictions for the  $\omega_1(a_1)$ ,  $\omega_2(a_1)$ , and  $\omega_3(b_2)$  harmonic vibrational frequencies of ozone obtained at the experimental geometry<sup>72</sup> are 1221, 726, and 747  $\text{cm}^{-1}$ , respectively, if the two O-O bond distances and the O-O-O valence bond angle are used as the internal coordinates but 1282, 768, and 709  $\text{cm}^{-1}$  if the nonbonded O-O distance and the two nonvalence O-O-O angles are employed.

The effects of various shift terms are elucidated by appropriate expansions of the shifted potential energy surface. Consider the expansion of  $\mathcal{R}$  in Eq. (3) in terms of an intermediate set of Cartesian coordinates:

$$\begin{aligned} \mathcal{R}_p - \mathcal{R}_p^{\text{shift}} = & \sum_{i_1}^{3N} B_{i_1}^p x_{i_1} + \frac{1}{2} \sum_{i_1 i_2}^{3N} B_{i_1 i_2}^p x_{i_1} x_{i_2} \\ & + \frac{1}{6} \sum_{i_1 i_2 i_3}^{3N} B_{i_1 i_2 i_3}^p x_{i_1} x_{i_2} x_{i_3} + \dots \end{aligned} \quad (45)$$

By employing Eq. (45) in conjunction with Eq. (31), it is found that<sup>73</sup>

$$\begin{aligned} \sum_p^M V^p(\mathcal{R}_p - \mathcal{R}_p^{\text{shift}}) = & \sum_{i_1}^{3N} V_{i_1} x_{i_1} + \frac{1}{2} \sum_{i_1 i_2}^{3N} U_{i_1 i_2} x_{i_1} x_{i_2} \\ & + \frac{1}{6} \sum_{i_1 i_2 i_3}^{3N} U_{i_1 i_2 i_3} x_{i_1} x_{i_2} x_{i_3} + \dots, \end{aligned} \quad (46)$$

in which

$$U_{i_1 i_2 \dots i_n} = \mathbf{G}^T (\mathbf{B}_1 \mathbf{B}_1^T)^{-1} \mathbf{D}_{i_1 i_2 \dots i_n}. \quad (47)$$

In Eq. (47) the  $p$ th element of the  $M$ -dimensional vector  $\mathbf{D}_{i_1 i_2 \dots i_n}$  is simply  $B_{i_1 i_2 \dots i_n}^p$ , and the internal gradient vector  $\mathbf{G}$  is equal to  $\mathbf{B}_1 \mathbf{h}$ , where  $\mathbf{h}$  contains the Cartesian gradient of the potential energy function at the reference geometry. By subtracting Eq. (46) from Eq. (44) and transforming the resulting surface to a representation involving a general set of internal coordinates  $\{s_p\}$ , one obtains

$$\begin{aligned} V^{\text{shift}}(\mathbf{s}; \mathcal{R}) = & V_0 + \frac{1}{2} \sum_{p_1 p_2}^M \tilde{V}^{p_1 p_2} s_{p_1} s_{p_2} \\ & + \frac{1}{6} \sum_{p_1 p_2 p_3}^M \tilde{V}^{p_1 p_2 p_3} s_{p_1} s_{p_2} s_{p_3} + \dots, \end{aligned} \quad (48)$$

where the transformed force constants are given by

$$\begin{aligned} \tilde{V}^{p_1 p_2} = & \sum_{i_1 i_2}^{3N} (V_{i_1 i_2} - U_{i_1 i_2}) A^{i_1 i_2} \{p_1, p_2\}, \\ \tilde{V}^{p_1 p_2 p_3} = & \sum_{i_1 i_2 i_3}^{3N} (V_{i_1 i_2 i_3} - U_{i_1 i_2 i_3}) A^{i_1 i_2 i_3} \{p_1, p_2, p_3\} \\ & - \sum_q^M \tilde{W}^q \{p_1, p_2, p_3\}, \end{aligned} \quad (49)$$

and higher-order analogs arising from Eq. (40), assuming the quantity  $\tilde{W}^q$  is constructed according to Eq. (36) using the  $V^{p_1 p_2}$  coefficients. Therefore, the shift term in Eq. (3) is

seen to remove the first-order term from Eq. (48) for all choices of coordinate sets  $\{\mathcal{R}_p\}$  and  $\{s_p\}$ , but the higher-order terms in the expansion of  $V^{\text{shift}}$  in the set  $\{s_p\}$  are concomitantly dependent on the selection of  $\{\mathcal{R}_p\}$ .

It is apparent from Eqs. (47), (49), and (50) that the contribution of the shift term to the higher-order force constants in Eq. (48) may become anomalously large if one or more of the following conditions are met: (a) the Cartesian gradient  $\mathbf{h}$  is large in magnitude; (b) the internal coordinate set  $\{\mathcal{R}_p\}$  is highly curvilinear whence the  $\mathbf{D}_{i_1 i_2 \dots i_n}$  vectors are sizeable; and (c) the set  $\{\mathcal{R}_p\}$  is nearly redundant and  $\mathbf{B}_1 \mathbf{B}_1^T$  is almost singular. This last circumstance can be particularly insidious, and a diagnostic for the linear independence of the set of coordinates used to form the shift term in Eq. (3) is thus desirable. In this regard note that the  $U_{i_1 i_2 \dots i_n}$  quantities in Eq. (47) are invariant to scaling of the individual internal coordinates. To gauge the relative importance of the  $(\mathbf{B}_1 \mathbf{B}_1^T)^{-1}$  factor therein, it is useful to employ a set of normalized internal coordinates for which the diagonal elements of  $\mathbf{B}_1 \mathbf{B}_1^T$  are unity. The appearance of one or more small eigenvalues of the normalized  $\mathbf{B}_1 \mathbf{B}_1^T$  matrix indicates a near redundancy in the set  $\{\mathcal{R}_p\}$  and predicts anomalously large  $U_{i_1 i_2 \dots i_n}$  elements. In brief, it is not advisable to choose a set of shift internal coordinates which exhibits a singularity in  $\mathbf{B}_1 \mathbf{B}_1^T$  anywhere in the nuclear configuration space of concern. The set of standard internal coordinates for various molecular fragments recommended by Pulay *et al.*<sup>9,53</sup> is generally sufficient for the purpose of averting singularities. However, it is clearly desirable to develop procedures for the construction of rotationally invariant shifted potential energy surfaces without reference to any particular set of internal coordinates.

## D. Cartesian projection scheme

A formalism whereby rotationally invariant shifted potential energy surfaces are obtained by implementing a projection scheme directly in the Cartesian space would allow any implicit internal coordinate dependence of the associated force fields to be circumvented. Consider an arbitrary, collective displacement of the Cartesian variables of the system which engenders both internal coordinate displacements according to

$$s_p = \sum_{i_1}^{3N} B_{i_1}^p x_{i_1} + \frac{1}{2} \sum_{i_1 i_2}^{3N} B_{i_1 i_2}^p x_{i_1} x_{i_2} + \frac{1}{6} \sum_{i_1 i_2 i_3}^{3N} B_{i_1 i_2 i_3}^p x_{i_1} x_{i_2} x_{i_3} + \frac{1}{24} \sum_{i_1 i_2 i_3 i_4}^{3N} B_{i_1 i_2 i_3 i_4}^p x_{i_1} x_{i_2} x_{i_3} x_{i_4} + \dots \quad (51)$$

as well as changes in the translational and rotational variables  $\tau_\eta$ . The projection of the Cartesian displacement  $\mathbf{x}$  onto the internal space can be performed to all orders by neglecting the associated changes in the external variables and substituting the internal coordinate variations given by Eq. (51) into Eq. (7). The relationship between the projected displacement  $\mathbf{x}^*$  and its antecedent vector  $\mathbf{x}$  thus becomes

$$\mathbf{x}_\sigma^* = \sum_{i_1}^{3N} P_{\sigma i_1} x_{i_1} + \frac{1}{2} \sum_{i_1 i_2}^{3N} P_{\sigma i_1 i_2} x_{i_1} x_{i_2} + \frac{1}{6} \sum_{i_1 i_2 i_3}^{3N} P_{\sigma i_1 i_2 i_3} x_{i_1} x_{i_2} x_{i_3} + \frac{1}{24} \sum_{i_1 i_2 i_3 i_4}^{3N} P_{\sigma i_1 i_2 i_3 i_4} x_{i_1} x_{i_2} x_{i_3} x_{i_4} + \dots, \quad (52)$$

where

$$P_{\sigma i_1} = \sum_{p_1}^M A_{p_1}^\sigma B_{i_1}^{p_1}, \quad (53)$$

$$P_{\sigma i_1 i_2} = \sum_{p_1}^M A_{p_1}^\sigma B_{i_1 i_2}^{p_1} + \sum_{p_1 p_2}^M A_{p_1 p_2}^\sigma B^{p_1 p_2} \{i_1, i_2\}, \quad (54)$$

$$P_{\sigma i_1 i_2 i_3} = \sum_{p_1}^M A_{p_1}^\sigma B_{i_1 i_2 i_3}^{p_1} + \sum_{p_1 p_2}^M A_{p_1 p_2}^\sigma B^{p_1 p_2} \{i_1, i_2, i_3\} + \sum_{p_1 p_2 p_3}^M A_{p_1 p_2 p_3}^\sigma B^{p_1 p_2 p_3} \{i_1, i_2, i_3\}, \quad (55)$$

and

$$P_{\sigma i_1 i_2 i_3 i_4} = \sum_{p_1}^M A_{p_1}^\sigma B_{i_1 i_2 i_3 i_4}^{p_1} + \sum_{p_1 p_2}^M A_{p_1 p_2}^\sigma [B^{p_1 p_2} \{i_1, i_2, i_3, i_4\} + B^{p_1 p_2} \{i_1, i_2, i_3, i_4\}] + \sum_{p_1 p_2 p_3}^M A_{p_1 p_2 p_3}^\sigma B^{p_1 p_2 p_3} \{i_1, i_2, i_3, i_4\} + \sum_{p_1 p_2 p_3 p_4}^M A_{p_1 p_2 p_3 p_4}^\sigma B^{p_1 p_2 p_3 p_4} \{i_1, i_2, i_3, i_4\}. \quad (56)$$

Note that  $P_{\sigma i_1}$  is an element of the conventional first-order projection matrix onto the internal space,<sup>74,75</sup> i.e.,  $\mathbf{P} = \mathbf{A}_1 \mathbf{B}_1 = \mathbf{u} \mathbf{B}_1^T (\mathbf{B}_1 \mathbf{u} \mathbf{B}_1^T)^{-1} \mathbf{B}_1$ . The sums in Eqs. (53)–(56) run over the particular set of internal coordinates employed for the projection in Eq. (51); however, it is shown in Appendix A that  $P_{\sigma i_1}$  and its higher-order counterparts are independent of the chosen set  $\{s_p\}$  and can actually be computed without reference to internal coordinates.

A shift term in projected Cartesian coordinates can now be defined:

$$f(\mathbf{x}^*) \equiv \sum_{\sigma} V_{\sigma} x_{\sigma}^* = \sum_{i_1}^{3N} V_{i_1} x_{i_1} + \frac{1}{2} \sum_{i_1 i_2}^{3N} c_{i_1 i_2} x_{i_1} x_{i_2} + \frac{1}{6} \sum_{i_1 i_2 i_3}^{3N} c_{i_1 i_2 i_3} x_{i_1} x_{i_2} x_{i_3} + \frac{1}{24} \sum_{i_1 i_2 i_3 i_4}^{3N} c_{i_1 i_2 i_3 i_4} x_{i_1} x_{i_2} x_{i_3} x_{i_4} + \dots \quad (57)$$

in which the form of the linear term in  $\mathbf{x}$  is a consequence of the matrix relation  $\mathbf{B}_1 \mathbf{P} = \mathbf{B}_1$ , and the expansion coefficients are determined by

$$c_{i_1 i_2 \dots i_n} = \sum_{\sigma} V_{\sigma} P_{\sigma i_1 i_2 \dots i_n}. \quad (58)$$

The use of  $f(\mathbf{x}^*)$  as the shift term in Eq. (3) removes the dependence of  $V^{\text{shift}}$  on  $\mathcal{R}$  and effectively modifies the original Cartesian force constants to  $V_{i_1 i_2 \dots i_n}^* = V_{i_1 i_2 \dots i_n} - c_{i_1 i_2 \dots i_n}$ .

Alternate forms of Eq. (58) can be derived which make the  $c_{i_1 i_2 \dots i_n}$  quantities more facile to computation and more amenable to interpretation. In the particular case of  $c_{i_1 i_2}$ , substitution into Eq. (58) of  $V_\sigma$  from Eq. (30) and  $P_{\sigma i_1 i_2}$  from Eq. (54) yields

$$c_{i_1 i_2} = \sum_{p_1}^M V^{p_1} \left[ \sum_{p_2}^M \left( \sum_{\sigma}^{3N} B_{\sigma}^{p_1} A_{\sigma}^{p_2} \right) B_{i_1 i_2}^{p_2} + \sum_{p_2 p_3}^M \left( \sum_{\sigma}^{3N} B_{\sigma}^{p_1} A_{\sigma}^{p_2 p_3} \right) B_{i_1}^{p_2} B_{i_2}^{p_3} \right]. \quad (59)$$

The first term in parentheses can be reduced via Eq. (8), and the second term in parentheses can be replaced according to Eq. (16), thus giving

$$c_{i_1 i_2} = \sum_{p_1}^M V^{p_1} \left( B_{i_1 i_2}^{p_1} - \sum_{j_1 j_2}^{3N} B_{j_1 j_2}^{p_1} P_{j_1 i_1} P_{j_2 i_2} \right) \\ = \sum_{j_1 j_2}^{3N} (\delta_{j_1 i_1} \delta_{j_2 i_2} - P_{j_1 i_1} P_{j_2 i_2}) \left( \sum_{p_1}^M V^{p_1} B_{j_1 j_2}^{p_1} \right). \quad (60)$$

A final form for  $c_{i_1 i_2}$  is obtained by replacement of the last factor in parentheses in Eq. (60) using Eq. (32):

$$c_{i_1 i_2} = \sum_{j_1 j_2}^{3N} (\delta_{j_1 i_1} \delta_{j_2 i_2} - P_{j_1 i_1} P_{j_2 i_2}) \\ \times \left( V_{j_1 j_2} - \sum_{p_1 p_2}^M V^{p_1 p_2} B_{j_1}^{p_1} B_{j_2}^{p_2} \right) \\ = V_{i_1 i_2} - \sum_{j_1 j_2}^{3N} V_{j_1 j_2} P_{j_1 i_1} P_{j_2 i_2}. \quad (61)$$

Note therein that the terms involving  $V^{p_1 p_2}$  cancel once  $\mathbf{B}_1 \mathbf{P} = \mathbf{B}_1$  is employed as before. As a consequence of Eq. (61), the projected, quadratic Cartesian force constants resulting from the shift term  $f(\mathbf{x}^*)$  in Eq. (57) are given by

$$V_{i_1 i_2}^* \equiv V_{i_1 i_2} - c_{i_1 i_2} = \sum_{j_1 j_2}^{3N} V_{j_1 j_2} P_{j_1 i_1} P_{j_2 i_2}. \quad (62)$$

This projection formula has been utilized in previous studies<sup>74</sup> and arises directly from the fact that to first order  $\mathbf{x}^* = \mathbf{P}\mathbf{x}$ . The purpose for presenting the derivation of Eq. (62) here is to illustrate the formalism by which the projection formulas for Cartesian force constants of all orders are obtained.

The manipulations required to derive the third- and fourth-order analogs of Eq. (62) are tedious and thus are not detailed here. The first step ensuing from Eq. (58) involves the replacement of  $V_\sigma$ ,  $P_{\sigma i_1 i_2 i_3}$ , and  $P_{\sigma i_1 i_2 i_3 i_4}$  by the expressions in Eqs. (30), (55), and (56), respectively. In turn the first terms in Eqs. (55) and (56) give rise to factors involving the internal force ( $V^p$ ) contributions in Eq. (34) and (37), thus facilitating substitutions which ultimately allow all terms involving first derivatives to be eliminated. After extensive rearrangements all quantities involving internal coordinate derivatives can be cancelled to provide forms containing only higher-order Cartesian force constants. The final results for the projected cubic and quartic Cartesian force constants are

$$V_{i_1 i_2 i_3}^* \equiv V_{i_1 i_2 i_3} - c_{i_1 i_2 i_3} \\ = \sum_{j_1 j_2 j_3}^{3N} V_{j_1 j_2 j_3} P_{j_1 i_1} P_{j_2 i_2} P_{j_3 i_3} + \sum_{j_1 j_2}^{3N} V_{j_1 j_2} (P_{j_1 i_1} P_{j_2 i_2} P_{j_3 i_3} \\ + P_{j_1 i_2} P_{j_2 i_1} + P_{j_1 i_3} P_{j_2 i_2}) \quad (63)$$

and

$$V_{i_1 i_2 i_3 i_4}^* \equiv V_{i_1 i_2 i_3 i_4} - c_{i_1 i_2 i_3 i_4} \\ = \sum_{j_1 j_2 j_3 j_4}^{3N} V_{j_1 j_2 j_3 j_4} P_{j_1 i_1} P_{j_2 i_2} P_{j_3 i_3} P_{j_4 i_4} + \sum_{j_1 j_2 j_3}^{3N} V_{j_1 j_2 j_3} (P_{j_1 i_1} P_{j_2 i_2} P_{j_3 i_3} P_{j_4 i_4} \\ + P_{j_1 i_1} P_{j_2 i_3} P_{j_3 i_2} P_{j_4 i_4} + P_{j_1 i_1} P_{j_2 i_4} P_{j_3 i_2} P_{j_4 i_3} \\ + P_{j_1 i_2} P_{j_2 i_3} P_{j_3 i_4} + P_{j_1 i_2} P_{j_2 i_4} P_{j_3 i_3} \\ + P_{j_1 i_3} P_{j_2 i_2} P_{j_3 i_4} + P_{j_1 i_3} P_{j_2 i_4} P_{j_3 i_2} \\ + P_{j_1 i_4} P_{j_2 i_2} P_{j_3 i_3} \\ + P_{j_1 i_2} P_{j_2 i_3} P_{j_3 i_4} + P_{j_1 i_3} P_{j_2 i_2} P_{j_3 i_4} \\ + P_{j_1 i_4} P_{j_2 i_2} P_{j_3 i_3}). \quad (64)$$

In examining Eqs. (62)–(64), two salient features become apparent: (a) The projected Cartesian derivatives of order  $n$  can be determined by utilizing projection matrices only through order  $n-1$ . Thus, by reducing the various cases of Eq. (58) to Eqs. (62)–(64), the computation of the  $n$ th-order projection matrix is obviated in the determination of the projected  $n$ th-order force constant matrix. For example, Eq. (64) allows  $V_{i_1 i_2 i_3 i_4}^*$  to be determined by using  $P_{\sigma i_1}$ ,  $P_{\sigma i_2}$ , and  $P_{\sigma i_1 i_2}$  without  $P_{\sigma i_1 i_2 i_3 i_4}$ . (b) The leading contributions to the projected  $n$ th-order Cartesian derivatives merely arise from a linear transformation of the corresponding unprojected derivatives via the first-order projection matrix  $\mathbf{P}$ . However, to obtain the projected higher-order force fields properly, this linear transformation alone is not sufficient, as contributions involving lower-order force constants and higher-order projection matrices must be included.

Replacement of  $c_{i_1 i_2}$ ,  $c_{i_1 i_2 i_3}$ , and  $c_{i_1 i_2 i_3 i_4}$  in Eqs. (62)–(64) according to Eq. (58) provides translational and rotational invariance relationships among the Cartesian force constants of various orders:

$$V_{i_1 i_2} - \sum_{j_1 j_2}^{3N} V_{j_1 j_2} P_{j_1 i_1} P_{j_2 i_2} = \sum_{j_1}^{3N} V_{j_1} P_{j_1 i_1 i_2}, \quad (65)$$

$$V_{i_1 i_2 i_3} - \sum_{j_1 j_2 j_3}^{3N} V_{j_1 j_2 j_3} P_{j_1 i_1} P_{j_2 i_2} P_{j_3 i_3} = \sum_{j_1}^{3N} V_{j_1} P_{j_1 i_1 i_2 i_3} + \sum_{j_1 j_2}^{3N} V_{j_1 j_2} (P_{j_1 i_1} P_{j_2 i_2 i_3} + P_{j_1 i_2} P_{j_2 i_1 i_3} + P_{j_1 i_3} P_{j_2 i_1 i_2}), \quad (66)$$

and

$$\begin{aligned} V_{i_1 i_2 i_3 i_4} - \sum_{j_1 j_2 j_3 j_4}^{3N} V_{j_1 j_2 j_3 j_4} P_{j_1 i_1} P_{j_2 i_2} P_{j_3 i_3} P_{j_4 i_4} \\ = \sum_{j_1}^{3N} V_{j_1} P_{j_1 i_1 i_2 i_3 i_4} + \sum_{j_1 j_2}^{3N} V_{j_1 j_2} (P_{j_1 i_1} P_{j_2 i_2 i_3 i_4} + P_{j_1 i_2} P_{j_2 i_1 i_3 i_4} + P_{j_1 i_3} P_{j_2 i_1 i_2 i_4} + P_{j_1 i_4} P_{j_2 i_1 i_2 i_3} + P_{j_1 i_1 i_2} P_{j_2 i_3 i_4} + P_{j_1 i_1 i_3} P_{j_2 i_2 i_4} + P_{j_1 i_1 i_4} P_{j_2 i_2 i_3}) \\ + \sum_{j_1 j_2 j_3}^{3N} V_{j_1 j_2 j_3} (P_{j_1 i_1} P_{j_2 i_2} P_{j_3 i_3 i_4} + P_{j_1 i_1} P_{j_2 i_3} P_{j_3 i_2 i_4} + P_{j_1 i_1} P_{j_2 i_4} P_{j_3 i_2 i_3} + P_{j_1 i_2} P_{j_2 i_3} P_{j_3 i_1 i_4} + P_{j_1 i_2} P_{j_2 i_4} P_{j_3 i_1 i_3} + P_{j_1 i_3} P_{j_2 i_4} P_{j_3 i_1 i_2}). \quad (67) \end{aligned}$$

These results reveal that for every  $n$  greater than 1, a relationship exists between the Cartesian force constants of order  $n$  and all Cartesian lower-order derivatives of order 1 to  $n-1$ . The origin of these invariance relationships is elucidated if Eq. (7) is substituted into Eq. (44) and it is recognized that all terms involving each power of the external displacement coordinates  $\{\tau_\eta\}$  must sum to zero. Alternatively, by exploiting the equivalence of the expansion of  $V(\mathbf{x})$  in projected and unprojected Cartesian variables,

$$\begin{aligned} V(\mathbf{x}) &= \sum_{n=1}^{\infty} \frac{1}{n!} \sum_{i_1 i_2 \dots i_n} V_{i_1 i_2 \dots i_n} x_{i_1} x_{i_2} \dots x_{i_n} \\ &= \sum_{n=1}^{\infty} \frac{1}{n!} \sum_{i_1 i_2 \dots i_n} V_{i_1 i_2 \dots i_n} x_{i_1}^* x_{i_2}^* \dots x_{i_n}^*, \quad (68) \end{aligned}$$

these invariance conditions can be extracted using Eq. (52). It is noteworthy that Eq. (68) and the invariance conditions ensuing from it provide a straightforward approach to the regeneration of Eqs. (62)–(64) for the projected Cartesian force constants on the basis of Eq. (58). In Appendix D an outline is given of the relationship between Eqs. (65)–(67) and the translational and rotational invariance conditions utilized by others<sup>76</sup> for analytic derivative evaluations in electronic structure calculations.

#### IV. COMPUTATIONAL DETAILS

*Ab initio* results for the  $F_2$ ,  $N_2$ ,  $F_2O$ , and  $N_2O$  molecules are reported in various parts of this paper as representative numerical case studies of the determination of anharmonic molecular force fields at nonstationary reference geometries. The atomic-orbital basis sets employed for nitrogen, oxygen, and fluorine are denoted as DZP, TZ(2d1f), and PZ(3d2f1g). The double- $\zeta$  *sp* sets in the DZP basis for each atom were comprised of the (9s5p) Gaussian primitives of Huzinaga<sup>77</sup> as contracted to (4s2p)

by Dunning,<sup>78</sup> similarly, the *sp* functions of the TZ(2d1f) sets consisted of Huzinaga–Dunning (10s6p/5s3p) contractions.<sup>77,79</sup> In the “penta”- $\zeta$  PZ(3d2f1g) case the *sp* sets were constructed from (13s8p/8s5p) contractions of the primitives of Partridge<sup>80</sup> according to (6,1,1,1,1,1,1) and (4,1,1,1,1) schemes for the *s* and *p* functions, respectively. The polarization functions complementing the *sp* core of the DZP basis set involved single sets of *d*-type functions with the exponents  $\alpha_d(N)=0.80$ ,  $\alpha_d(O)=0.85$ , and  $\alpha_d(F)=1.00$ , which are representative optimal exponents for uncorrelated wave functions.<sup>81</sup> For the TZ(2d1f) and PZ(3d2f1g) basis sets, correlation-optimized polarization function exponents were employed, as given by Dunning.<sup>82</sup> The exponents for the 2d, 3d, 1f, 2f, and 1g sets are, in order: nitrogen, (0.469, 1.654), (0.335, 0.968, 2.837), 1.093, (0.685, 2.027), 1.427; oxygen, (0.645, 2.314), (0.444, 1.300, 3.775), 1.428, (0.859, 2.666), 1.846; and fluorine, (0.855, 3.107), (0.586, 1.725, 5.014), 1.917, (1.148, 3.562), 2.376. In the DZP basis the *d* sets contained six Cartesian components, while the polarization functions in the TZ(2d1f) and PZ(3d2f1g) basis sets consisted of real combinations of only the true spherical harmonics for  $l=2, 3$ , and 4.

Reference electronic wave functions were determined in this study by the single-configuration, self-consistent-field, restricted Hartree–Fock (RHF) method.<sup>3,83,84</sup> Dynamical electron correlation was accounted for by the coupled-cluster singles and doubles method (CCSD),<sup>85–90</sup> augmented in most cases by the addition of a perturbative contribution from connected triple excitations [CCSD(T)].<sup>91,92</sup> In all correlation treatments the 1s core orbitals were excluded from the active space. Likewise, the highest-lying 1s\* virtual orbital for each atom was frozen in the correlation procedures, all of these orbitals lying higher than 20 a.u. in the DZP and TZ(2d1f) computations and above 150 a.u. in the PZ(3d2f1g) determinations. The electronic structure computations reported here

were performed by various implementations of the program packages TITAN<sup>93</sup> and PSI.<sup>94</sup>

The evaluation of quartic force fields was facilitated by analytic gradient techniques for the CCSD(T) method<sup>95</sup> and by analytic derivative methods from first through third order for RHF wave functions.<sup>2,6,7,34,96-99</sup> All DZP RHF cubic and lower-order force constants were determined analytically, whereas the corresponding quartic force constants were found numerically from finite differences of analytic third derivatives using internal-coordinate displacements sizes of  $\pm 0.005 \text{ \AA}$  or  $\pm 0.01 \text{ rad}$ . For F<sub>2</sub>O the DZP CCSD(T) quartic force field was evaluated with the aid of carefully constructed higher-order difference formulas<sup>100</sup> using analytic gradient data computed for 10 single and 8 double internal-coordinate displacements. The accuracy of this approach has been demonstrated previously in computational studies involving RHF and CISD anharmonic force fields of several small polyatomic molecules.<sup>11,12</sup> For the linear N<sub>2</sub>O molecule, 10 single, 12 double, and 2 triple internal-coordinate displacements<sup>100</sup> sufficed to determine the complete quartic force fields at the CCSD and CCSD(T) levels of theory from energy points computed to high precision ( $10^{-10}$  a.u. or better). The step sizes employed to generate the grid of energy and gradient data for F<sub>2</sub>O and N<sub>2</sub>O were 0.01  $\text{\AA}$  and 0.02 rad.

The nonlinear transformation equations of Sec. III B were implemented to fourth order in the program INTDER,<sup>65</sup> which performs both forward and backward transformations among internal- and Cartesian-coordinate force constants and thus provides for the representation of a given force field in any alternate coordinate set. The Cartesian projection scheme detailed in Sec. III D and Appendixes A–C was also coded in INTDER. Results for the projected Cartesian derivatives were tested by first transforming selected Cartesian force fields at nonstationary points to arbitrary internal coordinate representations while neglecting the Cartesian gradients and then transforming the internal derivatives back to the Cartesian space. Such sequential transformations effectively eliminate the rotationally variant parts of the Cartesian force field arising when the Cartesian gradients are discarded, thus constituting a circuitous route to the force constants given directly by the Cartesian projection scheme. Most quartic force fields were also transformed to reduced normal coordinate representations, after which vibrational anharmonic constants ( $\chi_{ij}$ ) and vibration–rotation interaction constants ( $\alpha_i^B$ ) were determined using formulas<sup>101</sup> derived from second-order perturbation theory as applied to the standard vibration–rotation Hamiltonian<sup>57,101-104</sup> for semirigid molecules. The utility of such vibrational analyses has been investigated extensively in the systematic studies of vibrational anharmonicity in linear and asymmetric top molecules by Allen and co-workers.<sup>11,12</sup>

## V. CASE STUDIES

### A. Diatomic molecules—N<sub>2</sub> and F<sub>2</sub>

In Sec. III C theoretical considerations were presented concerning the choice of internal coordinates used to ob-

TABLE VI. Analytic results for the expansion coefficients in the diatomic shift term.<sup>a</sup>

	Shift coordinate				
	$r$	$\xi$	$\rho$	$w$	$v$
$c_r$	1	1	1	1	1
$c_{rr}$	0	$-r_e^{-1}$	$-2r_e^{-1}$	$-\beta$	0
$c_{rrr}$	0	$r_e^{-2}$	$6r_e^{-2}$	$\beta^2$	$-2a^2$
$c_{rrrr}$	0	$r_e^{-3}$	$-24r_e^{-3}$	$-\beta^3$	0

<sup>a</sup>See Eq. (69) of the text.

tain the shifted potential energy surface in Eq. (3). It is instructive to briefly revisit the N<sub>2</sub> and F<sub>2</sub> paradigms in order to clarify the issues of relevance. As shown in Eq. (47), the degree of curvilinearity in the internal coordinates, which governs the magnitude of the  $\mathbf{D}_{i_1 i_2 \dots i_n}$  vectors, has important ramifications concerning the effect of the shift term on higher-order derivatives. To investigate this effect, five coordinates ( $\mathcal{R}$ ) are considered here for the shift term: the simple bond distance  $r$ , the Simons–Parr–Finlan coordinate  $\rho = (r - r_e)/r$ , the Morse coordinate  $w = 1 - \exp[-\beta(r - r_e)]$ , and two alternative coordinates  $\xi = \exp(\rho) - 1$  and  $v = \tan^{-1}[a(r - r_e)]$ . The Cartesian projection scheme is equivalent to the selection of simple bond distances for the shift term in the case of diatomic molecules. The shift contribution for each of the coordinates of concern can be expanded about  $r_e$  to provide a power series representation of the shifted potential energy curve in terms of the bond distance  $r$  and the corresponding gradient  $f$ :

$$\begin{aligned}
 V^{\text{shift}}(r; \mathcal{R}) = & V(r) - f_r \left[ c_r (r - r_e) + \frac{c_{rr}}{2} (r - r_e)^2 \right. \\
 & \left. + \frac{c_{rrr}}{6} (r - r_e)^3 + \frac{c_{rrrr}}{24} (r - r_e)^4 + \dots \right] \\
 = & \frac{f_{rr}^*}{2} (r - r_e)^2 + \frac{f_{rrr}^*}{6} (r - r_e)^3 \\
 & + \frac{f_{rrrr}^*}{24} (r - r_e)^4 + \dots \quad (69)
 \end{aligned}$$

In Table VI analytic results are given for the  $c_r$ ,  $c_{rr}$ ,  $c_{rrr}$  and  $c_{rrrr}$  coefficients. In Table VII numerical values for the modified force constants  $f_{rr}^*$ ,  $f_{rrr}^*$  and  $f_{rrrr}^*$  are listed along with associated spectroscopic constants for N<sub>2</sub> and F<sub>2</sub> for the various choices of the shift coordinate. The  $\beta$  parameters appearing in the Morse coordinate were determined from the experimental  $f_{rr}$  and  $D_e$  values according to  $\beta = [f_{rr}/(2D_e)]^{1/2}$ ; hence,  $\beta(\text{N}_2) = 2.6884$  and  $\beta(\text{F}_2) = 2.9749 \text{ \AA}^{-1}$ .<sup>105</sup>

The equilibrium bond lengths of diatomic molecules are typically predicted to be too short at the RHF level of theory, which means that the first derivative  $f_r$  in Eq. (69) is generally positive at the exact equilibrium bond length  $r_e$ . As indicated by the analytic results in Table VI, if the

TABLE VII. Force constants and spectroscopic constants for the DZP RHF shifted potential-energy curves of N<sub>2</sub> and F<sub>2</sub>.<sup>a</sup>

	Shift coordinate						Expt. <sup>b</sup>
	<i>r</i>	$\xi$	$\rho$	<i>w</i>	<i>v</i> ( <i>a</i> =1)	<i>v</i> ( <i>a</i> =10)	
N <sub>2</sub>							
$f_{rr}^*$	27.398	27.791	28.184	28.558	27.398	27.398	22.94
$f_{rrr}^*$	-183.30	-183.65	-185.45	-186.42	-182.43	-96.99	-169.6
$f_{rrrr}^*$	1037.0	1036.7	1044.8	1045.4	1037.0	1037.0	997.6
$\omega_e$	2577.1	2595.6	2613.8	2631.1	2577.1	2577.1	2358.6
$\omega_e x_e$	11.06	10.68	10.56	10.36	10.85	-5.11	14.32
$\alpha_e$	13.46	13.09	12.90	12.64	13.35	2.74	17.32
F <sub>2</sub>							
$f_{rr}^*$	5.365	5.745	6.125	6.961	5.365	5.365	4.703
$f_{rrr}^*$	-36.18	-36.45	-37.79	-40.93	-35.11	71.12	-36.39
$f_{rrrr}^*$	194.94	194.75	199.52	209.07	194.94	194.94	...
$\omega_e$	979.1	1013.2	1046.1	1115.2	979.1	979.1	916.6
$\omega_e x_e$	8.75	7.36	6.85	6.12	7.77	56.9	11.24
$\alpha_e$	10.56	9.32	8.65	7.53	10.10	-3.52	13.85

<sup>a</sup>See Eq. (69) and the associated text. The reference bond lengths are the experimental  $r_e$  values appearing in Table I. The force constants correspond to energies in aJ and distances in Å; the  $\omega_e$  and  $\omega_e x_e$  values are in cm<sup>-1</sup>, and the  $\alpha_e$  values are in 10<sup>-3</sup> cm<sup>-1</sup>.

<sup>b</sup>References 21–23.

coordinates  $\rho$  and  $w$  are utilized, the effect of the shift term is then to increase the magnitudes of the  $f_{rr}$ ,  $f_{rrr}$  and  $f_{rrrr}$  constants. If  $\xi$  is used instead, the magnitudes of  $f_{rr}$  and  $f_{rrr}$  are increased but that of  $f_{rrrr}$  is decreased. Finally, the shift coordinate  $v$  has the intriguing property that the even-order force constants are not altered while the magnitudes of odd-order force constants are concomitantly reduced. Recognizing that representative ranges of  $r_e$  and  $\beta$  are 1.0–2.5 Å and 2–3 Å<sup>-1</sup>, respectively, the results in Table VI also reveal that for  $\rho$  and  $w$  there is a numerical aggrandizement of the shift-term contribution to the force constants as one proceeds to higher order if aJ Å<sup>-*n*</sup> units are used. In the case of coordinate  $v$ , a similar effect is seen for the odd-order force constants. In contrast, for  $\xi$  the shift-term effect decreases numerically as the order of the derivative is increased. Perhaps the most salient result in Table VI is that for coordinates  $w$  and  $v$  the effect of the shift term can be made arbitrarily large by increasing the magnitude of the parameters  $\beta$  and  $a$ , which enhances the curvilinearity of the shift coordinate and gives rise to anomalously large  $\mathbf{D}_{i_1 i_2 \dots i_n}$  vectors in Eq. (47).

The numerical results in Table VII reveal substantial variations in the energy derivatives and spectroscopic constants derived from the various choices of shift coordinate. For N<sub>2</sub> and F<sub>2</sub> the original DZP RHF  $f_{rr}$  derivatives at the experimental geometry are too large in magnitude, and thus by shifting these quantities to larger values, the  $\rho$ ,  $\xi$ , and  $w$  choices diminish the agreement with experiment. The Morse coordinate is the most extreme in this regard, as  $\omega_e$  is shifted from 2577 to 2631 cm<sup>-1</sup> for N<sub>2</sub> and from 979 to 1115 cm<sup>-1</sup> for F<sub>2</sub>. On the other hand, the shifts in  $\omega_e$  for the  $\xi$  coordinate are much less significant. The same trends are observed for the anharmonic constants of the two molecules, i.e., the agreement with experiment be-

comes successively poorer as the shift coordinate is chosen in the series  $r \rightarrow \xi \rightarrow \rho \rightarrow w$ . Particularly striking is the fact that in going from  $r \rightarrow w$  the errors in  $\omega_e x_e$  and  $\alpha_e$  for F<sub>2</sub> increase from 22% to 46% and 24% to 46%, respectively. The data listed in Table VII also include two columns obtained from different choices of the coordinate  $v$ , one in which the parameter  $a=1$  Å<sup>-1</sup> and the other in which  $a=10$  Å<sup>-1</sup>. It is noteworthy that in the first case the accuracy of the predicted constants is generally better than that for either  $\rho$ ,  $\xi$ , or  $w$ . However, by increasing parameter  $a$  to 10 Å<sup>-1</sup>, unphysical values of  $f_{rrr}$ ,  $\omega_e x_e$ , and  $\alpha_e$  result merely as a consequence of the high curvilinearity of the shift coordinate. For example, for F<sub>2</sub> it is found that  $f_{rrr}=71.12$  aJ Å<sup>-3</sup>,  $\alpha_e=-3.52 \times 10^{-3}$  cm<sup>-1</sup>, and  $\omega_e x_e=56.9$  cm<sup>-1</sup>, the first two constants being of the wrong sign and the last value a factor of five too large! In summary, the data presented in this section show that the quality of the theoretical force constants is not improved by choosing variants of the simple bond-distance coordinate  $r$  for the shift term. Indeed, substantial deterioration of the predictions may be engendered if the curvilinearity of the shift coordinate is large.

## B. F<sub>2</sub>O

It is well known that electron correlation is unusually important in describing molecules with O–F bonds,<sup>106–112</sup> as indicated by the severe underestimation of equilibrium O–F distances typically observed in applying Hartree–Fock theory. For such molecules substantial improvements in predictions of force fields at the RHF level are thus anticipated by shifting the reference geometry to a nonstationary point. Indeed, as shown in this subsection, the oxygen difluoride molecule constitutes a remarkable example

TABLE VIII. Theoretical predictions of the quartic force field of F<sub>2</sub>O.<sup>a</sup>

Derivative	DZP RHF//DZP RHF		DZP RHF//expt			DZP CCSD(T)//expt <sup>b</sup>			Expt. <sup>c</sup>
	$E_e$	$V$	$E_e$	$V$	$V^{\text{proj}}$	$E_e$	$V$	$V^{\text{proj}}$	
$R$	[−125.35]	0.000	[−113.27]	0.4558	0.000	[−113.62]	−0.1018	0.000	...
$\theta$	[−35.01]	0.000	[−33.40]	0.0369	0.000	[−33.44]	0.0002	0.000	...
$RR$	[−147.04]	7.510	[−128.66]	4.826	4.848	[−128.95]	4.537	4.530	4.1045
$RR'$	[−31.49]	0.840	[−27.36]	0.614	0.591	[−27.17]	0.802	0.809	0.8595
$R\theta$	[−12.67]	0.380	[−11.64]	0.232	0.219	[−11.66]	0.209	0.209	0.2209
$\theta\theta$	[−47.77]	2.055	[−45.93]	1.663	1.984	[−46.09]	1.498	1.427	1.4709
$RRR$	[262.95]	−46.495	[223.15]	−31.344	−31.368	[222.92]	−31.570	−31.56	−29.256
$RRR'$	[34.16]	−1.979	[28.33]	−1.450	−1.442	[28.12]	−1.667	−1.670	−2.096
$RR\theta$	[−11.01]	−1.917	[−9.29]	−1.389	−1.390	[−9.27]	−1.367	−1.364	−1.501
$RR'\theta$	[27.67]	−0.880	[24.29]	−0.463	−0.461	[24.33]	−0.424	−0.427	−0.462
$R\theta\theta$	[15.19]	−3.381	[14.28]	−2.613	−2.499	[14.08]	−2.812	−2.840	−2.6843
$\theta\theta\theta$	[71.97]	−4.528	[69.75]	−3.428	−3.418	[69.62]	−3.554	−3.554	−3.5837
$RRRR$	[−625.30]	262.20	[−525.77]	169.38	169.41	[−521.45]	173.7(22)	173.6	187.97
$RRRR'$	[−18.11]	16.99	[−16.33]	11.16	11.16	[−23.89]	3.6(5)	3.6	...
$RRR\theta$	[57.62]	5.38	[47.48]	4.28	4.29	[47.20]	4.0(2)	4.0	...
$RRR'R'$	[−79.84]	−7.18	[−61.77]	−4.68	−4.69	[−55.39]	1.7(9)	1.7	...
$RRR'\theta$	[−27.81]	4.11	[−23.93]	2.43	2.43	[−23.61]	2.75(6)	2.76	...
$RR\theta\theta$	[37.43]	5.80	[31.88]	4.38	4.33	[31.10]	3.6(2)	3.7	(4.60)
$RR'\theta\theta$	[−51.59]	7.72	[−45.77]	5.71	5.76	[−44.88]	6.6(2)	6.6	...
$R\theta\theta\theta$	[−18.79]	9.72	[−18.63]	7.34	7.34	[−18.49]	7.48(1)	7.48	...
$\theta\theta\theta\theta$	[−155.90]	20.23	[−152.98]	15.65	15.57	[−159.93]	16.20(1)	16.22	(16.10)

<sup>a</sup>Derivatives of the electronic energy  $E_e$  are given in brackets along with the derivatives of the total energy  $V$ . The column headings are denoted as (method)//(geometry). The entries under  $V^{\text{proj}}$  are constants obtained from the complete quartic force field by application of the Cartesian projection scheme described in the text. Units are consistent with energy in aJ, distances in Å, and angles in radians. The experimental geometry is the  $r_0$  structure  $R(\text{O-F}) = 1.4087$  Å and  $\theta(\text{F-O-F}) = 103.32^\circ$ .

<sup>b</sup>Numerical uncertainties arising in the quartic force constants at the DZP CCSD(T) level are given in parentheses.

<sup>c</sup>See Ref. 118. Values in parentheses were constrained to the *ab initio* results of Ref. 13.

in which higher-order force constants determined using highly correlated methods are essentially reproduced by RHF predictions at shifted geometries.

Microwave studies by Pierce, DiCianni, and Jackson<sup>113</sup> in 1963 and by Morino and Saito<sup>114</sup> in 1966 of F<sub>2</sub>O in several low-lying vibrational states established the  $r_0$ ,  $r_z$ , and  $r_e$  structures of this  $C_{2v}$ -symmetry molecule; in particular,  $R_e(\text{O-F}) = 1.4053$  Å and  $\theta_e(\text{F-O-F}) = 103.07^\circ$ .<sup>114</sup> Early low-resolution infrared work<sup>115</sup> has largely been supplanted by recent high-resolution IR studies<sup>116,117</sup> of the  $\nu_2$ ,  $\nu_1$ , and  $2\nu_2$  bands, the latter two of which are involved in a strong Fermi resonance. The fundamental vibrational frequencies of F<sub>2</sub>O are currently accepted as  $\nu_1(a_1) = 928.1$  cm<sup>−1</sup>,  $\nu_2(a_1) = 460.6$  cm<sup>−1</sup>, and  $\nu_3(b_2) = 831$  cm<sup>−1</sup>.<sup>116,117</sup> The most recent experimental analysis of the vibrational spectrum and potential energy surface of F<sub>2</sub>O was performed by Saarinen, Kauppi, and Halonen<sup>118</sup> in 1990, in which a partial quartic force field was obtained. In a 1988 paper by Thiel *et al.*<sup>13</sup> the first state-of-the-art *ab initio* investigation of the anharmonic force field of F<sub>2</sub>O was reported. Therein the TZP RHF level of theory was shown to yield  $R_e(\text{O-F}) = 1.3428$  Å (a 0.06 Å underestimation), whereas the analogous length at the TZP CCSD level was found to be 1.4085 Å (within 0.004 Å of experiment). Consequently, the most reliable force field obtained by Thiel *et al.* involved a mixture of TZP CCSD quadratic

and cubic force constants with TZP RHF quartic constants determined at the TZP CCSD geometry. In the present analysis the force field of Thiel *et al.* is improved by determining a full quartic force field at the DZP CCSD(T) level using the experimental structure<sup>114</sup>  $R_0(\text{O-F}) = 1.4087$  Å and  $\theta_0(\text{F-O-F}) = 103.32^\circ$  as the reference geometry. In brief, not only is the accuracy of RHF predictions at non-stationary reference geometries investigated, but also correlated force fields of F<sub>2</sub>O of the highest quality yet determined are presented, providing data on anharmonic force constants not readily determined in parallel experimental efforts.

In Table VIII three separate predictions of the quartic force field of F<sub>2</sub>O are tabulated, as expressed in terms of the valence bond distances  $R(\text{O-F})$  and  $R'(\text{O-F})$  and the valence bond angle  $\theta(\text{F-O-F})$ . The first set of data (DZP RHF//DZP RHF) is comprised of DZP RHF derivatives computed at the corresponding optimum geometry, viz.,  $R_e(\text{O-F}) = 1.3416$  Å and  $\theta_e(\text{F-O-F}) = 103.43^\circ$ .<sup>13</sup> In the second set of predictions (DZP RHF//expt), the DZP RHF level of theory is used to evaluate the force constants at the experimental  $r_0$  structure. These constants are to be compared with the third set of predictions (DZP CCSD(T)//expt) determined at the same experimental geometry with the highly correlated CCSD(T) method. For each theoretical procedure the derivatives of the elec-

tronic energy  $E_e$  (in brackets) and the derivatives of the total energy  $V$  are tabulated, the electronic energy being related rather simply in atomic units to the total energy as

$$V(R, R', \theta) = E_e(R, R', \theta) + \frac{72}{R} + \frac{72}{R'} + \frac{81}{(R^2 + R'^2 - 2RR' \cos \theta)^{1/2}} \quad (70)$$

For the two procedures involving nonstationary reference geometries, additional sets of derivatives ( $V^{\text{proj}}$ ) are listed in Table VIII as given by the Cartesian projection scheme of Sec. III D followed by a curvilinear transformation of the projected Cartesian force constants into the internal coordinate representation. Note that the projected first derivatives are rigorously zero by construction but that the higher-order  $V^{\text{proj}}$  constants are quite similar to the corresponding  $V$  derivatives, the significance of which is discussed below. Experimentally derived force constants, where known, also appear in the table.

The results in Table VIII demonstrate in a vivid fashion that most of the "correlation error" in the DZP RHF//DZP RHF derivatives is, in fact, a consequence of the geometry shift. If the change in the derivatives of the total energy  $V$  in going from DZP RHF//DZP RHF to DZP CCSD(T)//expt is considered to be the "correlation contribution" to the force constants, then in the case of  $f_{RR}$ ,  $f_{RRR}$ , and  $f_{RRRR}$ , 90.3%, 101.5%, and 104.9% of this contribution, respectively, is recovered merely by shifting the reference geometry of the RHF analysis to a nonstationary point. Perhaps even more striking is the fact that this degree of improvement is not restricted to the bond stretching derivatives of  $V$  alone, even though the geometry shift is primarily an O–F bond length expansion with little change in the F–O–F angle. For example, the percent of the "correlation contribution" to  $f_{\theta\theta}$ ,  $f_{\theta\theta\theta}$ , and  $f_{\theta\theta\theta\theta}$  recovered by shifting the reference geometry is 70.4%, 112.9%, and 113.6%, respectively. Similarly, in the case of the  $f_{R\theta}$ ,  $f_{RR\theta}$ , and  $f_{RRR\theta}$  series these percentages are found to be 86.6%, 96.0%, and 79.7%, respectively. The only total energy derivatives at the DZP CCSD(T) level which are not well reproduced by the DZP RHF//expt procedure are the three off-diagonal stretching constants  $f_{RR'}$ ,  $f_{RRR'R'}$ , and  $f_{RRR'R'R'}$ . Finally, in comparing the DZP CCSD(T) force constants at the shifted geometry with those values which are known experimentally, it is seen that the agreement is excellent, and hence the entire force field at this level of theory must be considered very reliable.

For every force constant in Table VIII, the magnitude of the electronic energy derivative is immense in comparison to that of the total energy derivative, once again illustrating the delicate cancellation of  $E_e$  and  $V_N$  terms discussed in Sec. I. In the DZP RHF//expt case, the ratios  $E_e'/V_N'$ ,  $E_e''/V_N''$ ,  $E_e'''/V_N'''$ , and  $E_e''''/V_N''''$  for the diagonal stretching constants are  $-0.996$ ,  $-0.964$ ,  $-0.877$ , and  $-0.756$ , respectively, which is in accord with the observation made previously for  $N_2$  and  $F_2$  that the  $V_N$  terms become increasingly dominant in higher order. The trend

TABLE IX. DZP RHF force constants of  $F_2O$  in dimensionless normal coordinates determined at the experimental geometry by various procedures.<sup>a</sup>

Parameter	Shift term in internal coordinates <sup>b</sup>			Cartesian projection scheme
	(2 stre, 1 bend) <sup>c</sup>	(3 stre) <sup>d</sup>	(1 stre, 2 bend) <sup>e</sup>	
$\omega_1$	991.95	995.43	1041.41	1010.54
$\omega_2$	496.67	498.75	519.70	533.31
$\omega_3$	962.33	960.65	938.93	967.50
$\phi_{111}$	-229.5	-228.1	-210.6	-220.5
$\phi_{211}$	-48.3	-49.8	-65.2	-57.4
$\phi_{221}$	-18.4	-18.6	-22.5	-22.4
$\phi_{222}$	-85.1	-85.5	-91.3	-82.4
$\phi_{331}$	-276.4	-276.0	-270.1	-268.8
$\phi_{332}$	-55.2	-57.6	-85.6	-74.1
$\phi_{1111}$	35.1	34.4	27.0	30.7
$\phi_{2111}$	22.8	23.0	24.5	23.7
$\phi_{2211}$	-3.2	-2.9	1.2	-0.3
$\phi_{2221}$	7.3	7.1	5.5	5.7
$\phi_{2222}$	19.6	19.7	20.8	18.5
$\phi_{3311}$	68.4	68.2	64.6	65.4
$\phi_{3321}$	16.4	17.1	23.9	20.7
$\phi_{3322}$	-13.6	-13.2	-8.2	-9.8
$\phi_{3333}$	43.9	44.1	45.8	43.6

<sup>a</sup>All values in  $\text{cm}^{-1}$ . Geometry:  $R_0(\text{O-F}) = 1.4087 \text{ \AA}$  and  $\theta_0(\text{F-O-F}) = 103.32^\circ$  (Ref. 114). The positive phases of normal coordinates 1 and 2 are selected to correspond to increasing O–F bond lengths and an increasing F–O–F bond angle, respectively.

<sup>b</sup>The internal coordinates are defined assuming the numbering of the atoms is  $F_2-O-F_3$ .

<sup>c</sup>A valence internal coordinate set comprised of the two bond distances  $R(1-2)$  and  $R(1-3)$  and the bond angle  $\theta(2-1-3)$ .

<sup>d</sup>A set comprised of the three internuclear distances  $R(1-2)$ ,  $R(1-3)$ , and  $R(2-3)$ .

<sup>e</sup>Comprised of the internuclear distance  $R(2-3)$  and the angles  $\theta(1-2-3)$  and  $\theta(1-3-2)$ .

for the diagonal bending constants is similar but less pronounced, the corresponding ratios being  $-0.999$ ,  $-0.965$ ,  $-0.953$ , and  $-0.869$ . In brief, it is clear that the balance of  $E_e$  and  $V_N$  terms is a key issue not only in the evaluation of stretching force constants but also in the prediction of diagonal and off-diagonal constants involving the bending coordinate. In this regard it is remarkable that there is an essential reproduction of the DZP CCSD(T) electronic energy derivatives at the experimental geometry by the DZP RHF wave functions for all cases except the quartic  $RRRR'$  and  $RRR'R'$  constants. The mean absolute percentage error in the DZP RHF//expt values of  $E_e''$  is only 0.36%, and that for  $E_e'''$  only 0.47%. Excluding the two aforementioned spurious quartic constants, the corresponding error for  $E_e''''$  is a mere 1.77%.

With the success of the DZP RHF//expt predictions in Table VIII, a careful investigation of the coordinate dependence of the resulting shifted potential energy surfaces is necessitated. In Table IX DZP RHF//expt quartic force fields in dimensionless normal coordinates are presented as obtained by four different procedures. In the first set of results (2 stre, 1 bend), the shift term is applied using the standard valence internal coordinate set ( $R, R', \theta$ ), whereas the second (3 stre) and third (1 stre, 2 bend) sets involve alternate choices of the shift coordinates (see

TABLE X. DZP RHF fundamental vibrational frequencies ( $\nu_i$ ), total anharmonicities ( $\Delta_i$ ), vibration-rotation interaction constants ( $\alpha_i^B$ ), and vibrational anharmonic constants ( $\chi_{ij}$ ) of  $F_2O$  determined at the experimental geometry by various procedures.<sup>a</sup>

Parameter	Shift term in internal coordinates			Cartesian projection scheme
	(2 stre, 1 bend)	(3 stre)	(1 stre, 2 bend)	
$\nu_1$	975.26	978.77	1024.84	993.89
$\nu_2$	490.32	492.37	512.70	527.24
$\nu_3$	940.32	938.64	916.71	945.93
$\Delta_1$	-16.69	-16.66	-16.57	-16.09
$\Delta_2$	-6.35	-6.38	-7.00	-6.07
$\Delta_3$	-22.01	-22.01	-22.22	-21.57
$\alpha_1^A$	0.535	0.864	4.231	1.835
$\alpha_2^A$	-22.564	-22.254	-19.113	-20.922
$\alpha_3^A$	19.623	9.129	13.948	14.044
$\alpha_1^B$	2.356	2.359	2.383	2.271
$\alpha_2^B$	2.581	2.614	2.982	2.723
$\alpha_3^B$	3.522	3.527	3.634	3.259
$\alpha_1^C$	1.122	1.135	3.147	1.103
$\alpha_2^C$	1.781	1.809	0.231	1.905
$\alpha_3^C$	2.456	2.451	2.438	2.161
$\chi_{11}$	-3.906	-3.893	-3.740	-3.835
$\chi_{21}$	-4.274	-4.274	-4.278	-3.985
$\chi_{22}$	-0.344	-0.346	-0.436	-0.240
$\chi_{31}$	-13.465	-13.480	-13.891	-12.853
$\chi_{32}$	-7.040	-7.107	-7.977	-7.206
$\chi_{33}$	-5.879	-5.857	-5.641	-5.771

<sup>a</sup>All values in  $\text{cm}^{-1}$  except the  $\alpha_i^B$  constants, which are in  $10^{-3} \text{cm}^{-1}$ . For a description of the different procedures see footnotes a-e of Table IX. In all schemes the  $2\omega_2 - \omega_1$  Fermi resonance term has been excluded in the perturbation theory analysis.

footnotes b-e of Table IX). The last column in the table reports force constants obtained via the Cartesian projection scheme.<sup>119</sup> The variations in the sets of data in Table IX are significant but not blatant. The ranges of variation in the  $\omega_1$ ,  $\omega_2$ , and  $\omega_3$  values are 4.9%, 6.9%, and 3.0%, respectively, of the harmonic frequencies given by the Cartesian projection scheme. Such variations represent sizeable fractions of the respective errors in these harmonic frequencies as compared to experiment (see Table XI), viz., 6.9%, 13.7%, and 14.6%. On a relative basis the ranges of variation in the  $\phi_{ijk}$  and  $\phi_{ijkl}$  constants are much larger; for example, the  $\phi_{111}$ ,  $\phi_{211}$ ,  $\phi_{221}$ ,  $\phi_{222}$ ,  $\phi_{331}$ , and  $\phi_{332}$  ranges are 7.9%, 29.4%, 18.3%, 10.8%, 2.8%, and 41.0%, respectively, of the corresponding Cartesian projection values. It must be realized that some of these changes in the  $\phi_{ijk}$  and  $\phi_{ijkl}$  values arise from variations in the underlying  $\omega_i$  values, because the definition of the dimensionless normal coordinate on which these cubic and quartic constants are based involves a normalization factor of  $\omega_i^{1/2}$ . However, this effect only partially accounts for the observed trends and in some cases actually increases the range of values observed.

In Table X spectroscopic constants are given which arise from the various normal coordinate force constants in Table IX according to second-order perturbation theory. In an absolute sense it is seen that the anharmonic constants  $\chi_{ij}$  and the total anharmonicities  $\Delta_i$  are reasonably insensitive to changes in the shift term. In support of this characterization of the data is the observation that none of

the variations among the total anharmonicities is greater than  $1 \text{cm}^{-1}$ . The variations in the vibration-rotation interaction constants in Table X are much greater, however, particularly for  $\alpha_1^A$ ,  $\alpha_2^A$ ,  $\alpha_3^A$ ,  $\alpha_1^C$ , and  $\alpha_2^C$ . The sensitivity of these constants to the shift term is disturbing in that the observed changes are at least as large as the errors expected *a priori* of DZP RHF  $\alpha_i^B$  values (on the order of 10%).<sup>11,12</sup> While caution is thus dictated as to the effect of sundry shift terms on higher-order force constants, much of the fluctuation in the  $\alpha_i^B$  values may be related once again to changes in the associated  $\omega_i$  frequencies. For example, with regard to the anomalous  $\alpha_1^C$  entry for (1 stre, 2 bend), the associated  $\omega_1 - \omega_3$  difference is at least twice as large as in the other cases, and the Coriolis contribution to  $\alpha_1^C$  involving a  $\omega_1 - \omega_3$  resonance denominator is known to make this constant very sensitive to the level of theory.<sup>13</sup> In summary, the data in Tables IX and X clearly establish the shift-term dependence of spectroscopic constants predicted at nonstationary geometries, and while in most cases this dependence is not pernicious, the merits of an unambiguous shift procedure are clear.

In surveying the results in Tables IX and X, the conclusion arises that the valence (2 stre, 1 bend) set of shift coordinates is slightly better than (3 stre) and significantly better than (1 stre, 2 bend) in reproducing experiment, a fact not surprising to aficionados of vibrational analyses in internal coordinates. Comparing the various harmonic vibrational frequencies in Table IX to the experimental values  $\omega_1(a_1) = 945 \text{cm}^{-1}$ ,  $\omega_2(a_1) = 469 \text{cm}^{-1}$ , and  $\omega_3(b_2) = 844 \text{cm}^{-1}$ ,<sup>118</sup> the (2 stre, 1 bend) and (3 stre) sets appear essentially indistinguishable in accuracy, whereas the corresponding (1 stre, 2 bend) predictions are quite erratic in that the accuracy of  $\omega_1$  and  $\omega_2$  is deteriorated while the  $\omega_3$  value is significantly improved. Instructive comparisons can also be made for the vibration-rotation interaction constants in Table X, specifically,  $\alpha_1^A$ ,  $\alpha_2^A$ ,  $\alpha_3^A$ , and  $\alpha_1^C$ , whose experimental values (in  $10^{-3} \text{cm}^{-1}$ ) are 1.286, -23.316, 19.514, and 0.239, respectively.<sup>114</sup> The predictions for the (2 stre, 1 bend) case are in the very least reasonable in an absolute sense in all four instances; however,  $\alpha_3^A$  is anomalous in the (3 stre) case, and both  $\alpha_1^A$  and  $\alpha_1^C$  are spurious for (1 stre, 2 bend). It would be important to be able to judge *a priori* if a particular set of internal coordinates will give rise to anomalous spectroscopic constants. As discussed in Sec. III C, a diagnostic for this purpose is provided by the determinant of the normalized  $\mathbf{B}_1 \mathbf{B}_1^T$  matrix. For the (2 stre, 1 bend), (3 stre), and (1 stre, 2 bend) sets of shift coordinates, the determinants in question are 0.75, 0.64, and 0.78, respectively, so that there are no near redundancies and no clear distinctions between the three choices on this basis.

Having investigated the shift-term dependence of the DZP RHF//expt results for  $F_2O$ , a strong argument can be presented for the use of the Cartesian projection scheme. First, the cubic and quartic  $V^{\text{proj}}$  constants in Table VIII are in all cases almost identical to the analogous total energy derivatives obtained using the best set of internal shift coordinates (2 stre, 1 bend). Similar agreement is seen for all quadratic constants in the DZP CCSD(T)//expt case,

TABLE XI. Complete quartic force fields of F<sub>2</sub>O in dimensionless normal coordinates determined from various projected DZP Cartesian force fields.<sup>a</sup>

Anharmonic: Harmonic:	RHF//RHF RHF//RHF	RHF//RHF <sup>b</sup> CCSD(T)//expt	RHF//expt <sup>b,c</sup> CCSD(T)//expt	CCSD(T)//expt CCSD(T)//expt	Expt. <sup>d</sup>
$\omega_1$	1211.52	[976.50]	[976.50]	976.50	944.93
$\omega_2$	586.64	[463.05]	[463.05]	463.05	469.22
$\omega_3$	1211.61	[904.57]	[904.57]	904.57	843.86
$\phi_{111}$	-240.5	-347.1	-235.5(-240.4)	-247.2	-247.4
$\phi_{211}$	-52.4	-65.4	-45.3(-39.6)	-41.7	-48.4
$\phi_{221}$	-13.0	-24.7	-15.3(-19.8)	-17.4	-19.4
$\phi_{222}$	-91.8	-127.8	-92.0(-94.3)	-97.3	-97.6
$\phi_{331}$	-301.7	-441.9	-296.0(-296.1)	-295.9	-288.4
$\phi_{332}$	-37.0	-81.3	-51.7(-52.1)	-52.0	-63.4
$\phi_{1111}$	35.8	56.0	37.5(38.1)	35.2	
$\phi_{2111}$	23.0	36.1	22.8(22.4)	22.6	
$\phi_{2211}$	-4.9	-6.5	-5.0(-5.0)	-5.5	
$\phi_{2221}$	7.5	11.1	8.7(9.4)	9.6	
$\phi_{2222}$	21.4	27.4	22.8(20.9)	21.8	
$\phi_{3311}$	71.0	116.9	74.6(74.5)	73.3	
$\phi_{3321}$	12.1	22.0	15.1(15.2)	15.9	
$\phi_{3322}$	-16.3	-24.8	-16.7(-16.5)	-19.2	
$\phi_{3333}$	42.4	78.6	49.9(49.9)	81.4	

<sup>a</sup>All values in cm<sup>-1</sup>. The positive phases of normal coordinates 1 and 2 were selected to correspond to increasing O-F bond lengths and an increasing F-O-F bond angle, respectively.

<sup>b</sup>The RHF cubic and quartic force constants were first combined with CCSD(T)//expt first and second derivatives in the (2 stre, 1 bend) representation. The combined nonstationary force field was then transformed into the Cartesian space and projected as described in the text before the normal-coordinate force constants were computed.

<sup>c</sup>The values in parentheses were obtained by combining the RHF//expt third- and fourth-order projected Cartesian derivatives directly with the CCSD(T)//expt projected Cartesian harmonic force field.

<sup>d</sup>Reference 118.

and only for  $f_{\theta\theta}$  is there any significant modification of the original DZP RHF//expt second derivatives in arriving at the  $V^{\text{proj}}$  predictions. Thus, the effect of the projection scheme on the total energy derivatives expressed in a chemically relevant set of internal coordinates is greatest in first order and then falls off precipitously in higher order, a gratifying observation. Second, of the total reduction of the harmonic frequencies in going from DZP RHF//DZP RHF to DZP RHF//expt (2 stre, 1 bend), most is obtained via Cartesian projection of the DZP RHF//expt force constants. Note that for  $\omega_1$  and  $\omega_3$ , 201 and 244 cm<sup>-1</sup> out of the 220 and 250 cm<sup>-1</sup> shifts, respectively, are recovered by the Cartesian projection method. Third, the reproduction of the (2 stre, 1 bend)  $\phi_{ijk}$ ,  $\phi_{ijkl}$ ,  $\alpha_i^B$ ,  $\Delta_i$  and  $\chi_{ij}$  constants in Tables IX and X is generally good, and, in fact, excellent in all but a few cases. Finally, and most importantly, the Cartesian projection scheme is unambiguous and averts spurious shift term effects which might arise from high curvilinearity or near redundancy of the shift coordinate system.

In Table XI data are presented which illustrate the recommended procedure for obtaining accurate anharmonic force fields of small polyatomic molecules which are strongly bonded. In the third column of the table, the quartic force field of F<sub>2</sub>O in dimensionless normal coordinates appears, as determined by appending projected DZP RHF//expt Cartesian third and fourth derivatives to projected DZP CCSD(T)//expt Cartesian second derivatives via two different schemes (see footnotes b and c therein).

The agreement of the results obtained by both methods with the actual, projected DZP CCSD(T)//expt  $\phi_{ijk}$  and  $\phi_{ijkl}$  constants is exceptional in all cases but  $\phi_{3333}$ . The disparity for this constant arises from the discrepancies mentioned above in the  $RRRR'$  and  $RRR'R'$  derivatives in Table VIII. The high accuracy of the DZP RHF//expt  $\phi_{ijk}$  and  $\phi_{ijkl}$  constants is mitigated somewhat if the corresponding DZP RHF quadratic force field is used in the transformation to dimensionless normal coordinates, primarily because the  $V^{\text{proj}}$  value for  $f_{\theta\theta}$  is too large. Thus, it seems advisable to uncouple the harmonic and anharmonic components of the force field in performing such analyses. Finally, a comment on the misleading accuracy of the DZP RHF//DZP RHF results is apt. As shown in Table VIII, a substantial overestimation occurs for almost all of the internal coordinate derivatives obtained via the DZP RHF//DZP RHF procedure. It happens that the error in the quadratic constants balances the error in the cubic and quartic constants to give a fortuitously good set of predictions in Table XI. This effect is clearly exposed by using the more accurate CCSD(T)//expt quadratic force field with the RHF//RHF higher derivatives to obtain the  $\phi_{ijk}$  and  $\phi_{ijkl}$  data set, as shown in the second column of Table XI. The severe overestimation of the magnitudes of those constants is striking, and the anharmonicities derived from them are unreasonable. While a balance of errors may work to improve the values of  $\phi_{ijk}$  and  $\phi_{ijkl}$  constants determined at poor reference geometries, to rely on such an

effect to yield accurate results when a more viable option is available cannot be recommended.

### C. N<sub>2</sub>O

The rovibrational spectrum of the nitrous oxide molecule has been the subject of numerous theoretical and experimental investigations.<sup>120–134</sup> Rotational *l*-type doubling and the Fermi resonance between the  $\nu_3$  and  $2\nu_2$  vibrational states have been given particular attention in the experimental efforts. Empirical anharmonic force fields, even through sixth order, have been constructed for N<sub>2</sub>O by various approaches: (a) numerical, algebraic contact transformations;<sup>120</sup> (b) second-order perturbation theory;<sup>121</sup> and (c) direct numerical diagonalization.<sup>122,123</sup> Some of the higher-order constants in these force fields are likely to be phenomenological in nature, i.e., not directly correspondent with the associated derivatives of the potential energy surface. A synthesis of these results is encumbered by large variations in several of the empirical anharmonic  $\phi_{ijk}$  and  $\phi_{ijkl}$  force constants reported by Lacy and Whiffen,<sup>122</sup> Kobayashi and Suzuki,<sup>123</sup> and Teffo and Chédin.<sup>120</sup> For example, the ranges of the deduced values (in cm<sup>-1</sup>) for  $\phi_{111}$ ,  $\phi_{221}$ , and  $\phi_{311}$  are  $-271.8$  to  $-477.7$ ,  $38.7$  to  $106.4$ , and  $-82.6$  to  $+5.7$ , respectively. Such variations are maintained in internal-coordinate representations of these force fields.

In a recent *ab initio* study, Allen and co-workers<sup>12</sup> found considerable disparities between both TZ2P RHF//RHF and CISD//CISD force constants and their experimental counterparts. The force constants of Teffo and Chédin,<sup>120</sup> which constitute the most recent empirical force field, are in accord with theory in many cases, but the constants involving the N–N bond stretch ( $r$ ) and its coupling to the N–O stretch ( $R$ ) are generally in poor agreement with the TZ2P RHF//RHF and CISD//CISD predictions. For example, the (RHF, CISD) sets of values for  $f_{rrr}$ ,  $f_{rrrr}$  and  $f_{RRRr}$  are  $(-191.2, -161.1)$  aJ Å<sup>-3</sup>,  $(1074.1, 931.3)$  aJ Å<sup>-4</sup>, and  $(8.754, 5.699)$  aJ Å<sup>-4</sup>, respectively, as compared to the analogous experimental results of  $-133.6$ ,  $691.4$ , and  $46.45$ . The optimum TZ2P bond lengths underlying the *ab initio* predictions are  $r_e(\text{N–N})=1.0815$  and  $R_e(\text{N–O})=1.1723$  Å at the RHF level and  $r_e(\text{N–N})=1.1073$  and  $R_e(\text{N–O})=1.1809$  Å at the CISD level, the spectroscopically determined distances being  $r_e(\text{N–N})=1.1273$  and  $R_e(\text{N–O})=1.1851$  Å.<sup>120</sup> Because the underestimation of the N–N bond distance by both the TZ2P RHF and CISD methods is substantial, a redetermination of high-quality *ab initio* force fields at the experimental  $r_e$  structure is warranted to address the discrepancies present in the theoretical and empirical force fields.

The issues pertinent to the practical determination of spectroscopic constants at nonstationary reference geometries were discussed at length in the F<sub>2</sub>O case study above. Therefore, the analysis here is restricted to the force field data represented in terms of the valence internal coordinates  $r(\text{N–N})$ ,  $R(\text{N–O})$ , and  $\theta(\text{N–N–O})$ . The complete quartic force fields predicted for N<sub>2</sub>O at several levels of theory are given in Table XII. As shown therein, the DZP

RHF diagonal constants for N–N stretching undergo large reductions in magnitude upon shifting the reference geometry to the experimental structure, an occurrence manifested in the 264 cm<sup>-1</sup> reduction in the  $\omega_1$  harmonic stretching frequency. In each case these changes improve the agreement with the experimental constants of Teffo and Chédin.<sup>120</sup> The effects of the geometry shift on most of the other DZP RHF force constants are quite insignificant. Augmentation of the one-particle basis set to TZ(2d1f) in the RHF predictions at the experimental  $r_e$  structure leads to a further but less pronounced reduction in the size of the diagonal force constants involving  $r$ . In contrast, for the diagonal N–O stretching constants and many of the higher-order coupling constants, the DZP RHF//expt→TZ(2d1f) RHF//expt changes are larger than the effects of the geometry shift on the DZP RHF values, the case of  $f_{RRRr}$  being the most prominent in this regard.

Perhaps the most important characteristic of the data in Table XII is the impressive agreement of the TZ(2d1f) RHF//expt and CCSD(T)//expt values for the dominant diagonal stretching constants. The percent differences in the  $f_{rrr}$ ,  $f_{rrrr}$ ,  $f_{RRRr}$ , and  $f_{RRRR}$  predictions are only 4.5%, 3.6%, 5.3%, and 1.1%, respectively. The agreement for six other higher-order constants, viz.,  $f_{\theta\theta r}$ ,  $f_{\theta\theta R}$ ,  $f_{Rrrr}$ ,  $f_{\theta\theta rr}$ ,  $f_{\theta\theta RR}$ , and  $f_{\theta\theta\theta\theta}$ , must also be considered good. The remaining cubic and quartic constants involve coupling of the bond stretches. In the  $f_{RRrr}$  and  $f_{RRRr}$  cases, it is noteworthy that the differences between the CCSD and CCSD(T) predictions are sizeable in comparison with the deficiencies in the RHF values. Therefore, as observed in the F<sub>2</sub>O case, the small, higher-order bond–stretch coupling constants are very sensitive to the treatment of electron correlation.

Finally, it is possible to assess the accuracy of the experimental force constants on the basis of the TZ(2d1f) CCSD(T)//expt predictions in Table XII. As a point of reference, note that the CCSD(T) quadratic force constants represent only slight overestimations of the well-established empirical values, as displayed in the corresponding harmonic frequency predictions, which are only 1%–2% too large. The  $f_{rrr}$ ,  $f_{RRRr}$ , and  $f_{RRRR}$  values of both Teffo and Chédin<sup>120</sup> and Kobayashi and Suzuki<sup>123</sup> are supported by the theoretical results, although in the  $f_{RRRR}$  case the 634.9 aJ Å<sup>-4</sup> empirical value<sup>120</sup> may be slightly too large. In contrast, both of the empirical values for  $f_{rrrr}$  appear to be over 100 aJ Å<sup>-4</sup> too small, even though a large fraction of the previous discrepancy<sup>12</sup> with TZ2P RHF//RHF and CISD//CISD predictions is clearly a consequence of deficient theoretical reference geometries. For the five third- and fourth-order stretch–stretch coupling constants, the values of Teffo and Chédin<sup>120</sup> are clearly preferred over those of Kobayashi and Suzuki,<sup>123</sup> but the lack of agreement with theory makes the precise values suspect. For example,  $f_{RRRr}=-7.691$  aJ Å<sup>-4</sup> is probably of the wrong sign, and  $f_{Rrrr}=46.45$  aJ Å<sup>-4</sup> appears to be too large by a factor of 4–5. The agreement of all of the CCSD(T) force constants involving the N–N–O angle with the results of Teffo and Chédin<sup>120</sup> is remarkable, discrediting some of the analogous values of Ref. 123. It is

TABLE XII. *Ab initio* total energy derivatives from first through fourth order for N<sub>2</sub>O.

Derivative <sup>a</sup>	DZP RHF// DZP RHF	Reference geometry: expt. <sup>b</sup>				Expt.	
		DZP RHF	TZ(2d1f) RHF	TZ(2d1f) CCSD	TZ(2d1f) CCSD(T)	Ref. 120	Ref. 123
<i>r</i> (N–N)	...	0.7499	1.0805	0.1696	–0.0840	...	...
<i>R</i> (N–O)	...	0.0487	0.2896	–0.0228	–0.0545	...	...
<i>rr</i>	26.585	21.070	18.999	19.040	18.778	18.251	18.236
<i>Rr</i>	2.302	2.349	2.298	1.342	1.038	1.028	1.029
<i>RR</i>	11.704	11.824	10.195	11.964	12.374	11.960	11.966
<i>θθ</i>	0.813	0.759	0.799	0.713	0.689	0.666	0.666
<i>rrr</i>	–188.8	–159.1	–148.7	–143.1	–142.2	–133.6	–132.4
<i>Rrr</i>	1.12	1.33	0.78	–2.04	–2.93	–6.872	–9.842
<i>RRr</i>	–4.19	–3.88	–4.17	–1.46	–0.76	1.498	2.451
<i>RRR</i>	–114.9	–116.4	–106.0	–102.3	–100.5	–98.83	–96.33
<i>θθr</i>	–1.79	–1.85	–1.83	–1.69	–1.08	–1.580	–2.567
<i>θθR</i>	–1.92	–1.79	–1.86	–1.58	–1.52	–1.537	–1.101
<i>rrrr</i>	1027.9	847.6	803.6	828.9	833.0	691.4	674.7
<i>Rrrr</i>	6.08	8.42	12.64	9.30	10.48	46.45	65.61
<i>RRrr</i>	10.03	9.35	9.55	4.50	1.39	–3.485	8.771
<i>RRRr</i>	–1.42	–0.57	4.43	10.75	18.77	–7.691	–20.76
<i>RRRR</i>	640.6	641.8	597.1	608.5	603.9	634.9	590.3
<i>θθrr</i>	–1.52	–1.55	–1.58	0.47	0.92	1.808	12.67
<i>θθRr</i>	4.35	4.32	4.83	4.24	4.09	5.105	7.222
<i>θθRR</i>	1.94	1.83	1.82	2.24	2.43	1.491	–6.165
<i>θθθθ</i>	2.07	2.06	1.32	1.97	2.09	1.897	2.282
<i>ω</i> <sub>1</sub> (σ)	2589	2325	2184	2298	2318	2282.1	2281.7
<i>ω</i> <sub>2</sub> (π)	668	637	653	617	607	596.3	596.5
<i>ω</i> <sub>3</sub> (σ)	1358	1350	1264	1315	1319	1298.3	1298.5
Energy	–183.715 76	–183.712 93	–183.755 57	–184.386 04	–184.422 08	...	...

<sup>a</sup>Units are consistent with energy in aJ, distances in Å, and angles in deg. The associated harmonic frequencies in cm<sup>–1</sup> and total energies in hartree are also listed. The coordinate *θ* is the actual N–N–O angle and not the linear bending variable of Hoy, Mills, and Strey (Ref. 64).

<sup>b</sup>Geometry from Ref. 120: *r*<sub>e</sub>(N–N) = 1.1273 Å and *R*<sub>e</sub>(N–O) = 1.1851 Å. The harmonic frequencies listed at each level of theory were obtained by using *r*(N–N) and *R*(N–O) as shift coordinates.

hoped that the high-quality, state-of-the-art TZ(2d1f) CCSD(T)//expt cubic and quartic force constants will assist the continued refinement of the anharmonic force field of N<sub>2</sub>O.

## VI. RECOMMENDATIONS

The results of this investigation allow preliminary recommendations to be made concerning the *ab initio* prediction of anharmonic force fields for strongly bonded molecular systems. The treatment of weak intermolecular interactions or large-amplitude vibrational motions in general is a more intricate topic which is the subject of a forthcoming paper;<sup>135</sup> such cases are precisely those which are not amenable *a priori* to vibrational analyses based on force field representations of the local potential energy surface. The electronic energy and its derivatives through fourth order are typically predicted by Hartree–Fock theory at a given geometry to within a few percent in the bonding regions of the potential energy surfaces for the types of molecules considered here. The percent errors appear to be slowly varying functions of the internuclear distances, and there seems to be little correspondence between percent error and order of derivative. The cancellations of the lower-order derivatives of the electronic energy occurring when the nuclear repulsion terms are appended are almost complete, thus making the precise determination of first and second derivatives of the total energy problematic.

In contrast, in higher orders the loss of numerical significance in the total energy derivatives is diminished because the nuclear repulsion terms become increasingly dominant. Consequently, higher-order derivatives can be predicted to high relative accuracy even by modest levels of theory. The associated caveat is that these derivatives are rapidly varying functions of the internuclear distances, and if the reference geometry is not precisely known, the numerical advantage in their evaluation is lost.

It is recommended that in *ab initio* predictions of anharmonic molecular force fields the most accurate reference geometry available be employed, even if it is not a stationary point at the level of theory used to determine the higher-order derivatives. If the use of an experimental *r*<sub>e</sub> structure or an empirically corrected theoretical geometry is not feasible or preferred, this recommendation entails the augmentation of second derivatives given by a correlated level of theory at the corresponding optimum geometry with RHF third and fourth derivatives computed at the same point. Of course, for small molecules it may be both possible and preferable to determine a consistent and complete anharmonic force field at a highly correlated level of theory to achieve improved accuracy. Some correlated electronic structure methods are inappropriate for the provision of the underlying structure and harmonic force field because the imbalance of basis set and correlation errors creates a propensity for the overestimation of bond lengths.

Valence complete-active-space SCF (CASSCF) procedures frequently employed for small molecules and second-order Møller–Plesset perturbation (MP2) theory as applied to multiply bonded species are examples of such methods. For many systems CISD wave functions constructed with polarized basis sets of moderate size constitute a counterexample, as basis set incompleteness and the neglect of higher-order excitations tend to advantageously cancel in geometric structure determinations. To base predictions of vibrational anharmonicities on RHF//RHF quartic force fields is to rely on the sizeable overestimation of harmonic frequencies to cancel the overestimation of the magnitudes of the cubic and quartic force constants in the evaluation of the  $\chi_{ij}$  constants appearing in the vibrational term value expansion. In many cases such cancellations indeed occur, but deficiencies in RHF//RHF anharmonic force fields can clearly be detected by substituting the associated RHF//RHF harmonic frequencies with correlated values obtained at an improved reference structure in the computation of the vibrational anharmonic constants. The dominant diagonal stretching constants are those most sensitive to geometric structure in an absolute sense, and RHF predictions for these quantities at proper reference geometries typically reproduce highly correlated predictions extremely well. The RHF cubic and quartic force constants involving bond-angle bends are also quite accurate, but the values of the higher-order, stretch–stretch coupling constants are difficult to pinpoint theoretically. In the latter cases, predictions obtained using moderate treatments of electron correlation may not be much more reliable.

It is important to understand the conceptual basis for constructing anharmonic force fields from RHF higher derivatives at a nonstationary point, *viz.*, that a shift term is being formally added to the RHF potential energy surface to bring its equilibrium point into coincidence with the reference structure. The predicted spectroscopic constants from the RHF force field are not invariant to the choice of the shift internal coordinate set. The variations in the predictions can be as large as the uncertainties expected *a priori* for the given level of theory; nevertheless, standard valence internal coordinate sets seem to give reliable results if the Cartesian gradient is not too large and there are no singularities in the coordinate set within the nuclear configuration space of concern. The use of specially designed coordinates such as Simons–Parr–Finlan or Morse variables is not recommended for the shift term because the nature of the curvilinearity exhibited therein tends to change the RHF stretching constants in the wrong direction. To circumvent ambiguities arising from the choice of shift coordinates, the Cartesian projection formalism detailed here is a viable alternative, particularly if large-amplitude bending vibrations are absent. For strongly bonded systems the results given by the Cartesian projection scheme appear to be only slightly different from those obtained using chemically relevant sets of shift coordinates. More extensive testing of this procedure is underway. In conclusion, the use of nonstationary reference structures in the determination of improved anharmonic molecular

force fields shows much promise. The primary obstacles to be overcome are the development of widespread understanding of the conceptual basis for performing vibrational analyses at nonstationary points and the establishment of standard procedures for dealing with the nonzero force dilemma.

## ACKNOWLEDGMENT

The research was supported by the U.S. National Science Foundation, Grant No. CHEM-8821737.

## APPENDIX A: HIGHER-ORDER PROJECTION MATRICES

The essential results of Sec. III D are contained in Eqs. (62)–(64), where projected Cartesian force constants are expressed in terms of their unprojected analogs transformed via the projection matrices appearing in Eqs. (53)–(56). The utility of these expressions is predicated on the fact that at each order the projection matrices are independent of the internal coordinate set  $\{s_p\}$  selected in Eqs. (53)–(56), thus allowing the shift term in Eq. (57) to be unambiguously defined. The challenge is then to derive formulas for the projection matrices which only contain derivatives of the external variables  $\{\tau_\eta\}$  with respect to the Cartesian coordinates of the system. The formalism in Appendixes A and B is constructed for the general case of nonlinear molecular reference configurations. The special case of linear molecules is discussed in Appendix C.

In order to derive expressions of the desired form, it is necessary to establish orthogonality conditions of various degrees relating the  $B_{i_1 i_2 \dots i_p}^p$  derivatives to quantities involving external variables alone. Let  $\mathbf{s}_0$  denote the internal coordinates of a molecule for a given set of lab-fixed nuclear position vectors, denoted collectively as  $\mathbf{x}$  and individually as  $\mathbf{x}_\alpha$ . The level sets of composite Cartesian vectors  $\mathbf{r}$  determined by the condition  $\mathbf{s}(\mathbf{r}) = \mathbf{s}_0$  are comprised of the collections of points  $\{\mathbf{r}_\alpha\}$  satisfying

$$\mathbf{r}_\alpha(\lambda) = - \begin{pmatrix} \lambda_1 \\ \lambda_2 \\ \lambda_3 \end{pmatrix} + \exp \left[ \begin{pmatrix} 0 & -\lambda_6 & \lambda_5 \\ \lambda_6 & 0 & -\lambda_4 \\ -\lambda_5 & \lambda_4 & 0 \end{pmatrix} \right] (\mathbf{x}_\alpha - \mathbf{R}), \quad (\text{A1})$$

where  $\lambda$  consists of translational and rotational parameters,  $(\lambda_1, \lambda_2, \lambda_3)$  and  $(\lambda_4, \lambda_5, \lambda_6)$ , respectively, lying in the domain  $(-\infty, +\infty)$ , and  $\mathbf{R}$  is an arbitrary, fixed position vector. Orthogonality conditions result from Eq. (A1) by invoking a general theorem<sup>136</sup> involving multivariable functions  $f(\mathbf{z})$ : *The gradient vector  $\nabla f(\mathbf{z}_0)$  is orthogonal to the tangent vector at  $\mathbf{z}_0$  of any smooth curve passing through this point on the level set defined by  $f(\mathbf{z}) = f_0$ .* In the current context this theorem is applied to each internal coordinate  $s_p(\mathbf{r})$ . The gradient vectors of concern are comprised simply of the quantities  $B_{j_1}^p$ , whereas the elements  $N_{j_1}^\eta$  of the  $3N$ -dimensional tangent vectors are given by the derivatives  $\mathbf{n}_{j_1}^\eta \equiv (\partial \mathbf{r}_\alpha / \partial \lambda_\eta)$ . Hence, the following first-order orthogonality condition is revealed by the theorem for all  $p$  and  $\eta$ :

$$\sum_{j_1}^{3N} B_{j_1}^p(\mathbf{x}) N_{j_1}^\eta(\mathbf{x}) = 0. \quad (\text{A2})$$

The individual tangent vectors  $\mathbf{n}_\alpha^\eta$  given by Eq. (A1) at  $\lambda = \mathbf{0}$  yield

$$N_{j_1}^\eta = \begin{cases} -\mathbf{e}_\eta \cdot \mathbf{e}_{\beta_1} & \text{for } \eta = 1, 2, 3 \\ \mathbf{e}_{\eta-3} \cdot [\mathbf{e}_{\beta_1} \times (\mathbf{x}_{\alpha_1} - \mathbf{R})] & \text{for } \eta = 4, 5, 6, \end{cases} \quad (\text{A3})$$

assuming a notation used henceforth in which  $\alpha_n = 3^{-1}[j_n + 2 - \text{mod}(j_n - 1, 3)]$  is the nucleus to which Cartesian coordinate  $x_{j_n}$  refers,  $\beta_n = j_n - 3(\alpha_n - 1)$  is the associated component of  $\mathbf{x}_{\alpha_n}$ , and  $\mathbf{e}_\gamma$  denotes the unit vector  $(\delta_{\gamma 1}, \delta_{\gamma 2}, \delta_{\gamma 3})$ .

The first-order condition embodied in Eq. (A2) is valid for all nuclear configurations  $\mathbf{x}$ , as suggested by the functional dependence indicated therein. Consequently, the differentiation of Eq. (A2) with respect to Cartesian coordinate  $x_{j_2}$  provides a second-order orthogonality condition

$$\sum_{j_1}^{3N} B_{j_1 j_2}^p N_{j_1}^\eta + \sum_{j_1}^{3N} B_{j_1}^p N_{j_1 j_2}^\eta = 0, \quad (\text{A4})$$

in which

$$N_{j_1 j_2}^\eta = \begin{cases} 0 & \text{for } \eta = 1, 2, 3 \\ \delta_{\alpha_1 \alpha_2} \mathbf{e}_{\eta-3} \cdot (\mathbf{e}_{\beta_1} \times \mathbf{e}_{\beta_2}) & \text{for } \eta = 4, 5, 6. \end{cases} \quad (\text{A5})$$

Finally, Eq. (A4) can be differentiated in turn to obtain a third-order orthogonality condition of the form

$$\sum_{j_1}^{3N} B_{j_1 j_2 j_3}^p N_{j_1}^\eta + \sum_{j_1}^{3N} (B_{j_1 j_2}^p N_{j_1 j_3}^\eta + B_{j_1 j_3}^p N_{j_1 j_2}^\eta) = 0, \quad (\text{A6})$$

since all derivatives of  $N_{j_1 j_2}^\eta$  vanish.

The tangent vector elements  $N_{j_1}^\eta$  are closely related to the first derivatives  $B_{j_1}^\eta$  of the standard set of external displacement coordinates. As shown in Appendix B, the matrix relation

$$\mathbf{N} = -\Lambda \mathbf{B}_2 \mathbf{u} \quad (\text{A7})$$

holds when the rotational derivatives  $B_{j_1}^\eta$  are evaluated at the reference orientation of the molecule, wherein  $\Lambda$  is an  $L \times L$  matrix prescribed by

$$\Lambda = \begin{bmatrix} M \mathbf{I}_3 & \mathbf{0} \\ \mathbf{0} & \mathbf{I}_0 \end{bmatrix} = \mathbf{N} \mathbf{u}^{-1} \mathbf{N}^T, \quad (\text{A8})$$

$\mathbf{u}$  is the diagonal matrix mentioned in Sec. III A containing triads of reciprocal atomic masses,  $M$  is the total molecular mass,  $\mathbf{I}_3$  is the  $3 \times 3$  identity matrix, and  $\mathbf{I}_0$  is the inertia tensor computed in the molecule-fixed axis system. In matrix form Eq. (A2) is merely  $\mathbf{N} \mathbf{B}_1^T = \mathbf{0}$ , and thus Eqs. (10) and (11) follow trivially from Eq. (A7) because  $\Lambda$  is nonsingular for nonlinear reference configurations. Despite the isomorphism of Eqs. (10) and (A2), the second-order condition expressed in Eq. (A4) does not have an analog involving  $B_{j_1 j_2}^\eta$ , i.e.,

$$\sum_{j_1}^{3N} B_{j_1 j_2}^p B_{j_1}^\eta + \sum_{j_1}^{3N} B_{j_1}^p B_{j_1 j_2}^\eta \neq 0 \quad (\text{A9})$$

because  $N_{j_1 j_2}^\eta$  represents  $(\partial^2 r_{j_1} / \partial \lambda_\eta \partial x_{j_2})_0$  with  $\mathbf{r}$  from Eq. (A1) and not  $(\partial^2 \tau_\eta / \partial x_{j_1} \partial x_{j_2})_0$ .

An important consequence of Eqs. (A7) and (A8) is that  $\mathbf{A}_2 = -\mathbf{N}^T$  and

$$\mathbf{Q} = \mathbf{A}_2 \mathbf{B}_2 = \mathbf{u}^T \mathbf{B}_2^T (\mathbf{B}_2 \mathbf{u}^T \mathbf{B}_2^T)^{-1} \mathbf{B}_2 = -\mathbf{N}^T \mathbf{B}_2, \quad (\text{A10})$$

the matrix  $\mathbf{Q}$  being the first-order projection matrix onto the external space. Equation (A4) can thus be multiplied by  $A_p^\sigma$  and  $B_{i_1}^\eta$  and successively summed over  $p$  and  $\eta$  to give

$$\sum_{j_1}^{3N} Q_{j_1 i_1} F_{\sigma j_1 j_2} = \sum_{j_1}^{3N} P_{\sigma j_1} \Gamma_{j_1 j_2 i_1}, \quad (\text{A11})$$

where

$$\Gamma_{j_1 j_2 j_3 \dots j_n} = \sum_{\eta} N_{j_1 j_2}^\eta B_{j_3 \dots j_n}^\eta = \delta_{\alpha_1 \alpha_2} (\mathbf{e}_{\beta_1} \times \mathbf{e}_{\beta_2}) \cdot \mathbf{k}^{\alpha_3 \beta_3 \dots \alpha_n \beta_n}. \quad (\text{A12})$$

The form involving  $\mathbf{k}^{\alpha_3 \beta_3 \dots \alpha_n \beta_n}$  in Eq. (A12) assumes a notation used henceforth in which  $\mathbf{t}$  and  $\mathbf{k}$  are three-dimensional vectors containing the translational and rotational variables, respectively, and superscripts on these quantities denote derivatives with respect to a component  $\beta$  of the Cartesian vector for atom  $\alpha$ . The result of Eq. (A11) is very useful in replacing terms involving  $F_{\sigma j_1 j_2}$ , which is defined by direct reference to a specific internal coordinate set, with terms containing  $\Gamma_{j_1 j_2 j_3}$ , which depends only on external variables. In an analogous fashion, Eq. (A6) yields

$$\sum_{j_1}^{3N} Q_{j_1 i_1} F_{\sigma j_1 j_2 j_3} = \sum_{j_1}^{3N} (F_{\sigma j_1 j_2} \Gamma_{j_1 j_3 i_1} + F_{\sigma j_1 j_3} \Gamma_{j_1 j_2 i_1}), \quad (\text{A13})$$

which later provides a key first step in the reduction of  $F_{\sigma j_1 j_2 j_3}$  to quantities involving external variables alone.

The mathematical form for the first-order projection matrix  $\mathbf{P} = \mathbf{A}_1 \mathbf{B}_1$  is well known. Since  $\mathbf{Y}$  in Eq. (14) is equivalent to the  $3N \times 3N$  identity matrix  $\mathbf{I}_{3N}$ ,

$$\mathbf{P} = \mathbf{I}_{3N} - \mathbf{Q} = \mathbf{I}_{3N} + \mathbf{N}^T \mathbf{B}_2. \quad (\text{A14})$$

This equation can be simplified to a form involving derivatives of  $\mathbf{t}$  and  $\mathbf{k}$ , namely,

$$P_{\alpha_1 \beta_1, \alpha_2 \beta_2} = \delta_{\alpha_1 \alpha_2} \delta_{\beta_1 \beta_2} - \mathbf{e}_{\beta_1} \cdot \boldsymbol{\rho}_{\alpha_1}^{\alpha_2 \beta_2}, \quad (\text{A15})$$

where

$$\boldsymbol{\rho}_{\alpha_1}^{\alpha_2 \beta_2} \equiv \mathbf{t}^{\alpha_2 \beta_2} + \mathbf{k}^{\alpha_2 \beta_2} \times (\mathbf{x}_{\alpha_1} - \mathbf{R}). \quad (\text{A16})$$

If a canonical set  $\{\tau_\eta^o\}$  of external displacement variables is assumed, then  $\mathbf{u} = \mathbf{I}_{3N}$  in Eqs. (12) and (13). The resulting  $\mathbf{P}^o$  and  $\mathbf{Q}^o$  matrices are symmetric and satisfy the simplified relation

$$\mathbf{P}^o = \mathbf{B}_1^T [\mathbf{B}_1 \mathbf{B}_1^T]^{-1} \mathbf{B}_1 = \mathbf{I}_{3N} - \mathbf{Q}^o = \mathbf{I}_{3N} - \mathbf{N}^T [\mathbf{N} \mathbf{N}^T]^{-1} \mathbf{N}.$$

The derivation of the expression for  $P_{\sigma i_1 i_2}$  begins by noting that the first term in Eq. (54) is simply  $F_{\sigma i_1 i_2}$  by definition, whereas the second term satisfies

$$H_{\sigma i_1 i_2} \equiv \sum_{\rho_1 \rho_2}^M A_{\rho_1 \rho_2}^\sigma B_{i_1}^{\rho_1} B_{i_2}^{\rho_2} = - \sum_{j_1 j_2}^{3N} P_{j_1 i_1} P_{j_2 i_2} (F_{\sigma j_1 j_2} + G_{\sigma j_1 j_2}) \quad (\text{A17})$$

as a consequence of Eq. (25). Hence,

$$P_{\sigma i_1 i_2} = F_{\sigma i_1 i_2} + H_{\sigma i_1 i_2} = \sum_{j_1 j_2}^{3N} (\delta_{j_1 i_1} \delta_{j_2 i_2} - P_{j_1 i_1} P_{j_2 i_2}) F_{\sigma j_1 j_2} - \sum_{j_1 j_2}^{3N} P_{j_1 i_1} P_{j_2 i_2} G_{\sigma j_1 j_2}. \quad (\text{A18})$$

As shown by Eq. (A14), the Kronecker  $\delta$  symbols in Eq. (A18) can be replaced using  $\delta_{i_1 i_2} = P_{i_1 i_2} + Q_{i_1 i_2}$ , and after some rearrangement

$$P_{\sigma i_1 i_2} = \sum_{j_1 j_2}^{3N} (P_{j_2 i_2} Q_{j_1 i_1} + \delta_{j_1 i_1} Q_{j_2 i_2}) F_{\sigma j_1 j_2} - \sum_{j_1 j_2}^{3N} P_{j_1 i_1} P_{j_2 i_2} G_{\sigma j_1 j_2} \quad (\text{A19})$$

is obtained. Because each  $F_{\sigma i_1 i_2}$  term in Eq. (A19) is accompanied by a factor involving a component of  $\mathbf{Q}$ , Eq. (A11) can be invoked to provide  $P_{\sigma i_1 i_2}$  in terms of  $P_{\sigma i_1}$  and  $G_{\sigma i_1 i_2}$  only. The resulting final form for  $P_{\sigma i_1 i_2}$  is

$$P_{\sigma i_1 i_2} = \sum_{j_1}^{3N} P_{\sigma j_1} \Theta_{j_1 i_1 i_2} - \sum_{j_1 j_2}^{3N} P_{j_1 i_1} P_{j_2 i_2} G_{\sigma j_1 j_2}, \quad (\text{A20})$$

where

$$\Theta_{j_1 i_1 i_2} \equiv \Gamma_{j_1 i_1 i_2} + \sum_{j_2}^{3N} P_{j_2 i_2} \Gamma_{j_1 j_2 i_1} = \Gamma_{j_1 i_1 i_2} + \Gamma_{j_1 i_2 i_1} + \Xi_{j_1 i_1 i_2}, \quad (\text{A21})$$

and

$$\Xi_{j_1 j_2 j_3} \equiv - \sum_{i_1}^{3N} \Gamma_{j_1 i_1 j_2} Q_{i_1 j_3} = \mathbf{e}_{\beta_1} \cdot (\mathbf{k}^{\alpha_2 \beta_2, \alpha_3 \beta_3, \dots, \alpha_n \beta_n}). \quad (\text{A22})$$

To facilitate the evaluation of the second-order projection matrix via Eq. (A20), it is useful to note that Eq. (27) reduces to

$$G_{j_1 j_2 \dots j_n} = [(\mathbf{x}_{\alpha_1} - \mathbf{R}) \times \mathbf{e}_{\beta_1}] \cdot \mathbf{k}^{\alpha_2 \beta_2, \alpha_3 \beta_3, \dots, \alpha_n \beta_n}. \quad (\text{A23})$$

The manipulations required to derive an appropriate form for the third-order projection matrix  $P_{\sigma i_1 i_2 i_3}$  proceed in an analogous fashion to the  $P_{\sigma i_1 i_2}$  case but are significantly more involved. By employing Eq. (29) the following result is obtained for the quantity  $H_{\sigma i_1 i_2 i_3}$ , which comprises the third term in Eq. (55) for  $P_{\sigma i_1 i_2 i_3}$ :

$$H_{\sigma i_1 i_2 i_3} \equiv \sum_{\rho_1 \rho_2 \rho_3}^M A_{\rho_1 \rho_2 \rho_3}^\sigma B_{i_1}^{\rho_1} B_{i_2}^{\rho_2} B_{i_3}^{\rho_3} = - \sum_{j_1 j_2}^{3N} (P_{j_1 i_1} H_{j_2 i_2 i_3} + P_{j_1 i_2} H_{j_2 i_1 i_3} + P_{j_1 i_3} H_{j_2 i_1 i_2}) \times (F_{\sigma j_1 j_2} + G_{\sigma j_1 j_2}) - \sum_{j_1 j_2 j_3}^{3N} P_{j_1 i_1} P_{j_2 i_2} P_{j_3 i_3} \times (F_{\sigma j_1 j_2 j_3} + G_{\sigma j_1 j_2 j_3}). \quad (\text{A24})$$

A useful modification of the second term in Eq. (55),  $L_{\sigma i_1 i_2 i_3}$ , can be achieved via Eq. (25), viz.,

$$L_{\sigma i_1 i_2 i_3} \equiv \sum_{\rho_1 \rho_2}^M A_{\rho_1 \rho_2}^\sigma (B_{i_1}^{\rho_1} B_{i_2 i_3}^{\rho_2} + B_{i_2}^{\rho_1} B_{i_1 i_3}^{\rho_2} + B_{i_3}^{\rho_1} B_{i_1 i_2}^{\rho_2}) = - \sum_{j_1 j_2}^{3N} (P_{j_1 i_1} F_{j_2 i_2 i_3} + P_{j_1 i_2} F_{j_2 i_1 i_3} + P_{j_1 i_3} F_{j_2 i_1 i_2}) \times (F_{\sigma j_1 j_2} + G_{\sigma j_1 j_2}). \quad (\text{A25})$$

These results can then be combined to provide an important intermediate expression for  $P_{\sigma i_1 i_2 i_3}$ :

$$P_{\sigma i_1 i_2 i_3} = F_{\sigma i_1 i_2 i_3} + L_{\sigma i_1 i_2 i_3} + H_{\sigma i_1 i_2 i_3} = \sum_{j_1 j_2 j_3}^{3N} (\delta_{j_1 i_1} \delta_{j_2 i_2} \delta_{j_3 i_3} - P_{j_1 i_1} P_{j_2 i_2} P_{j_3 i_3}) F_{\sigma j_1 j_2 j_3} - \sum_{j_1 j_2 j_3}^{3N} P_{j_1 i_1} P_{j_2 i_2} P_{j_3 i_3} G_{\sigma j_1 j_2 j_3} - \sum_{j_1 j_2}^{3N} (P_{j_1 i_1} P_{j_2 i_2 i_3} + P_{j_1 i_2} P_{j_2 i_1 i_3} + P_{j_1 i_3} P_{j_2 i_1 i_2}) (F_{\sigma j_1 j_2} + G_{\sigma j_1 j_2}). \quad (\text{A26})$$

The first term in Eq. (A26), denoted as  $S_{\sigma i_1 i_2 i_3}$ , can be reduced as before by replacing each Kronecker  $\delta$  symbol with the sum  $\delta_{i_1 i_2} = P_{i_1 i_2} + Q_{i_1 i_2}$ , hence

$$S_{\sigma i_1 i_2 i_3} \equiv \sum_{j_1 j_2 j_3}^{3N} (\delta_{j_1 i_1} \delta_{j_2 i_2} \delta_{j_3 i_3} - P_{j_1 i_1} P_{j_2 i_2} P_{j_3 i_3}) F_{\sigma j_1 j_2 j_3} = \sum_{j_1 j_2 j_3}^{3N} (P_{j_1 i_1} P_{j_2 i_2} Q_{j_3 i_3} + P_{j_1 i_1} Q_{j_2 i_2} \delta_{j_3 i_3} + Q_{j_1 i_1} \delta_{j_2 i_2} \delta_{j_3 i_3}) F_{\sigma j_1 j_2 j_3}. \quad (\text{A27})$$

Subsequently all terms involving  $F_{\sigma i_1 i_2 i_3}$  can be replaced using Eq. (A13) to provide

$$S_{\sigma i_1 i_2 i_3} = \sum_{j_1 j_2}^{3N} F_{\sigma j_1 j_2} (P_{j_1 i_1} \Theta_{j_2 j_3 i_2} + P_{j_1 i_2} \Theta_{j_2 j_3 i_1} + P_{j_1 i_3} \Theta_{j_2 j_3 i_1}) + Q_{j_1 i_1} \Gamma_{j_2 j_3 i_1} + Q_{j_1 i_3} \Theta_{j_2 j_3 i_1}. \quad (\text{A28})$$

Accordingly, Eq. (A26) can be written in the form

$$\begin{aligned}
P_{\sigma i_1 i_2 i_3} = & T_{\sigma i_1 i_2 i_3} + \sum_{j_1 j_2}^{3N} F_{\sigma j_1 j_2} [P_{j_1 i_1} (\Theta_{j_2 i_3 i_2} - P_{j_2 i_3 i_2}) \\
& + P_{j_1 i_2} (\Theta_{j_2 i_3 i_1} - P_{j_2 i_3 i_1}) + P_{j_1 i_3} (\Theta_{j_2 i_2 i_1} - P_{j_2 i_2 i_1})] \\
& + \sum_{j_1 j_2}^{3N} F_{\sigma j_1 j_2} (\mathcal{Q}_{j_1 i_2} \Gamma_{j_2 i_3 i_1} + \mathcal{Q}_{j_1 i_3} \Theta_{j_2 i_2 i_1}), \quad (A29)
\end{aligned}$$

where

$$\begin{aligned}
T_{\sigma i_1 i_2 i_3} \equiv & - \sum_{j_1 j_2 j_3}^{3N} P_{j_1 i_1} P_{j_2 i_2} P_{j_3 i_3} G_{\sigma j_1 j_2 j_3} - \sum_{j_1 j_2}^{3N} (P_{j_1 i_1} P_{j_2 i_2 i_3} \\
& + P_{j_1 i_2} P_{j_2 i_1 i_3} + P_{j_1 i_3} P_{j_2 i_1 i_2}) G_{\sigma j_1 j_2}. \quad (A30)
\end{aligned}$$

By some means the  $F_{\sigma i_1 i_2}$  terms in Eq. (A29) must be eliminated, and the key observation for this purpose is that

$$\begin{aligned}
\Theta_{\sigma i_2 i_1} - P_{\sigma i_1 i_2} = & \Xi_{\sigma i_2 i_1} - \Xi_{\sigma i_1 i_2} + \sum_{j_1}^{3N} \mathcal{Q}_{\sigma j_1} \Theta_{j_1 i_1 i_2} \\
& + \sum_{j_1 j_2}^{3N} P_{j_1 i_1} P_{j_2 i_2} G_{\sigma j_1 j_2}. \quad (A31)
\end{aligned}$$

Upon substitution of Eq. (A31) into Eq. (A29), it is found after invoking Eq. (A11) that

$$\begin{aligned}
P_{\sigma i_1 i_2 i_3} = & T_{\sigma i_1 i_2 i_3} + \sum_{j_1 j_2 j_3}^{3N} P_{\sigma j_2} \Gamma_{j_2 j_1 j_3} (P_{j_1 i_3} \Theta_{j_3 i_1 i_2} + P_{j_1 i_2} \Theta_{j_3 i_1 i_3} \\
& + P_{j_1 i_1} \Theta_{j_3 i_2 i_3}) + \sum_{j_1}^{3N} (P_{j_1 i_3} \Delta_{\sigma j_1 i_1 i_2} + P_{j_1 i_2} \Delta_{\sigma j_1 i_1 i_3} \\
& + P_{j_1 i_1} \Delta_{\sigma j_1 i_2 i_3}) + \sum_{j_1 j_2 j_3}^{3N} P_{j_1 i_1} P_{j_2 i_2} P_{j_3 i_3} (R_{\sigma j_1 j_2 j_3} \\
& + R_{\sigma j_2 j_1 j_3} + R_{\sigma j_3 j_1 j_2}) + \sum_{j_1 j_2}^{3N} P_{\sigma j_1} (\Gamma_{j_1 j_2 i_2} \Gamma_{j_2 i_3 i_1} \\
& + \Gamma_{j_1 j_2 i_3} \Theta_{j_2 i_2 i_1}), \quad (A32)
\end{aligned}$$

where

$$\Delta_{\sigma i_1 i_2 i_3} \equiv \sum_{j_2}^{3N} F_{\sigma i_1 j_2} (\Xi_{j_2 i_3 i_2} - \Xi_{j_2 i_2 i_3}) = \omega_{\sigma i_1} \cdot (\mathbf{k}^{\alpha_2 \beta_2} \times \mathbf{k}^{\alpha_3 \beta_3}), \quad (A33)$$

$$(\omega_{\sigma i_1})_{\eta} = - \sum_{j_2}^{3N} P_{\sigma j_2} N_{j_2 i_1}^{\eta}, \quad (A34)$$

and

$$R_{\sigma i_1 i_2 i_3} \equiv \sum_{j_1}^{3N} F_{\sigma i_1 j_1} G_{j_1 i_2 i_3} = \sum_{j_1}^{3N} P_{\sigma j_1} \Gamma_{j_1 i_1 i_2 i_3}. \quad (A35)$$

The reductions of  $\Delta_{\sigma i_1 i_2 i_3}$  and  $R_{\sigma i_1 i_2 i_3}$  in Eqs. (A33) and (A35) to the forms on the right sides therein, which contain no reference to internal coordinates, proceed by ex-

pansion of  $F_{\sigma j_1 j_2}$  and  $G_{\sigma j_1 j_2}$  according to Eqs. (26) and (27) followed by substitutions arising from Eq. (A4). Finally, by defining

$$M_{\sigma i_1 i_2 i_3} \equiv \Delta_{\sigma i_1 i_2 i_3} - \sum_{j_2}^{3N} G_{\sigma i_1 j_2} P_{j_2 i_2 i_3} + \sum_{j_2 j_3}^{3N} P_{\sigma j_2} \Gamma_{j_2 i_1 j_3} \Theta_{j_3 i_2 i_3}, \quad (A36)$$

a final form for the third-order projection matrix is found:

$$\begin{aligned}
P_{\sigma i_1 i_2 i_3} = & \sum_{j_1 j_2 j_3}^{3N} P_{j_1 i_1} P_{j_2 i_2} P_{j_3 i_3} (R_{\sigma j_1 j_2 j_3} + R_{\sigma j_2 j_1 j_3} + R_{\sigma j_3 j_1 j_2} \\
& - G_{\sigma j_1 j_2 j_3}) + \sum_{j_1}^{3N} (P_{j_1 i_1} M_{\sigma j_1 i_2 i_3} + P_{j_1 i_2} M_{\sigma j_1 i_1 i_3} \\
& + P_{j_1 i_3} M_{\sigma j_1 i_1 i_2}) + \sum_{j_1 j_2}^{3N} P_{\sigma j_1} (\Gamma_{j_1 j_2 i_2} \Gamma_{j_2 i_3 i_1} \\
& + \Gamma_{j_1 j_2 i_3} \Theta_{j_2 i_2 i_1}). \quad (A37)
\end{aligned}$$

All quantities appearing in this equation can be evaluated from expressions involving external variables alone, viz. Eqs. (A12), (A15), (A16), (A20)–(A23), and (A33)–(A35).

## APPENDIX B: HIGHER-ORDER DERIVATIVES OF EXTERNAL DISPLACEMENT VARIABLES

In Appendix A, Eqs. (A15), (A20), and (A37) were presented which allow the projection matrices  $P_{\sigma i_1}$ ,  $P_{\sigma i_1 i_2}$ , and  $P_{\sigma i_1 i_2 i_3}$ , respectively, to be determined solely from the derivatives of the external displacement variables  $\tau_{\eta}$ . Thus, the procedure for performing higher-order projections of Cartesian force constants at nonstationary points is fully specified upon the formulation of higher-order derivatives of the  $\tau_{\eta}$  variables. A formalism for accomplishing this task is detailed in this section.

The generalized external displacement variables specify the position and orientation of the molecule-fixed coordinate system relative to the lab-fixed system. In particular, the Cartesian coordinates in the two frames,  $\mathbf{x}^{\text{mol}}$  and  $\mathbf{x}$ , respectively, are related by

$$\mathbf{x} = \mathbf{R} + \mathcal{U}(\theta, \phi, \chi) \mathbf{x}^{\text{mol}}, \quad (B1)$$

where vector  $\mathbf{R}$  connects the origins of the two systems, and  $\mathcal{U}$  is a  $3 \times 3$  orthogonal matrix which may be considered a function of the three Euler angles of orientation  $\theta$ ,  $\phi$ , and  $\chi$ . The  $\mathcal{U}$  matrix in Eq. (B1) can alternatively be represented as  $e^{\kappa}$ , where  $\kappa$  is a  $3 \times 3$  antisymmetric matrix containing three rotational parameters  $\mathbf{k} = (k_1, k_2, k_3)$ ; specifically,

$$\kappa = \begin{pmatrix} 0 & -k_3 & k_2 \\ k_3 & 0 & -k_1 \\ -k_2 & k_1 & 0 \end{pmatrix}. \quad (B2)$$

By selecting the translational variables  $\mathbf{t} = (t_1, t_2, t_3)$  as the components of  $\mathbf{R}$ , the full parametric dependence of  $\mathbf{x}$  on the internal ( $\mathbf{s}$ ) and external ( $\boldsymbol{\tau}$ ) variables thus becomes

$$\mathbf{x}(\mathbf{s}, \boldsymbol{\tau}) = \mathbf{t} + e^{\kappa} \mathbf{x}^{\text{mol}}(\mathbf{s}). \quad (B3)$$

There are many choices of conditions which prescribe the attachment of the molecule-fixed axes to the molecular system, thus specifying  $\mathbf{x}^{\text{mol}}$  as a function of the internal variables alone. The six Sayvetz conditions,<sup>56,59</sup> which are also referred to as the Eckart conditions<sup>58</sup> by many authors, are the most widely used. The first three Sayvetz conditions,

$$\sum_{\alpha}^N m_{\alpha} \mathbf{x}_{\alpha}^{\text{mol}} = \sum_{\alpha}^N m_{\alpha} e^{-\kappa} (\mathbf{x}_{\alpha} - \mathbf{t}) = \mathbf{0}, \quad (\text{B4})$$

are satisfied trivially by selecting  $\mathbf{t}$  as the position of the center of mass, i.e.,

$$\mathbf{t} = M^{-1} \sum_{\alpha}^N m_{\alpha} \mathbf{x}_{\alpha}, \quad (\text{B5})$$

where  $m_{\alpha}$  is the mass of nucleus  $\alpha$ , and  $M$  is the total mass of the system. The last three Sayvetz conditions,

$$\sum_{\alpha}^N m_{\alpha} (\mathbf{a}_{\alpha} \times \mathbf{x}_{\alpha}^{\text{mol}}) = \sum_{\alpha}^N m_{\alpha} [\mathbf{a}_{\alpha} \times e^{-\kappa} (\mathbf{x}_{\alpha} - \mathbf{t})] = \mathbf{0}, \quad (\text{B6})$$

determine the values of the rotational variables. Implicit in Eq. (B6) is the choice of an arbitrary, fixed reference orientation of the molecule represented by the nuclear position vectors  $\mathbf{a}_{\alpha}$ , which are subject to the center-of-mass condition

$$\sum_{\alpha}^N m_{\alpha} \mathbf{a}_{\alpha} = \mathbf{0}. \quad (\text{B7})$$

As a consequence of Eq. (B7), the conditions which determine the rotational parameters  $\mathbf{k}$  become

$$\sum_{\alpha}^N m_{\alpha} (\mathbf{a}_{\alpha} \times \mathbf{y}_{\alpha}) = \mathbf{0}, \quad (\text{B8})$$

in which

$$\mathbf{y}_{\alpha} \equiv e^{-\kappa} \mathbf{x}_{\alpha}. \quad (\text{B9})$$

In analyses of molecular vibration-rotation dynamics, the internal coordinates underlying the reference positions  $\mathbf{a}_{\alpha}$  usually correspond to the equilibrium geometry of the system, but for convenience here, the  $\mathbf{a}_{\alpha}$  vectors are chosen as  $\mathbf{x}_{\alpha}^{\text{ref}} - \mathbf{t}^{\text{ref}}$  to represent the nonstationary reference geometry at which the unprojected Cartesian force field is computed. Thus by construction the solution to Eq. (B8) at the geometry at which the  $\mathbf{t}$  and  $\mathbf{k}$  derivatives are to be determined is  $\mathbf{k} = \mathbf{0}$ , a fact greatly facilitating the evaluation of these quantities.

The Sayvetz conditions define a canonical set of external variables satisfying Eq. (10) only if all nuclear masses are identical. However, the Cartesian projection formalism presented above is valid for arbitrary choices of the  $\{m_{\alpha}\}$  set. The mass dependence due to the specification of the external variables by the Sayvetz conditions is contained completely in the  $\mathbf{t}$  and  $\mathbf{k}$  derivatives occurring in Appendix A, and thus is incorporated by the general formulas presented below for arbitrary nuclear masses. It should be recognized that the projected higher-order Cartesian force constants are mass invariant for the triatomic systems in-

vestigated here but do not possess this property in general. Therefore, the spectroscopic constants derived from projected Cartesian force fields generated with mass-dependent external variables may differ slightly from those derived using canonical sets of external variables defined for identical masses.

The first derivative of the translational variables in Eq. (B5) with respect to Cartesian component  $\beta$  of nucleus  $l$  ( $\beta = x, y, \text{ or } z, \text{ and } l = 1, 2, \dots, N$ ) is simply given by

$$\mathbf{t}^{l\beta} = \left( \frac{m_l}{M} \right) \mathbf{e}_{\beta}, \quad (\text{B10})$$

where  $\mathbf{e}_{\beta} = (1, 0, 0)$ ,  $(0, 1, 0)$ , or  $(0, 0, 1)$  depending on whether  $\beta = x, y, \text{ or } z$ , respectively, and the superscript  $l\beta$  denotes the derivative of concern. Taking the  $l\beta$  derivative of Eq. (B9) and evaluating the result at  $\mathbf{k} = \mathbf{0}$  yields

$$\mathbf{y}_{\alpha}^{l\beta} = -\kappa^{l\beta} (\mathbf{t}^{\text{ref}} + \mathbf{a}_{\alpha}) + \mathbf{x}_{\alpha}^{l\beta} = -\mathbf{k}^{l\beta} \times (\mathbf{t}^{\text{ref}} + \mathbf{a}_{\alpha}) + \mathbf{x}_{\alpha}^{l\beta}. \quad (\text{B11})$$

Substitution of this equation into the first derivative of Eq. (B8) provides the following relation for the derivatives of the rotational parameters at  $\mathbf{k} = \mathbf{0}$ :

$$\mathbf{I}_0 \mathbf{k}^{l\beta} = m_l (\mathbf{a}_l \times \mathbf{e}_{\beta}), \quad (\text{B12})$$

where  $\mathbf{I}_0$  is the  $3 \times 3$  inertia tensor in the center-of-mass frame at the reference geometry, i.e.,

$$(\mathbf{I}_0)_{\gamma\delta} = \sum_{\alpha}^N m_{\alpha} [(a_{\alpha,x}^2 + a_{\alpha,y}^2 + a_{\alpha,z}^2) \delta_{\gamma\delta} - a_{\alpha,\gamma} a_{\alpha,\delta}]. \quad (\text{B13})$$

The first derivatives  $\mathbf{k}^{l\beta}$  can then be found by inversion of  $\mathbf{I}_0$  in Eq. (B12). By comparing Eqs. (B10) and (B12) with Eq. (A3), the relationship between the tangent vector elements  $N_{j_1}^{\eta}$  and the derivatives  $B_{j_1}^{\eta}$  is revealed, as embodied in Eq. (A7) above. The derivative relations of Eqs. (B10) and (B12) give the same results for the  $\mathbf{B}_2$  matrix reported by many other authors. The crux is that in this formalism higher-order derivatives follow readily.

The second derivatives of  $\mathbf{y}_{\alpha}$  with respect to Cartesian coordinates  $l\beta$  and  $m\gamma$  are obtained straightforwardly from Eq. (B9) as

$$\begin{aligned} \mathbf{y}_{\alpha}^{l\beta, m\gamma} &= -\kappa^{l\beta, m\gamma} (\mathbf{t}^{\text{ref}} + \mathbf{a}_{\alpha}) + \mathbf{w}_{\alpha}^{l\beta, m\gamma} \\ &= -\mathbf{k}^{l\beta, m\gamma} \times (\mathbf{t}^{\text{ref}} + \mathbf{a}_{\alpha}) + \mathbf{w}_{\alpha}^{l\beta, m\gamma} \end{aligned} \quad (\text{B14})$$

upon evaluation at  $\mathbf{k} = \mathbf{0}$ , provided that

$$\begin{aligned} \mathbf{w}_{\alpha}^{l\beta, m\gamma} &\equiv -\kappa^{l\beta} \mathbf{x}_{\alpha}^{m\gamma} - \kappa^{m\gamma} \mathbf{x}_{\alpha}^{l\beta} + \frac{1}{2} (\kappa^{l\beta} \kappa^{m\gamma} + \kappa^{m\gamma} \kappa^{l\beta}) (\mathbf{t}^{\text{ref}} + \mathbf{a}_{\alpha}) \\ &= -(\mathbf{k}^{l\beta} \times \mathbf{x}_{\alpha}^{m\gamma}) - (\mathbf{k}^{m\gamma} \times \mathbf{x}_{\alpha}^{l\beta}) \\ &\quad + \frac{1}{2} \mathbf{k}^{l\beta} \times [\mathbf{k}^{m\gamma} \times (\mathbf{t}^{\text{ref}} + \mathbf{a}_{\alpha})] \\ &\quad + \frac{1}{2} \mathbf{k}^{m\gamma} \times [\mathbf{k}^{l\beta} \times (\mathbf{t}^{\text{ref}} + \mathbf{a}_{\alpha})]. \end{aligned} \quad (\text{B15})$$

Thus, from the second derivative of Eq. (B8) it follows that

$$\begin{aligned} \mathbf{I}_0 \mathbf{k}^{l\beta, m\gamma} &= \sum_{\alpha}^N m_{\alpha} (\mathbf{a}_{\alpha} \times \mathbf{w}_{\alpha}^{l\beta, m\gamma}) \\ &= m_l [(\mathbf{a}_l \cdot \mathbf{k}^{m\gamma}) \mathbf{e}_{\beta} - (\mathbf{a}_l \cdot \mathbf{e}_{\beta}) \mathbf{k}^{m\gamma}] + m_m [(\mathbf{a}_m \cdot \mathbf{k}^{l\beta}) \mathbf{e}_{\gamma} \\ &\quad - (\mathbf{a}_m \cdot \mathbf{e}_{\gamma}) \mathbf{k}^{l\beta}] + \frac{1}{2} \sum_{\alpha}^N m_{\alpha} [(\mathbf{a}_{\alpha} \cdot \mathbf{k}^{l\beta}) (\mathbf{a}_{\alpha} \times \mathbf{k}^{m\gamma}) \\ &\quad + (\mathbf{a}_{\alpha} \cdot \mathbf{k}^{m\gamma}) (\mathbf{a}_{\alpha} \times \mathbf{k}^{l\beta})]. \end{aligned} \quad (\text{B16})$$

Analogously, the results for the third-derivative quantities are

$$\begin{aligned} \mathbf{y}_{\alpha}^{l\beta, m\gamma, n\delta} &= -\mathbf{k}^{l\beta, m\gamma, n\delta} (\mathbf{t}^{\text{ref}} + \mathbf{a}_{\alpha}) + \mathbf{w}_{\alpha}^{l\beta, m\gamma, n\delta} \\ &= -\mathbf{k}^{l\beta, m\gamma, n\delta} \times (\mathbf{t}^{\text{ref}} + \mathbf{a}_{\alpha}) + \mathbf{w}_{\alpha}^{l\beta, m\gamma, n\delta}, \end{aligned} \quad (\text{B17})$$

where

$$\begin{aligned} \mathbf{w}_{\alpha}^{l\beta, m\gamma, n\delta} &\equiv \mathbf{v}_{\alpha}(l\beta, m\gamma, n\delta) + \mathbf{v}_{\alpha}(l\beta, n\delta, m\gamma) \\ &\quad + \mathbf{v}_{\alpha}(m\gamma, l\beta, n\delta) + \mathbf{v}_{\alpha}(n\delta, l\beta, m\gamma) \\ &\quad + \mathbf{v}_{\alpha}(n\delta, m\gamma, l\beta) + \mathbf{v}_{\alpha}(m\gamma, n\delta, l\beta), \end{aligned} \quad (\text{B18})$$

and

$$\begin{aligned} \mathbf{v}_{\alpha}(l\beta, m\gamma, n\delta) &= \frac{1}{4} (\mathbf{k}^{l\beta, m\gamma} \mathbf{k}^{n\delta} + \mathbf{k}^{n\delta} \mathbf{k}^{l\beta, m\gamma}) (\mathbf{t}^{\text{ref}} + \mathbf{a}_{\alpha}) \\ &\quad - \frac{1}{6} \mathbf{k}^{l\beta} \mathbf{k}^{m\gamma} \mathbf{k}^{n\delta} (\mathbf{t}^{\text{ref}} + \mathbf{a}_{\alpha}) - \frac{1}{2} \mathbf{k}^{l\beta, m\gamma} \mathbf{x}_{\alpha}^{n\delta} \\ &\quad + \frac{1}{2} \mathbf{k}^{l\beta} \mathbf{k}^{m\gamma} \mathbf{x}_{\alpha}^{n\delta}. \end{aligned} \quad (\text{B19})$$

Therefore, from Eq. (B8)

$$\begin{aligned} \mathbf{I}_0 \mathbf{k}^{l\beta, m\gamma, n\delta} &= \sum_{\alpha}^N m_{\alpha} (\mathbf{a}_{\alpha} \times \mathbf{w}_{\alpha}^{l\beta, m\gamma, n\delta}) \\ &= \sum_{\mathcal{P}} \left\{ \frac{1}{2} m_p [(\mathbf{a}_p \cdot \mathbf{k}^{q\nu, r\sigma}) \mathbf{e}_{\mu} - (\mathbf{a}_p \cdot \mathbf{e}_{\mu}) \mathbf{k}^{q\nu, r\sigma} + (\mathbf{k}^{q\nu} \cdot \mathbf{e}_{\mu}) (\mathbf{a}_p \times \mathbf{k}^{r\sigma})] - \frac{1}{3} m_p (\mathbf{k}^{q\nu} \cdot \mathbf{k}^{r\sigma}) (\mathbf{a}_p \times \mathbf{e}_{\mu}) \right. \\ &\quad \left. + \frac{1}{4} \sum_{\alpha}^N m_{\alpha} [(\mathbf{a}_{\alpha} \cdot \mathbf{k}^{q\nu, r\sigma}) (\mathbf{a}_{\alpha} \times \mathbf{k}^{l\mu}) + (\mathbf{a}_{\alpha} \cdot \mathbf{k}^{l\mu}) (\mathbf{a}_{\alpha} \times \mathbf{k}^{q\nu, r\sigma})] \right\}, \end{aligned} \quad (\text{B20})$$

in which the sum on the right side is over all permutations  $\mathcal{P}(l\beta, m\gamma, n\delta) = (p\mu, q\nu, r\sigma)$ . By inverting  $\mathbf{I}_0$  in Eqs. (B16) and (B20),  $\mathbf{k}^{l\beta, m\gamma}$  and  $\mathbf{k}^{l\beta, m\gamma, n\delta}$  are evaluated, allowing the  $G_{j_1 j_2 j_3}$ ,  $G_{j_1 j_2 j_3 j_4}$ , and  $\Gamma_{j_1 j_2 j_3 j_4}$  matrices in Eqs. (A23) and (A12) to be computed and completing the determination of  $P_{\sigma i_1 i_2}$  and  $P_{\sigma i_1 i_2 i_3}$ .

### APPENDIX C: MODIFICATION OF THE CARTESIAN PROJECTION SCHEME FOR LINEAR MOLECULES

The partitioning of the internal and external variables of a molecular system must be reconsidered in order to apply the Cartesian projection scheme of Sec. III D to linear molecular reference configurations. While the potential energy function of an N-atom molecule is fully specified by  $3N-6$  internal variables for all nuclear configurations, transformations between Cartesian and internal spaces become indeterminate for linear structures unless the external space partition includes only two rotational variables. The axis containing the nuclear centers defines the molecule-fixed  $z$  axis at the linear reference configuration, and the Sayvetz conditions determine the orientation of this axis for arbitrary displacements from linearity. By setting  $k_3$  and all of its derivatives to zero, all formulas in Appendix B are applicable, provided that the vanishing  $z$  components of the inertia tensor are discarded in Eqs. (B12), (B16), and (B20), which are understood to be  $2 \times 2$  linear systems for the derivatives of  $k_1$  and  $k_2$  alone. The  $3N-5$  dimensional "internal" space is that which re-

mains after  $k_1$  and  $k_2$  and the translational variables  $\mathbf{t}$  are partitioned into the external space. Assuming the atoms are indexed from 1 to N in order of increasing  $z$ , the internuclear distances  $r_{\alpha} = |\mathbf{x}_{\alpha+1} - \mathbf{x}_{\alpha}|$  for  $\alpha = 1, 2, \dots, N-1$  suffice for  $N-1$  of the internal variables. Two linear bending coordinates,  $\theta_{\alpha}^x$  and  $\theta_{\alpha}^y$ , for each atom  $\alpha = 3, 4, \dots, N$  complete the specification of the "internal" space. It is critical to explicitly define these variables for all instantaneous linear and nonlinear configurations. Here  $\theta_{\alpha}^x$  and  $\theta_{\alpha}^y$  are taken to be the  $x$  and  $y$  components of the unit vector directed from  $\alpha-1$  to  $\alpha$  in a local coordinate frame in which the  $(\alpha-2) - (\alpha-1)$  bond axis defines the  $z$  direction and the component of the space-fixed  $X$  axis orthogonal to this bond vector is the local  $x$  direction. These linear bending variables are invariant to molecular translations as well as changes in the polar and azimuthal angles ( $\lambda_4$  and  $\lambda_5$ ) of the molecular system relative to the space-fixed  $X$  axis. Accordingly, the analog of Eq. (A1) becomes<sup>137</sup>

$$\begin{aligned} \mathbf{r}_{\alpha}(\boldsymbol{\lambda}) &= - \begin{pmatrix} \lambda_1 \\ \lambda_2 \\ \lambda_3 \end{pmatrix} \\ &\quad + \begin{pmatrix} \cos \lambda_4 & \sin \lambda_4 \sin \lambda_5 & -\sin \lambda_4 \cos \lambda_5 \\ 0 & \cos \lambda_5 & \sin \lambda_5 \\ \sin \lambda_4 & -\cos \lambda_4 \sin \lambda_5 & \cos \lambda_4 \cos \lambda_5 \end{pmatrix} \\ &\quad \times (\mathbf{x}_{\alpha} - \mathbf{R}). \end{aligned} \quad (\text{C1})$$

By differentiating this parametric equation with respect to

the  $\lambda_\eta$  quantities and evaluating the results at  $\lambda=0$ , tangent vector formulas identical to those of Eqs. (A2)–(A6) are recovered except that  $\eta=6$  is omitted. Hence, Eqs. (A7) and (A8) hold as before except that the  $\mathbf{N}$  and  $\mathbf{B}_2$  matrices are of dimensionality  $5 \times 3N$  and  $\mathbf{A}$  is a  $5 \times 5$  matrix. All subsequent formulas in Appendix A apply for linear molecules if the  $\eta=6$  elements of the  $B_{i_1 i_2 \dots i_n}^\eta$  quantities and the third elements of  $\mathbf{k}$  and all of its derivatives are formally set to zero.

#### APPENDIX D: INVARIANCE RELATIONS FOR ANALYTIC DERIVATIVE EVALUATIONS

In 1984, Page, Saxe, Adams, and Lengsfeld<sup>76</sup> brought attention to a set of translational and rotational invariance relations which can be exploited to enhance the efficiency of analytic derivative evaluations of various orders in electronic structure calculations. Because the potential energy of a molecular system is a function of the internal variables alone,

$$\sum_{j_1}^{3N} V_{j_1}(\mathbf{x}) N_{j_1}^\eta(\mathbf{x}) = 0, \quad (\text{D1})$$

by analogy with Eq. (A2). Successive differentiation of Eq. (D1) with respect to Cartesian variables  $x_{j_2}$  and  $x_{j_3}$  yields the potential energy analogs of Eqs. (A4) and (A6):

$$\sum_{j_1}^{3N} V_{j_1 j_2} N_{j_1}^\eta + \sum_{j_1}^{3N} V_{j_1} N_{j_1 j_2}^\eta = 0 \quad (\text{D2})$$

and

$$\sum_{j_1}^{3N} V_{j_1 j_2 j_3} N_{j_1}^\eta + \sum_{j_1}^{3N} (V_{j_1 j_2} N_{j_1 j_3}^\eta + V_{j_1 j_3} N_{j_1 j_2}^\eta) = 0. \quad (\text{D3})$$

These expressions are simply Eqs. (8) and (12) of Page *et al.*<sup>76</sup> as written in our formalism, which facilitates analytic manipulations of these invariance conditions via the expressions of Appendix A. Multiplication of Eqs. (D2) and (D3) by  $B_{j_3}^\eta$  and summation over the external index  $\eta$  provides the alternate forms

$$\sum_{j_1}^{3N} V_{j_1 j_2} Q_{j_1 i_1} = \sum_{j_1}^{3N} V_{j_1} \Gamma_{j_1 j_2 i_1} \quad (\text{D4})$$

and

$$\sum_{j_1}^{3N} V_{j_1 j_2 j_3} Q_{j_1 i_1} = \sum_{j_1}^{3N} (V_{j_1 j_2} \Gamma_{j_1 j_3 i_1} + V_{j_1 j_3} \Gamma_{j_1 j_2 i_1}). \quad (\text{D5})$$

The conditions embodied in Eqs. (65)–(67) can be shown to arise from Eqs. (D4) and (D5) and higher-order analogs by a series of summations and algebraic manipulations. To illustrate the procedure it is worthwhile to demonstrate the equivalence of the two sides of Eq. (65). Substitution into the right side of Eq. (65) using  $P_{j_1 i_1 i_2}$  from Eq. (A20) gives

$$\begin{aligned} \sum_{j_1}^{3N} V_{j_1} P_{j_1 i_1 i_2} &= \sum_{j_1}^{3N} V_{j_1} \left( \sum_{j_2}^{3N} P_{j_1 j_2} \theta_{j_2 i_1 i_2} - \sum_{j_2 j_3}^{3N} P_{j_2 i_1} P_{j_3 i_2} G_{j_1 j_2 j_3} \right) \\ &= \sum_{j_1}^{3N} V_{j_1} \theta_{j_1 i_1 i_2}, \end{aligned} \quad (\text{D6})$$

by examining the form of  $G_{\sigma i_1 i_2}$  in Eq. (27) and noting that the Cartesian gradient vector  $\mathbf{h}$  satisfies  $\mathbf{P}\mathbf{h}=\mathbf{h}$  and  $\mathbf{Q}\mathbf{h}=\mathbf{0}$  as a consequence of Eq. (D1). Subsequent utilization of Eq. (A21) for  $\theta_{j_1 i_1 i_2}$  followed by the implementation of Eq. (D4) provides

$$\sum_{j_1}^{3N} V_{j_1} P_{j_1 i_1 i_2} = \sum_{j_2}^{3N} V_{j_2 i_1} Q_{j_2 i_2} + \sum_{j_1 j_2}^{3N} V_{j_1 j_2} Q_{j_1 i_1} P_{j_2 i_2}, \quad (\text{D7})$$

the right side of which can be readily shown to equal the left side of Eq. (65) by using Eq. (A14). Equations (65)–(67) provide an alternate route to the determination of complete Cartesian force fields from minimal, nonredundant sets of Cartesian derivatives through the inversion of the supermatrix  $L_{i_1 i_2 \dots i_n j_1 j_2 \dots j_n} = \delta_{i_1 j_1} \delta_{i_2 j_2} \dots \delta_{i_n j_n} - P_{i_1 j_1} P_{i_2 j_2} \dots P_{i_n j_n}$  within a selected set of redundant force constants  $V_{j_1 j_2 \dots j_n}$ . This approach is direct, whereas the procedure of Page *et al.*<sup>76</sup> is sequential for higher-order derivatives; however, as the molecular system becomes larger the inversion of the burgeoning supermatrix is likely to make the direct approach computationally less efficient.

<sup>1</sup>G. Fogarasi and P. Pulay, in *Vibrational Spectra and Structure*, edited by J. R. Durig (Elsevier, Amsterdam, 1985), Vol. 14, p. 125.

<sup>2</sup>P. Pulay, in *Modern Theoretical Chemistry*, edited by H. F. Schaefer III (Plenum, New York, 1977), Vol. 4, p. 153.

<sup>3</sup>W. J. Hehre, L. Radom, P. v. R. Schleyer, and J. A. Pople, *Ab Initio Molecular Orbital Theory* (Wiley-Interscience, New York, 1986).

<sup>4</sup>B. A. Hess, Jr., L. J. Schaad, P. Čársky, and R. Zahradník, *Chem. Rev.* **86**, 709 (1986).

<sup>5</sup>W. D. Allen, A. G. Császár, and D. A. Horner, *J. Am. Chem. Soc.* **114**, 6834 (1992).

<sup>6</sup>P. Pulay, *Mol. Phys.* **17**, 197 (1969).

<sup>7</sup>P. Pulay, *Mol. Phys.* **18**, 473 (1970).

<sup>8</sup>C. E. Blom and C. Altona, *Mol. Phys.* **31**, 1377 (1976).

<sup>9</sup>P. Pulay, G. Fogarasi, F. Pang, and J. E. Boggs, *J. Am. Chem. Soc.* **101**, 2550 (1979).

<sup>10</sup>P. Pulay, G. Fogarasi, G. Pongor, J. E. Boggs, and A. Vargha, *J. Am. Chem. Soc.* **105**, 7037 (1983).

<sup>11</sup>D. A. Clabo, Jr., W. D. Allen, R. B. Remington, Y. Yamaguchi, and H. F. Schaefer III, *Chem. Phys.* **123**, 187 (1988).

<sup>12</sup>W. D. Allen, Y. Yamaguchi, A. G. Császár, D. A. Clabo, Jr., R. B. Remington, and H. F. Schaefer III, *Chem. Phys.* **145**, 427 (1990).

<sup>13</sup>W. Thiel, G. Scuseria, H. F. Schaefer III, and W. D. Allen, *J. Chem. Phys.* **89**, 4965 (1988).

<sup>14</sup>T. J. Lee, W. D. Allen, and H. F. Schaefer III, *J. Chem. Phys.* **87**, 7062 (1987).

<sup>15</sup>J. F. Gaw and N. C. Handy, *Chem. Phys. Lett.* **128**, 182 (1986).

<sup>16</sup>E. D. Simandiras, J. F. Gaw, and N. C. Handy, *Chem. Phys. Lett.* **141**, 166 (1987).

<sup>17</sup>W. H. Green, D. Jayatilaka, A. Willets, R. D. Amos, and N. C. Handy, *J. Chem. Phys.* **93**, 4965 (1990).

<sup>18</sup>(a) R. H. Schwendeman, *J. Chem. Phys.* **44**, 556 (1966); (b) **44**, 2115 (1966).

<sup>19</sup>R. Rydberg, *Ann. Phys.* **73**, 376 (1931); O. Klein, *Z. Phys.* **76**, 226 (1932); A. L. G. Rees, *Proc. Phys. Soc. London, Sect. A* **59**, 998 (1947).

<sup>20</sup>See Sec. IV for computational details.

<sup>21</sup>A. Lofthus and P. H. Krupenie, *J. Phys. Chem. Ref. Data* **6**, 113 (1977).

- <sup>22</sup>E. A. Colbourn, M. Dagenais, A. E. Douglas, and J. W. Raymond, *Can. J. Phys.* **54**, 1343 (1976).
- <sup>23</sup>K. P. Huber and G. Herzberg, *Constants of Diatomic Molecules* (Van Nostrand, Princeton, NJ, 1979).
- <sup>24</sup>Y. P. Varshni, *Rev. Mod. Phys.* **29**, 664 (1957).
- <sup>25</sup>D. Steele, E. R. Lippincott, and J. T. Vanderslice, *Rev. Mod. Phys.* **34**, 239 (1962).
- <sup>26</sup>G. Simons, R. G. Parr, and J. M. Finlan, *J. Chem. Phys.* **59**, 3229 (1973); G. Simons, *ibid.* **61**, 369 (1974).
- <sup>27</sup>The absolute total energy of the nitrogen atom ( $-54.5958$  a.u.) was obtained by summing successive experimental ionization potentials, which are tabulated in C. E. Moore, *Atomic Energy Levels*, Natl. Stand. Ref. Data Ser. Natl. Bur. Stand. (U.S. GPO, Washington, DC, 1971). For the fluorine atom the observed ionization potentials give an energy of  $-59.2688(36)$  a.u. for  $F^{8+}$ , but the energy required to remove the last electron is not known accurately. The measured ionization potentials of the  $B^{4+}$ - $O^{7+}$  ions are uniformly larger than those predicted by the nonrelativistic energy formula for hydrogenlike atoms. In particular, the relativistic corrections (in  $\text{cm}^{-1}$ ) for these IP values are  $B^{4+}(767)$ ,  $C^{5+}(1588)$ ,  $N^{6+}(2943)$ , and  $O^{7+}(5024)$ , which fit the scaling relation  $1.2262 Z^2$  remarkably well. Accordingly, a relativistic contribution of  $8045 \text{ cm}^{-1}$  is surmised for the ionization potential of  $F^{8+}$ , whence the total energy of the fluorine atom is ascertained to be  $-99.8043(36)$  a.u.
- <sup>28</sup>The assumed absolute atomic energies  $E(\text{Si}) = -289.94$  and  $E(\text{Ar}) = -529.40$  a.u. are those predicted by a correlated, relativistic local-density method. See M. Vijayakumar, N. Vaidehi, and M. S. Gopinathan, *Phys. Rev. A* **40**, 6834 (1989).
- <sup>29</sup>Spectroscopic constants for  $N_2$  obtained with the CCSD(T) method and large atomic-natural-orbital basis sets have also been reported recently by T. J. Lee and J. E. Rice, *J. Chem. Phys.* **94**, 1220 (1991). Their  $[5s4p3d2f1g]$  CCSD(T) predictions at the corresponding theoretical geometry yield  $\omega_e = 2352 \text{ cm}^{-1}$  and  $\omega_e x_e = 14.2 \text{ cm}^{-1}$ , as compared to the experimental values (Ref. 23) of  $\omega_e = 2359 \text{ cm}^{-1}$  and  $\omega_e x_e = 14.3 \text{ cm}^{-1}$ , and our PZ( $3d2f1g$ ) CCSD(T)/expt results of  $\omega_e = 2378 \text{ cm}^{-1}$  and  $\omega_e x_e = 13.9 \text{ cm}^{-1}$ . The cubic force constant for  $N_2$  reveals that almost all of the improvement in the prediction of Lee and Rice relative to ours is a consequence of their use of a reference bond distance  $0.0030 \text{ \AA}$  longer than experiment. To wit, when the quartic force field of  $N_2$  is explicitly evaluated at their optimum  $[5s4p3d2f1g]$  CCSD(T) distance of  $r_e = 1.100688 \text{ \AA}$  using the PZ( $3d2f1g$ ) CCSD(T) method,  $\omega_e = 2352 \text{ cm}^{-1}$  and  $\omega_e x_e = 14.0 \text{ cm}^{-1}$  are obtained, in near perfect agreement with the original results of Lee and Rice.
- <sup>30</sup>As shown in Table III,  $V''''(r_e)$  for  $F_2$  is predicted to be  $176.8 \text{ aJ \AA}^{-4}$  by the PZ( $3d2f1g$ ) CCSD(T) method, a value which differs by 25% from the spectroscopic result of  $231.0 \text{ aJ \AA}^{-4}$ . When used as constraints in Eqs. (1) and (2), both of these  $V''''(r_e)$  values engender anomalous fifth derivatives in the fit to the RKR data. The unconstrained  $z_4$  result listed in Table I gives an intermediate value of  $211.3 \text{ aJ \AA}^{-4}$ , which appears to be the  $V''''(r_e)$  constant most consistent with the RKR points. The discrepancies among the various fourth-derivative values of  $F_2$  warrant further study because the high accuracy normally observed for CCSD(T) predictions with large basis sets makes the empirically derived values suspect.
- <sup>31</sup>F. Jenc and B. A. Brandt, *J. Mol. Spectrosc.* **138**, 13 (1989).
- <sup>32</sup>J. F. Gaw, Y. Yamaguchi, and H. F. Schaefer III, *J. Chem. Phys.* **81**, 6395 (1984).
- <sup>33</sup>J. F. Gaw, Y. Yamaguchi, H. F. Schaefer III, and N. C. Handy, *J. Chem. Phys.* **85**, 5132 (1986).
- <sup>34</sup>J. F. Gaw and N. C. Handy, *Annu. Rep. R. Soc. Chem. C* **81**, 291 (1984).
- <sup>35</sup>J. F. Gaw and N. C. Handy, in *Geometrical Derivatives of Energy Surfaces and Molecular Properties*, edited by P. Jørgensen and J. Simons (Reidel, Dordrecht, 1986), p. 79.
- <sup>36</sup>For  $N_2$  unconstrained numerical fits gave  $V''''$  and  $V''''''$  results which differed from the directly determined values by only 1.6% and 2.0%, respectively. For  $F_2$  the analogous percent differences in the  $V''''$  and  $V''''''$  values were 0.3% and 3.1%.
- <sup>37</sup>P. Pulay, W. Meyer, and J. E. Boggs, *J. Chem. Phys.* **68**, 5077 (1978).
- <sup>38</sup>D. Michalska, L. J. Schaad, P. Čárský, B. A. Hess, Jr., and C. S. Ewig, *J. Comput. Chem.* **9**, 495 (1988).
- <sup>39</sup>The correlation energy is usually defined as the difference between the exact, nonrelativistic energy of the system and the Hartree-Fock limiting value. As such, the quantity  $W(r)$  deviates slightly from the true correlation energy because the RKR energies contain relativistic contributions and the DZP RHF results are only upper bounds to the Hartree-Fock energies.
- <sup>40</sup>K. Jankowski, R. Becherer, P. Scharf, H. Schiffer, and R. Ahlrichs, *J. Chem. Phys.* **82**, 1413 (1985).
- <sup>41</sup>K. Kuchitsu and S. J. Cyvin, in *Molecular Structures and Vibrations*, edited by S. J. Cyvin (Elsevier, Amsterdam, 1972), p. 183.
- <sup>42</sup>J. A. Pople and M. Gordon, *J. Am. Chem. Soc.* **89**, 4253 (1967).
- <sup>43</sup>P. Császár, A. G. Császár, A. Somogyi, Z. Dinya, S. Holly, M. Gál, and J. E. Boggs, *Spectrochim. Acta* **42A**, 473 (1986).
- <sup>44</sup>P. Pulay, J. Lee, and J. E. Boggs, *J. Chem. Phys.* **79**, 3382 (1983).
- <sup>45</sup>V. J. Klimkowski, J. D. Ewbank, C. van Alsenoy, J. N. Scarsdale, and L. Schäfer, *J. Am. Chem. Soc.* **104**, 1476 (1982).
- <sup>46</sup>C. van Alsenoy, V. J. Klimkowski, and L. Schäfer, *J. Mol. Struct. Theochem.* **109**, 321 (1984).
- <sup>47</sup>H. J. Geise and W. Pyckhout, in *Stereochemical Applications of Gas-Phase Electron Diffraction*, edited by I. Hargittai and M. Hargittai (VCH, New York, 1988), p. 321.
- <sup>48</sup>J. E. Boggs, *Pure Appl. Chem.* **60**, 175 (1988).
- <sup>49</sup>G. Hafelinger, C. U. Regelman, T. M. Krygowski, and K. Wozniak, *J. Comput. Chem.* **10**, 329 (1989).
- <sup>50</sup>W. J. Bouma and L. Radom, *J. Mol. Struct.* **43**, 267 (1978).
- <sup>51</sup>B. J. Smith and L. Radom, *J. Am. Chem. Soc.* **112**, 7525 (1990).
- <sup>52</sup>H. Guo and M. Karplus, *J. Chem. Phys.* **91**, 1719 (1989).
- <sup>53</sup>G. Fogarasi, X. Zhou, P. W. Taylor, and P. Pulay, *J. Am. Chem. Soc.* **114**, 8191 (1992).
- <sup>54</sup>M. V. Volkenstein, M. A. Eliashevich, and B. I. Stepanov, *Kolebanija Molekul* (Gostechizdat, Moscow, 1949).
- <sup>55</sup>E. B. Wilson Jr., J. C. Decius, and P. C. Cross, *Molecular Vibrations* (McGraw-Hill, New York, 1955).
- <sup>56</sup>S. Califano, *Vibrational States* (Wiley, New York, 1976).
- <sup>57</sup>D. Papoušek and M. R. Aliev, *Molecular Vibrational-Rotational Spectra* (Elsevier, Amsterdam, 1982).
- <sup>58</sup>C. Eckart, *Phys. Rev.* **47**, 552 (1935).
- <sup>59</sup>A. Sayvetz, *J. Chem. Phys.* **7**, 383 (1939).
- <sup>60</sup>B. L. Crawford, Jr. and W. H. Fletcher, *J. Chem. Phys.* **19**, 141 (1951).
- <sup>61</sup>Z. Cihla and J. Plíva, *Coll. Czech. Chem. Commun.* **28**, 1232 (1963).
- <sup>62</sup>M. A. Pariseau, I. Suzuki, and J. Overend, *J. Chem. Phys.* **42**, 2335 (1965).
- <sup>63</sup>Y. Morino, K. Kuchitsu, and S. Yamamoto, *Spectrochim. Acta* **24A**, 335 (1968).
- <sup>64</sup>A. R. Hoy, I. M. Mills, and G. Strey, *Mol. Phys.* **24**, 1265 (1972).
- <sup>65</sup>W. D. Allen, Program INTDER, Stanford University, Stanford, CA.
- <sup>66</sup>J. Plíva, *Coll. Czech. Chem. Commun.* **23**, 777 (1958).
- <sup>67</sup>J. Plíva, *Coll. Czech. Chem. Commun.* **23**, 1839 (1958).
- <sup>68</sup>J. Plíva, *Coll. Czech. Chem. Commun.* **23**, 1846 (1958).
- <sup>69</sup>Z. Cihla and J. Plíva, *Coll. Czech. Chem. Commun.* **28**, 1232 (1962).
- <sup>70</sup>Since the potential-energy function is invariant to molecular translations and rotations,  $\mathbf{Q}^0 \mathbf{h} = 0$ , where  $\mathbf{Q}^0$  is the first-order projection matrix onto the space of canonical external variables and  $\mathbf{h}$  is the Cartesian gradient vector. As discussed in Appendix A,  $\mathbf{Q}^0 = \mathbf{I}_{3N} - \mathbf{B}_1^T (\mathbf{B}_1 \mathbf{B}_1^T)^{-1} \mathbf{B}_1$ , and thus the condition  $\mathbf{h}^T = \mathbf{h}^T \mathbf{B}_1^T (\mathbf{B}_1 \mathbf{B}_1^T)^{-1} \mathbf{B}_1$  arises. The internal gradient vector  $\mathbf{G}^T$  is given by  $\mathbf{G}^T = \mathbf{h}^T \mathbf{u} \mathbf{B}_1^T (\mathbf{B}_1 \mathbf{B}_1^T)^{-1}$  according to Eq. (31), which simplifies to  $\mathbf{G}^T = \mathbf{h}^T \mathbf{B}_1^T (\mathbf{B}_1 \mathbf{B}_1^T)^{-1}$  if the preceding condition on  $\mathbf{h}$  is used. Thus, it is seen that  $V^0$  in Eq. (31) is invariant to the choice of  $\mathbf{u}$ .
- <sup>71</sup>A. G. Császár, *J. Phys. Chem.* **96**, 7898 (1992).
- <sup>72</sup>T. Tanaka and Y. Morino, *J. Mol. Spectrosc.* **33**, 538 (1970).
- <sup>73</sup>The first-order term on the right-hand side of Eq. (46) is a consequence of the fact that the Cartesian gradient  $\mathbf{h}$  satisfies  $\mathbf{P}^0 \mathbf{h} = \mathbf{h}$ , where  $\mathbf{P}^0 = \mathbf{B}_1^T (\mathbf{B}_1 \mathbf{B}_1^T)^{-1} \mathbf{B}_1$  is the first-order projection matrix onto the internal space.
- <sup>74</sup>I. H. Williams, *J. Mol. Struct.* **94**, 275 (1983).
- <sup>75</sup>W. H. Miller, N. C. Handy, and J. E. Adams, *J. Chem. Phys.* **72**, 99 (1980).
- <sup>76</sup>M. Page, P. Saxe, G. F. Adams, and B. H. Lengsfeld III, *Chem. Phys. Lett.* **104**, 587 (1984). See also T. Helgaker and P. Jørgensen, *Adv. Quantum Chem.* **19**, 183 (1988), and references therein.
- <sup>77</sup>S. Huzinaga, *J. Chem. Phys.* **42**, 1293 (1965).
- <sup>78</sup>T. H. Dunning, Jr., *J. Chem. Phys.* **53**, 2823 (1970).
- <sup>79</sup>T. H. Dunning, Jr., *J. Chem. Phys.* **55**, 716 (1971).
- <sup>80</sup>H. Partridge, NASA Technical Memorandum 101044, 1989.
- <sup>81</sup>M. W. Wong, P. M. W. Gill, R. H. Nobes, and L. Radom, *J. Phys. Chem.* **92**, 4875 (1988).

- <sup>82</sup>T. H. Dunning, Jr., *J. Chem. Phys.* **90**, 1007 (1989).
- <sup>83</sup>C. C. J. Roothaan, *Rev. Mod. Phys.* **23**, 69 (1951).
- <sup>84</sup>A. Szabó and N. S. Ostlund, *Modern Quantum Chemistry* (McGraw-Hill, New York, 1989).
- <sup>85</sup>R. J. Bartlett, *Annu. Rev. Phys. Chem.* **32**, 359 (1981).
- <sup>86</sup>G. D. Purvis and R. J. Bartlett, *J. Chem. Phys.* **76**, 1910 (1982).
- <sup>87</sup>J. Paldus, in *New Horizons of Quantum Chemistry*, edited by P. O. Löwdin and B. Pullmann (Reidel, Dordrecht, 1983), p. 31.
- <sup>88</sup>R. J. Bartlett, C. E. Dykstra, and J. Paldus, in *Advanced Theories and Computational Approaches to the Electronic Structure of Molecules*, edited by C. E. Dykstra (Reidel, Dordrecht, 1984), p. 127.
- <sup>89</sup>G. E. Scuseria, A. C. Scheiner, T. J. Lee, J. E. Rice, and H. F. Schaefer III, *J. Chem. Phys.* **86**, 2881 (1987).
- <sup>90</sup>A. C. Scheiner, G. E. Scuseria, J. E. Rice, T. J. Lee, and H. F. Schaefer III, *J. Chem. Phys.* **87**, 5361 (1987).
- <sup>91</sup>K. Raghavachari, G. W. Trucks, J. A. Pople, and M. Head-Gordon, *Chem. Phys. Lett.* **157**, 479 (1989).
- <sup>92</sup>G. E. Scuseria and T. J. Lee, *J. Chem. Phys.* **93**, 5851 (1990).
- <sup>93</sup>TITAN is a set of electronic structure programs written by T. J. Lee, A. P. Rendell, and J. E. Rice.
- <sup>94</sup>PSI 2.0 (PSITECH Inc., Watkinsville, GA, 1991).
- <sup>95</sup>T. J. Lee and A. P. Rendell, *J. Chem. Phys.* **94**, 6229 (1991).
- <sup>96</sup>H. F. Schaefer III and Y. Yamaguchi, *J. Mol. Struct. Theochem.* **135**, 369 (1986).
- <sup>97</sup>P. Jørgensen and J. Simons, *Geometrical Derivatives of Energy Surfaces and Molecular Properties* (Reidel, Dordrecht, 1986).
- <sup>98</sup>Y. Osamura, Y. Yamaguchi, P. Saxe, M. A. Vincent, J. F. Gaw, and H. F. Schaefer III, *Chem. Phys.* **72**, 131 (1982).
- <sup>99</sup>Y. Osamura, Y. Yamaguchi, P. Saxe, D. J. Fox, M. A. Vincent, and H. F. Schaefer III, *J. Mol. Struct. Theochem.* **103**, 183 (1983).
- <sup>100</sup>The explicit finite-difference formulas used in the evaluation of the quartic force fields of F<sub>2</sub>O and N<sub>2</sub>O are available from the authors upon request.
- <sup>101</sup>I. M. Mills, in *Molecular Spectroscopy: Modern Research*, edited by K. N. Rao and C. W. Mathews (Academic, New York, 1972), Vol. 1, p. 115.
- <sup>102</sup>H. H. Nielsen, *Rev. Mod. Phys.* **23**, 90 (1951).
- <sup>103</sup>J. K. G. Watson, in *Vibrational Spectra and Structure*, edited by J. R. Durig (Elsevier, Amsterdam, 1977), Vol. 6, p. 1.
- <sup>104</sup>J. K. G. Watson, *J. Chem. Phys.* **48**, 4517 (1968).
- <sup>105</sup>See Tables II and III and footnote f of Table I.
- <sup>106</sup>K. E. Valenta, K. Vasudevan, and F. Grein, *J. Chem. Phys.* **72**, 2148 (1980).
- <sup>107</sup>R. Ahlrichs and P. R. Taylor, *Chem. Phys.* **72**, 287 (1982).
- <sup>108</sup>D. A. Clabo, Jr. and H. F. Schaefer III, *Int. J. Quantum Chem.* **31**, 429 (1987).
- <sup>109</sup>C. M. Rohlfing and P. J. Hay, *J. Chem. Phys.* **86**, 4518 (1987).
- <sup>110</sup>T. J. Lee, J. E. Rice, G. E. Scuseria, and H. F. Schaefer III, *Theor. Chim. Acta* **75**, 81 (1989).
- <sup>111</sup>T. J. Lee and J. E. Rice, *J. Chem. Phys.* (in press).
- <sup>112</sup>G. E. Scuseria, *J. Chem. Phys.* **94**, 442 (1991).
- <sup>113</sup>L. Pierce, N. DiCianni, and R. H. Jackson, **38**, 730 (1963).
- <sup>114</sup>Y. Morino and S. Saito, *J. Mol. Spectrosc.* **19**, 435 (1966).
- <sup>115</sup>E. A. Jones, J. S. Kirby-Smith, P. J. H. Woltz, and A. H. Nielsen, *J. Chem. Phys.* **19**, 337 (1951).
- <sup>116</sup>G. Taubmann, H. Jones, H. D. Rudolph, and M. Takami, *J. Mol. Spectrosc.* **120**, 90 (1986).
- <sup>117</sup>H. Bürger and G. Schippel, *J. Mol. Spectrosc.* **121**, 238 (1987).
- <sup>118</sup>T. Saarinen, E. Kauppi, and L. Halonen, *J. Chem. Phys.* **142**, 175 (1990).
- <sup>119</sup>It is possible to perform a linear transformation of the complete Cartesian force field to the dimensionless normal-coordinate space without making corrections for the rotational variance of the surface resulting from neglect of the Cartesian first derivatives. These unprojected Cartesian results differ from their projected counterparts only in those cases involving normal coordinate 3, the antisymmetric O–F stretch, since for a C<sub>2v</sub>-symmetry triatomic molecule, only the b<sub>2</sub> normal mode is of the proper symmetry to couple with rotational motion. Specifically, the unprojected force field yields the modified constants (in cm<sup>-1</sup>)  $\omega_3=968.74$ ,  $\phi_{331}=-268.3$ ,  $\phi_{332}=-73.3$ ,  $\phi_{3311}=65.6$ ,  $\phi_{3321}=20.3$ ,  $\phi_{3322}=-10.0$ , and  $\phi_{3333}=42.3$  (cf. Table IX). Thus, in the case of F<sub>2</sub>O the differences in the spectroscopic constants derived from the projected and unprojected Cartesian force fields are quite small.
- <sup>120</sup>J.-L. Teffo and A. Chédin, *J. Mol. Spectrosc.* **135**, 389 (1989).
- <sup>121</sup>I. Suzuki, *J. Mol. Spectrosc.* **32**, 54 (1969).
- <sup>122</sup>M. Lacy and D. H. Whiffen, *Mol. Phys.* **45**, 241 (1982).
- <sup>123</sup>M. Kobayashi and I. Suzuki, *J. Mol. Spectrosc.* **125**, 24 (1987).
- <sup>124</sup>A. G. Maki, J. S. Wells, and M. D. Vanek, *J. Mol. Spectrosc.* **138**, 84 (1989).
- <sup>125</sup>M. D. Vanek, M. Schneider, J. S. Wells, and A. G. Maki, *J. Mol. Spectrosc.* **134**, 154 (1989).
- <sup>126</sup>J. S. Wells, A. Hinz, and A. G. Maki, *J. Mol. Spectrosc.* **114**, 84 (1985).
- <sup>127</sup>J. M. L. J. Reinartz, W. L. Meerts, and A. Dymanus, *Chem. Phys.* **31**, 19 (1978).
- <sup>128</sup>H. Jalink, D. H. Parker, and S. Stolte, *J. Mol. Spectrosc.* **121**, 236 (1987).
- <sup>129</sup>J. Plíva, *J. Mol. Spectrosc.* **27**, 461 (1968).
- <sup>130</sup>S. D. Peyerimhoff and R. J. Buenker, *J. Chem. Phys.* **49**, 2473 (1968).
- <sup>131</sup>R. E. Bruns and W. B. Person, *J. Chem. Phys.* **53**, 1413 (1970).
- <sup>132</sup>D. G. Hopper, A. C. Wahl, R. L. C. Wu, and T. O. Tiernan, *J. Chem. Phys.* **65**, 5474 (1976).
- <sup>133</sup>J. L. Griggs, Jr., K. N. Rao, L. H. Jones, and R. M. Potter, *J. Mol. Spectrosc.* **25**, 34 (1968).
- <sup>134</sup>J. Plíva, *J. Mol. Spectrosc.* **25**, 62 (1968).
- <sup>135</sup>W. D. Allen, A. L. L. East, and A. G. Császár, *Structures and Conformations of Non-Rigid Molecules*, edited by J. Laane and M. Dakkouri (Kluwer, Dordrecht, in press).
- <sup>136</sup>R. E. Williamson and H. F. Trotter, *Multivariable Mathematics*, 2nd ed. (Prentice-Hall, Englewood Cliffs, NJ, 1979), p. 244.
- <sup>137</sup>H. Goldstein, *Classical Mechanics*, 2nd ed. (Addison-Wesley, Reading, MA, 1981).